BIOLOGY AND RECEPTOR INTERACTIONS OF P97 AND THE TRANSFERRIN RECEPTORS

by

BRANDIE LAUREL WALKER

B.Sc., University of Calgary, 1994

A THESIS SUBMITTED IN PARTIAL FULFILLMENT OF THE REQUIREMENTS FOR THE DEGREE OF

DOCTOR OF PHILOSOPHY

In

THE FACULTY OF GRADUATE STUDIES

Department of Zoology
and the Biotechnology Laboratory

We accept this thesis as conforming
to the required standard

THE UNIVERSITY OF BRITISH COLUMBIA

June 2002

In presenting this thesis in partial fulfilment of the requirements for an advanced degree at the University of British Columbia, I agree that the Library shall make it freely available for reference and study. I further agree that permission for extensive copying of this thesis for scholarly purposes may be granted by the head of my department or by his or her representatives. It is understood that copying or publication of this thesis for financial gain shall not be allowed without my written permission.

Department of Zoology

The University of British Columbia
Vancouver, Canada

Date July 31/02

DE-6 (2/88)

Abstract

Melanotransferrin, or p97, is an iron binding protein that is expressed as both a glycosylphosphatidylinositol-anchored form and as a soluble form. While the anchored form internalizes iron, the function of the soluble form is still unknown. Soluble p97 levels are increased in the serum and cerebral spinal fluid of Alzheimer disease patients, but the reasons for this increase are undetermined. In order to begin to address the question of function for this soluble protein, possible receptor interactions were studied.

The interaction of p97 and transferrin receptor 1 was characterized with radio-ligand assays and immunofluorescent labeling assays. These experiments demonstrated that p97 interacts with the transferrin receptor 1 in cell binding experiments. However, p97 was not able to deliver iron into the cells via transferrin receptor 1. Furthermore, BIAcore studies were not able to measure any interaction between p97 and transferrin receptor 1.

In the search for other likely candidate receptors of p97, a novel homologue of the transferrin receptor 1 was discovered through mining of the EST database. Expression of this protein was revealed by Northern blot to be largely restricted to the liver. In embryogenesis, the mouse transferrin receptor 2 is present by E15 and continues to increase in expression through E17, in contrast to transferrin receptor 1 that is discernable by E7, increases until E15 and decreases by E17. Transferrin receptor 2 is present on the brain endothelial cells that form the blood-brain barrier implicating it as a candidate receptor for transport of p97 (and iron) into or out of the brain. Interestingly, in

transfected cells that over express both transferrin receptor 1 and 2, the receptor is present at the cell surface as a heterodimeric combination of the two receptors.

p97 binds to the mouse transferrin receptor 2, and unlike transferrin receptor 1, also facilitates the uptake of ^{55}Fe through this interaction. Thus, in addition to receptor binding, the functional aspect of this interaction can be demonstrated. Clearly, identification of transferrin receptor 2 as a receptor of p97 is only one of the first important steps toward the ultimate goal of clarifying the function of soluble p97.

Table of Contents

List of Figures

List of Tables

List of Abbreviations:

AP-1	Activator protein 1
ATCC	American Type Culture Collection
ATP	Adenosine triphosphate
BBB	Blood-brain barrier
BSA	Bovine serum albumin
cDNA	Complementary deoxyribonucleotide
CHO	Chinese hamster ovary
C-lobe	Carboxyl-terminal lobe
CNS	Central nervous system
Cp	Ceruloplasmin
CREB	Cyclic adenosine monophosphate response element binding protein
CSF	Cerebral spinal fluid
Dcytb	Duodenal cytochrome b
DIG	Digoxigenin
DMEM	Dulbecco modified eagle's media
DMT-1	Divalent metal transporter 1
DPM	Disintegrations per minute
E7	Embryological day 7
EDC	N-ethyl-N'-(dimethyl-aminopropyl) carbodiimide
EDTA	Ethylenediaminetetraacetic acid
EEA1	Early endosome associated antigen 1
EST	Expressed sequence tag

FACS	Flow cytometry
Fe^{2+}	Ferrous iron
Fe^{3+}	Ferric iron
FITC	Fluorescein isothiocyanate
GPI	Glycosylphosphatidylinositol
HEPES	2-hydroxyethyl-piperazine-2-ethansulfonic acid
HepG2	Human hepatocellular carcinoma derived cell line
HFE	Protein responsible for hereditary hemochromatosis
HH	Hereditary hemochromatosis
HO-1	Heme oxygenase 1
IRE	Iron responsive element
IRP	Iron regulatory protein
K562	Human erythroid leukemia cell line
mRNA	Messenger ribonucleotide
NHS	N-hydroxysuccinimide
N-lobe	Amino terminal lobe
PBS	Phosphate buffered saline
RNA	Ribonucleotide
RT-PCR	Reverse transcription and polymerase chain reaction
RU	Resonance units
SDS-PAGE	Sodium dodecyl sulfate-polyacrylamide gel electrophoresis
SFT	Stimulator of iron transport
SK-MEL-28	Human melanoma derived cell line

TCA	Trichloroacetic acid
Tf	Transferrin
TfR1	Transferrin receptor 1
TfR2	Transferrin receptor 2
TRA	Transferrin receptor transcriptional control element
TRAC	Transferrin receptor transcriptional control element specific complex
TRVb	Chinese hamster ovary cell with defective endogenous transferrin receptor

Acknowledgements and Dedication

Thanks are due to many individuals who have helped me with this work, directly or indirectly, over the years. To begin, I must acknowledge the guidance and encouragement of my supervisor, Dr. Wilf Jefferies. Wilf has always had a vision for this research, and an unshakeable faith in both the direction of study and in my ability to complete it. Many people in the lab were also essential to the progression of this thesis, including Dr. Maki Ujiie, who believed in and encouraged me constantly; and Dr. Jacqueline Tiong, who completed her thesis one year ahead of me (inspiring me and proving that it could be done). Dr. Cheryl Pfeifer, Maya Kotturi, and Dara Dickstein, helped with extensive proof-reading (and coffee break) duties.

I would also like to acknowledge the contribution of all the other lab members (past and present) who have made my time at UBC enjoyable over the years. Thanks to Ian, Forrest, Gregor, Iku, Cyp, Joe, Judie, Daphne, Gaba, Malcolm, Greg, Ana Luiza, Alex, Kyung Bok (K.B.), Kendra, Siri, Jason X, Jason G, Laura, Quin Jin, Mei Mei, Kaan, Matt, Joanne, Mei, Linda, Genc, Ray, Andy, Francesca, and Sarah.

I must also thank Dr. Alex Law of Oxford for allowing me to come to his facility to carry out BIAcore studies with the integrin $\alpha_V\beta_3$. His generous gift of reagents and friendly welcome were appreciated. Thank-you also to Dr. Alister Dodds for his technical assistance with the BIAcore assays in Oxford. Similarly, Dr. Pamela Bjorkman allowed me to work in her laboratory at Caltech for BIAcore studies with transferrin receptor 1 and 2. The BIAcore work could not have been accomplished without the help of Ph.D. candidate Anthony Giannetti in the Bjorkman lab, who worked very hard at trouble-shooting to get the assay working.

Finally, but most importantly, I must acknowledge my family for their indispensable contribution. My Mom, who is my greatest cheerleader and unwavering support system. My Dad, who believes I can accomplish anything. My sisters, who understand the ups and downs of research and are always there with good advice, or just to listen when I need to vent. The rest of my family (old and new) who have refrained from asking "when will you be done?" Most of all, I need to thank my husband: without Greg, none of this could have been done or would have been worth doing. Greg, this thesis is dedicated to you.

Chapter 1: Introduction

I. General introduction

Protein-protein interactions are involved in some of the most important biological processes discovered to date. From the development of the immune system to nerve impulse transmission, the ability of one protein to interact with another in a specific fashion to elicit a particular response is one fundamental way in which biological systems function. This thesis examines one protein-protein interaction: namely the receptor binding properties of melanotransferrin, a protein that binds iron and is a biomarker of Alzheimer disease. Melanotransferrin, also known as p97, shares significant sequence homology with the well-characterized transferrin receptor ligand, transferrin (Tf), and is implicated in iron transport across the blood-brain barrier. One of the main goals of p97 research has been to establish a function for the soluble form of the p97 protein. This investigation has begun to identify p97 receptors, including the binding to transferrin receptor 1 (TfR1). After the characterization of this interaction, the search for additional receptors for p97 led to the discovery of a novel transferrin receptor, now called transferrin receptor 2 (TfR2), which is characterized in detail.

II. Iron absorption in the intestine

p97 and the transferrin receptors make up only a few components in a very complex group of players involved in iron uptake, transport, and storage. Iron is an essential element for life. However, it can also catalyze the formation of free radicals, and for this reason the uptake and dissemination of iron is closely regulated. Iron absorption takes place mainly in the duodenum and jejunum. It is a complex process

involving many proteins that play roles in the uptake and transfer of iron, or in the regulation of iron uptake.

A. Divalent metal transporter 1

In the intestine, the uptake of inorganic iron occurs through the duodenal villus cells via a protein called divalent metal transporter-1 (DMT-1). Divalent metal transporter-1 is a 561 amino acid protein with 12 membrane spanning regions. It is found on many different cell types in the body, with high levels of expression exhibited in the intestine, brain, thymus, proximal kidney and bone marrow (Griffiths *et al.*, 2000; Gruenheid *et al.*, 1995; Rabin *et al.*, 1985). The highest concentration of DMT-1 protein is found in the upper villus region of the duodenum, and upon ingestion of high levels of iron, a redistribution of DMT-1 protein occurs from the apical cell surface to the cytosol (Sharp *et al.*, 2002). Divalent metal transporter-1's role in the iron uptake pathway is to transport the Fe^{2+} (ferrous) form of iron across the plasma membrane into the duodenal cell (see Figure 1.1). Since dietary inorganic iron is largely in the Fe^{3+} (ferric) form, it must be reduced by an NADH-ferric reductase before transport by DMT-1 (Conrad *et al.*, 1999). The activity of this reductase has been demonstrated in both a cell culture model of the duodenal mucosa, and in the mucosa itself (Raja *et al.*, 1992; Riedel *et al.*, 1995). One candidate for the NADH-ferric reductase is duodenal cytochrome b (Dcytb). Recently it was shown that Dcytb is localized to the upper villus region of the duodenum, and that it has ferric reductase activity (McKie *et al.*, 2001). Furthermore, both protein levels and mRNA levels of Dcytb are increased by iron deficiency as well as in a mouse model of chronic anemia (McKie *et al.*, 2001). Based on these studies, Dcytb may be the

Figure 1.1: Flowchart of iron absorption pathway from the intestine. Ingested inorganic ferric iron is reduced to the ferrous form by a ferric reductase, possibly Dcytb, in the enterocyte, and transported across the cell membrane by DMT-1. Iron from heme is absorbed, possibly through a heme receptor, and reduced to the ferrous form by heme oxygenase 1 (HO-1). Ferric iron can also be associated with mucin in the gut, and absorbed by parraferritin which solubilizes the ferric iron, which is then reduced by mono-oxygenase. The ferrous iron is transported out of the cell to the blood stream. It is transported across the membrane by ferroportin, in association with hephaestin that oxidizes the ferrous iron to the ferric form that is bound by transferrin. Ceruloplasmin (Cp) oxidizes ferrous iron in serum for delivery to transferrin (Tf).

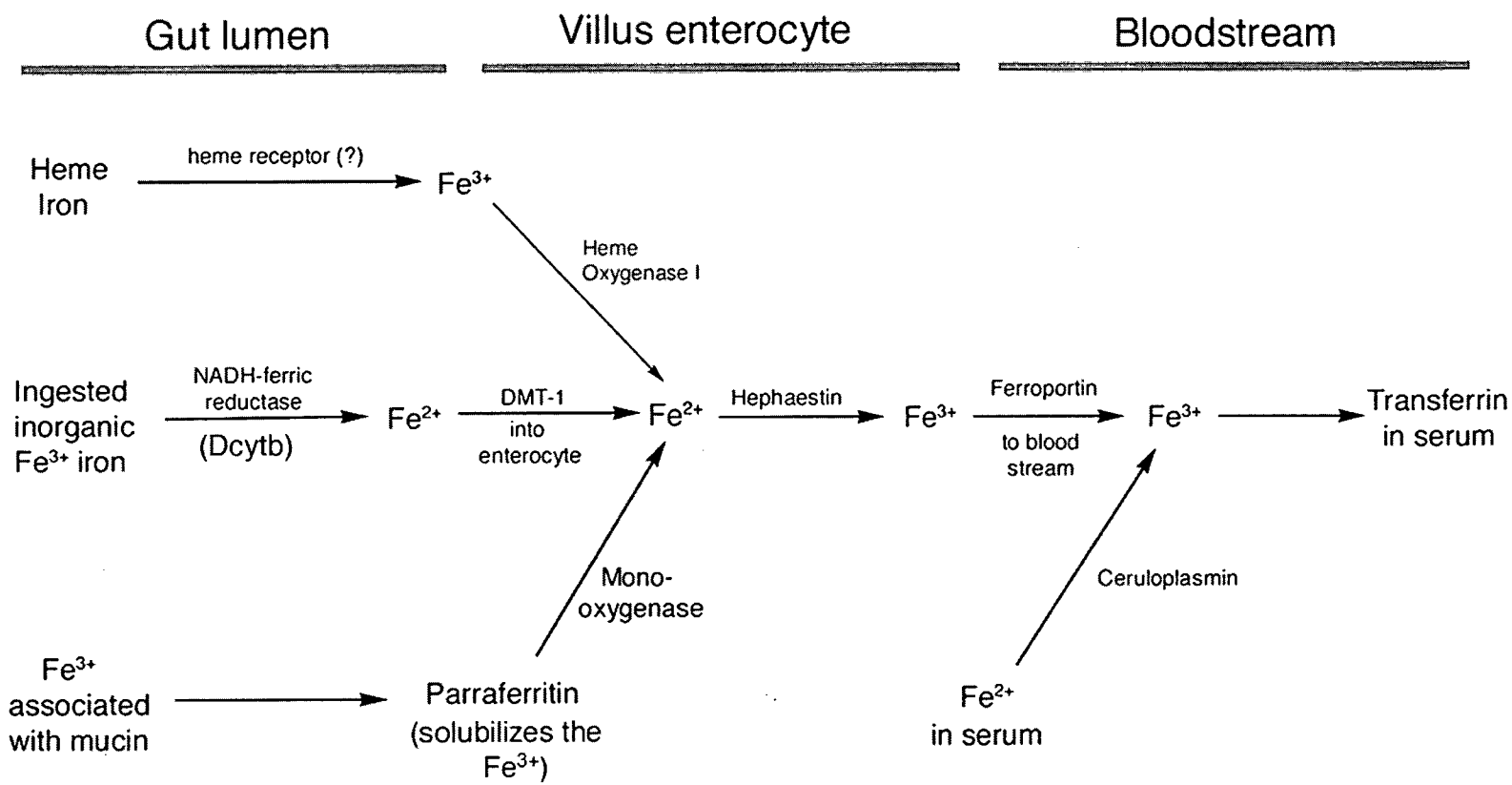
Gut lumen
Villus enterocyte
Bloodstream
Heme Iron
heme receptor (?)
Fe^{3+}
Heme Oxygenase I
Ingested inorganic Fe^{3+} iron
NADH-ferric reductase
(Dcytb)
Fe^{2+}
DMT-1
into enterocyte
Fe^{2+}
Hephaestin
Fe^{3+}
Ferroportin
to blood stream
Fe^{3+}
Transferrin in serum
Mono-oxygenase
Ceruloplasmin
Fe^{3+} associated with mucin
Parraferritin (solubilizes the Fe^{3+})
Fe^{2+} in serum

iron reductase that works in concert with DMT-1 to bring dietary non-heme iron into the body. It should be noted that DMT-1 is not specific for Fe^{2+}, but also transports other metals such as Zn^{2+}, Mn^{2+}, Co^{2+}, Cd^{2+}, Cu^{2+}, Ni^{2+}, and Pb^{2+} (Sharp *et al.*, 2002).

Divalent metal transporter-1 expression, like the expression of a number of proteins involved in the iron uptake, transport and storage pathways, is regulated through the elegant iron responsive element (IRE)/ iron regulatory protein (IRP) system (Andrews, 1999). In this system, the IRE can be found at either the 3' or the 5' end of the mRNA. In general, IREs located at the 5' end of mRNA allow the IRP to bind in low iron conditions and thus result in decreased translation of the iron binding protein. The iron storage protein ferritin is an example of this regulation (Aziz and Munro, 1987). In this case, low levels of iron cause IRPs to bind to the IREs, thereby blocking translation of the ferritin mRNA and preventing the ferritin protein from being synthesized. When intracellular levels of iron are high, the IRPs change conformation and can no longer bind to the IREs. If this occurs, ferritin synthesis will proceed, resulting in a greater capacity to store pools of iron intracellularly.

Conversely, if IREs are found within the 3' end of mRNAs, IRPs will bind to the nascent mRNA molecule under low cellular iron conditions and stabilize it, thus allowing more protein to be translated. The IREs within the TfR1 and DMT-1 are located in the 3' untranslated region of the mRNA. When iron concentrations are low and the IRPs are able to bind, the transcript is stabilized and increased amounts of the protein are produced (Mullner and Kuhn, 1988). If iron concentrations are high, the IRP cannot bind to the 5' IRE and the transcript becomes targeted for rapid degradation. Unlike the TfR1, which has five sets of IREs, and needs at least three to be bound by the

IRPs for stabilization of the mRNA (Casey *et al.*, 1989), the common isoform of DMT-1 has only one IRE (while the other splice variant of DMT-1 has none) (Gunshin *et al.*, 1997; Wardrop and Richardson, 1999). This single IRE within DMT-1 mRNA may lead to a less sensitive response to iron than that observed for the TfR1 (Sharp *et al.*, 2002).

B. Heme absorption

Dietary iron from heme is absorbed through a different mechanism than inorganic iron. Hemoglobin and myoglobin-derived iron are absorbed more efficiently by the intestine than inorganic iron since the presence of amino acids from proteolytic digestion prevents polymerization and precipitation of heme (Majuri and Grasbeck, 1987; Raffin *et al.*, 1974; Turnbull *et al.*, 1989). There is evidence to support the presence of a heme receptor on the luminal side of villus cells that brings iron into the intestinal cell, largely in the metalloporphyrin form (Grasbeck *et al.*, 1982), but this notion remains controversial. Once heme is inside the cell, iron is released via heme oxygenase 1 (HO-1), which cleaves the heme ring to generate bilirubin, carbon monoxide, and ferrous iron (see Figure 1.1) (Maines, 1997). In mice deficient in HO-1, tissue iron stores are high while serum iron is low, suggesting that the enzyme is involved in the discharge of iron from certain cells (Poss and Tonegawa, 1997a; Poss and Tonegawa, 1997b). The mechanism by which the iron liberated from heme is subsequently routed for systemic use is not well understood. The liberation of iron from spent erythrocytes is of vital importance, because almost all of the iron required for erythropoiesis is recycled in this manner (Andrews, 2000). Reticuloendothelial macrophages ingest senescent erythrocytes and the iron is either stored within the ferritin of the macrophage, or released

to the serum where it can be oxidized by ceruloplasmin and bound by Tf (Fleming and Sly, 2001).

Recently, a mammalian iron ATPase (Fe-ATPase) associated with the microsomal membrane and co-distributed in tissues with HO-1 was identified (Baranano *et al.*, 2000). There is some evidence to suggest that HO-1 is functionally coupled to this Fe-ATPase (Ferris *et al.*, 1999; Poss and Tonegawa, 1997b). The novel Fe-ATPase is enriched in spleen, and the iron transport it mediates is dependent upon hydrolyzable nucleotide triphosphate, magnesium, time and temperature. Barañano and associates suggest a new model in which Fe-ATPase and HO-1 colocalize to the endoplasmic reticulum where heme is first degraded by HO-1 and the liberated iron is transported by the Fe-ATPase to the luminal side of the endoplasmic reticulum (Baranano *et al.*, 2000). Moreover, they propose that the iron in the endoplasmic reticulum can then bind to Tf and can be recycled back to the cell surface for exocytosis, rather than being released into the serum.

C. Parraferritin

The parraferritin complex is made up of β-integrin, mobilferrin (a homologue of the molecular chaperone calreticulin) and flavin mono-oxygenase. Although the mechanism is not well understood, parraferritin mediates the uptake of ferric iron associated with mucin in the gut lumen (Umbreit *et al.*, 1998). The proposed mechanism is that ferric iron is solubilized by mucin in the intestinal lumen, and then transferred to parraferritin complexes containing β-integrin and mobilferrin (Conrad *et al.*, 1999). Following internalization of the iron, the complex becomes associated with the mono-oxygenase, and the ferric iron is reduced (see Figure 1.1). Thus, the parraferritin

complex acts as an NADPH-dependent ferrireductase, and serves to make reduced iron available to the various iron transport proteins.

D. Ferroportin and hephaestin

Once inside the duodenal cell the absorbed iron can be stored in ferritin, or it can be transported into the blood stream via the iron exporter protein ferroportin, (also known as iron regulated transporter-1) which is located on the basolateral surface of the duodenal enterocytes. Ferroportin also plays an important role in the release of iron from body stores in reticuloendothelial cells (Abboud and Haile, 2000). Furthermore, missense mutations in the ferroportin gene have been implicated in hereditary hemochromatosis (HH) (Montosi *et al.*, 2001). In this disease, the loss of function mutation causes problems with iron recycling from the reticuloendothelial macrophages, leading to a decrease in iron available for the hematopoeitic system. This in turn leads to a feedback mechanism that increases iron absorption through the intestine, and thus to iron overload.

Ferroportin was initially discovered through positional cloning of a zebrafish mutant with defects in circulating erythroid cells (Donovan *et al.*, 2000). The mammalian version is expressed in the placenta, liver, spleen, macrophages and kidneys. Ferroportin has an IRE in the 5' untranslated region, much like ferritin, while its response to iron levels mimics that of the TfR1 (McKie *et al.*, 2000). When rodents are fed diets high in iron, ferritin expression increases while ferroportin expression decreases (Abboud and Haile, 2000). Furthermore, in HH, the duodenal expression of ferroportin is stimulated despite the increased level of iron in the body, perhaps due to a defect in the

iron-sensing mechanisms of the enterocyte (Zoller *et al.*, 2001). The potential regulatory mechanisms of the promoter for this gene have yet to be elucidated.

Ferroportin works in concert with a multicopper ferroxidase called hephaestin, which is closely related to ceruloplasmin (Vulpe *et al.*, 1999). Hephaestin seems to oxidize iron so that it can be transported by ferroportin into the bloodstream and ultimately be delivered throughout the body via Tf (see Figure 1.1). How these proteins interact to achieve this phenomenon has yet to be determined.

E. Regulation of iron uptake

Intestinal iron uptake is regulated in at least three distinct ways. The first regulatory mechanism is the mucosal block, and refers to the fact that once a large oral dose of iron is received, enterocytes do not absorb iron again for 48 hours. While this has been shown experimentally, there is some dispute whether this would explain the ineffectiveness of daily oral iron supplementation (Benito *et al.*, 1998). The molecular mechanism of this mucosal block is still under investigation.

The second mechanism for iron uptake regulation is the stores regulator which seems to function at the level of the duodenal crypt cell and involves cell programming in response to existing body iron stores (Finch, 1994). An absorptive capacity for the villus cell is thus established, and in this manner the amount of iron routed to the ferritin stores within the villus cells versus the amount transported across into the blood is regulated. If the body iron stores are high, more iron will be stored in the ferritin of the villus cells, and be expelled from the body as the villus cells are shed, reducing the overall amount of iron in the body. The current understanding is that iron levels are sensed via the iron

saturation level of the circulating soluble TfR1 (Andrews, 2000). This in turn dictates the expression levels of DMT-1 and ferroportin on the villus cell.

A recently discovered protein called hepcidin is also believed to be involved in communicating body iron storage levels to the intestine. Hepcidin was identified as a circulating antimicrobial peptide, and is produced in hepatocytes (Krause *et al.*, 2000) (Park *et al.*, 2001). In mice with a targeted disruption of the gene encoding upstream stimulatory factor 2 (USF2), an additional unintended knockout of the hepcidin gene (downstream of USF2) created a situation in which no hepcidin was expressed, and iron overload was observed (Nicolas *et al.*, 2001). Deficiencies in four different proteins have now been shown to lead to the hereditary hemochromatosis-like iron overload phenotype in mice. These include deficiencies in HFE (Feder *et al.*, 1996), β2microglobulin (Rothenberg and Voland, 1996), TfR2 (Camaschella *et al.*, 2000) and hepcidin (Nicolas *et al.*, 2001). This fact led to the hypothesis that hepcidin expression may be modulated by iron levels in hepatocytes, then function by interacting with the HFE, β2microglobulin, and TfR1 system to regulate iron uptake by the crypt cells of the duodenum (Nicolas *et al.*, 2001). This theory has yet to be tested experimentally, although it is now confirmed that an overexpression of hepcidin leads to a severe iron deficiency condition in transgenic mice (Nicolas *et al.*, 2002).

The final known regulation mechanism is the erythropoietic regulator (Finch, 1994). Using this mechanism, the body can adjust the level of intestinal iron absorption to the current demands of erythropoiesis, a major iron sink. It is speculated that an as yet unknown soluble signal from the hematopoeitic bone marrow to the duodenum must exist (Finch, 1994) that signals the need for increased dietary iron uptake. A great deal of

further work is necessary to fully understand how iron uptake is regulated in the dietary uptake system.

III. Serum iron transport proteins

A. Transferrin

The major iron transport protein in the body is transferrin (Tf). Transferrin has two lobes that possess about 40% sequence homology between them, connected by a short bridging peptide. The crystal structure of rabbit Tf produced by Bailey and associates shows that there are 13 disulphide bridges within the protein, and that six of those are in homologous positions in each lobe (Bailey *et al.*, 1988). The Tf gene is located at 3q21-25, which is in close proximity to the TfR1 gene (Rabin *et al.*, 1985).

Transferrin is mainly synthesized in the liver, and then is secreted into the plasma where it can transport iron to all areas of the body. Transferrin expression is controlled by both positive and negative regulatory elements found 5' of the transcription start site, although no IRE exists in the mRNA of this molecule.

Transferrin binds one ferric ion in each lobe. Anderson *et. al.* have proposed a model where the open lobe structure of the protein changes configuration by closing tightly when the iron and its synergistic anion bind in the binding site (called the 'Venus fly-trap' mechanism) (Anderson *et al.*, 1990). Since iron binds to Tf with very high affinity, in order for Tf to effectively supply iron to the cells, Tf must also possess an efficient release mechanism. This mechanism appears to be quite complex. While past studies on iron release from Tf have been conducted on either single lobe or monoferric Tf, it has become clear that the physiological mechanism can only be understood by

taking into account the active role that the TfR1 plays in iron release (Bali and Aisen, 1992). As will be discussed later, in the acidic environment of the endosome, iron is released from Tf, while the Tf remains tightly bound to the TfR1. In general, iron release is thought to occur most readily from the amino-terminal-lobe (N-lobe) of the protein than the carboxyl-terminal-lobe (C-lobe), and has been proposed to involve a dilysine trigger mechanism (Dewan *et al.*, 1993). The dilysine motif is, however, missing from lactoferrin (a Tf-like protein found in human milk and other epithelial secretions (Lonnerdal *et al.*, 1987)) and the C-lobe of Tf. In addition, mutation of the iron ligand histidine at position 249 to glutamine in the N-lobe of human Tf removes the dilysine "trigger" but does not significantly affect iron release (MacGillivray *et al.*, 2000). Comparison of the two different conformations of the recombinant N-lobe of the human Tf crystal structure revealed that the protonation of the carbonate anion and the resulting partial removal of the anion from arginine 124 may be the initial step in pH-induced release of iron from Tf (MacGillivray *et al.*, 1998). Our understanding of the release of iron from Tf will not be complete until iron release from the Tf/TfR1 complex is directly examined.

B. Ceruloplasmin

Ceruloplasmin (Cp) is a copper binding protein secreted by hepatocytes into the plasma, but interestingly, it plays no known role in copper transport (Gitlin, 1998). However, Cp does seem to be a vital component in the iron transport system, since it functions as a serum ferroxidase required to oxidate iron before the iron can be incorporated into transferrin (Osaki and Johnson, 1969; Roeser *et al.*, 1970). It has also

been observed that under iron deficient conditions, the transcription and translation of Cp significantly increases (Mukhopadhyay *et al.*, 2000). The role of this multicopper oxidase has been more clearly defined in yeast, where a species orthologue multicopper oxidase protein (fet3P) is required for high affinity iron uptake (de Silva *et al.*, 1997; Stearman *et al.*, 1996). In a study on iron uptake using a human erythroleukemia (K562) cell line grown in iron deficient conditions, Cp was able to induce a 2- to 3-fold increase in non-Tf bound iron uptake, through a transcription-dependent manner (Attieh *et al.*, 1999). In the presence of excess trivalent cations this effect could be completely inhibited, suggesting the involvement of a trivalent cation specific mechanism (Attieh *et al.*, 1999).

Ceruloplasmin has three pairs of consensus hypoxia response elements in the 5' untranslated region of the gene (Mukhopadhyay *et al.*, 2000). Hypoxic inducible factor 1 is believed to bind hypoxia response elements and increase transcription of the Cp, which is consistent with the fact that an iron deficiency leads to an increase in the level of Cp in the plasma

Ceruloplasmin has been demonstrated to exist in both a soluble form and a glycosylphospatidylinositol (GPI)-linked cell surface form. Recently, the GPI-linked form was shown to be a result of alternative splicing (Patel *et al.*, 2000), and to be expressed in glial cells associated with brain microvasculature. This may indicate a specialized role for Cp in iron metabolism and homeostasis within the central nervous system (Klomp and Gitlin, 1996; Sheth and Brittenham, 2000). In the brain, all of the Cp appears to be in the GPI-linked form, whereas the soluble form has been shown to be unable to cross the blood-brain barrier (BBB).

C. Melanotransferrin (p97)

Melanotransferrin, referred to as p97 in this thesis, is a 97 kDa protein which shares 39% sequence identity with human transferrin (Rose *et al.*, 1986). It was first identified as a cell surface marker for human skin cancer (Brown *et al.*, 1981; Woodbury *et al.*, 1981; Woodbury *et al.*, 1980). However, the protein was subsequently found to be expressed at various levels in other tissues such as the liver, intestine, umbilical cord, placenta, sweat gland and more recently on human brain endothelium (Barresi and Tuccari, 1994; Rothenberger *et al.*, 1996; Sciot *et al.*, 1989). Unlike the other members of the transferrin family, p97 is present as two distinct forms. It can be found as a membrane protein attached to the cell surface via a GPI-anchor and as a soluble form in the serum and cerebrospinal fluid (Alemany *et al.*, 1993; Brown *et al.*, 1981; Food *et al.*, 1994; Kennard *et al.*, 1996).

Like other members of the transferrin family, p97 is a bilobed metal binding protein. Sequence alignment with other members of the family (such as Tf, lactoferrin, and ovotransferrin) show that the amino acids involved in coordinating the iron atom of the N-lobe are precisely conserved (Rose *et al.*, 1986). However, there is an aspartic acid at position 395 in the sequence of the C-lobe of Tf that is a serine in the p97 sequence, which could affect iron binding to the C-lobe of the latter. Baker and associates have shown that p97 has only one functional iron binding site, but recent data using various techniques suggests that under certain conditions, both lobes are able to bind iron (Baker *et al.*, 1992; Tiong, 2001; Tiong and Jefferies, 2002).

Metal binding studies on a Chinese hamster ovary cell line transfected with human p97 show the iron uptake process by surface GPI-linked p97 is both temperature

dependent and saturable (Kennard *et al.*, 1995). The GPI-linked cell surface form of p97 has been shown to deliver the internalized iron to ferritin (Tiong, 2001). This internalization, shown through immunofluorescence co-localization, is mediated through caveolae rather than clathrin coated pits (Tiong, 2001). The iron delivery to ferritin requires the presence of Rab 5 in the cells, which indicates that at some point the caveolae vesicle merges with the endosomal pathway (Tiong *et al.*, 2002).

Similar to Tf, p97 is able to bind to other metals in addition to iron. Using a competitive metal binding assay, it has been demonstrated that metals such as Al^{3+}, Cu^{3+} and Zn^{3+} are able to compete for the iron binding site in p97 (Tiong, 2001). Also as with Tf, there is no identifiable iron responsive element in p97 (Richardson, 2000). However, a regulatory element is located 2 kilobases (Kb) upstream from the promoter region of the p97 gene, and deletion of this element severely impairs the expression of p97 (Duchange *et al.*, 1992). This regulatory element was shown to be part of an enhancer composed of two binding sites for the AP-1 transcription factor. AP-1 is formed by the dimerization of the proteins Jun and Fos through their leucine zipper motifs, and is upregulated after ultraviolet irradiation (a suspected risk factor in melanoma) (Devary *et al.*, 1991). The transcription factor recognizes the phorbol 12-myristate 13-acetate responsive element (Angel and Karin, 1991), (Sassone-Corsi, 1994). By gel retardation assays it has been shown that the expression of p97 correlates with increased AP-1 binding activity (Roze-Heusse *et al.*, 1996). A secondary unidentified nuclear factor is involved with AP-1 to form a ternary complex at the two AP-1 sites in the p97 enhancer region (Roze-Heusse *et al.*, 1996). This may explain how p97 is upregulated in melanoma cells.

It has long been believed that the Tf/TfR1system is exclusively responsible for iron delivery to the brain, but recent studies suggest this may not be the case. For example, hypotransferrinemic mice, deficient in Tf, have normal brain iron levels. Many pieces of evidence point to a role for p97 in iron transport to the brain. Expression of p97 has been examined in brains from Alzheimer disease patients as well as in brains from patients suffering from other neurological diseases. While immunohistochemical staining of p97 in normal brains shows distribution limited to the BBB, p97 in Alzheimer disease is also found to be highly expressed in a subset of reactive microglia cells associated with β-amyloid plaques (Jefferies *et al.*, 1996). This was further confirmed by *in situ* hybridization of p97 mRNA, which shows p97 is expressed in the reactive microglia cells in the Alzheimer disease brain but not in normal brain or non-reactive microglia in Alzheimer disease brains (Yamada *et al.*, 1999). Soluble p97 was also found to be elevated 2 to 4 fold in the cerebral spinal fluid and serum of patients with Alzheimer disease compared with healthy age matched controls and patients with other forms of dementia (Feldman *et al.*, 2001; Kennard *et al.*, 1996; Kim, 2001; Moroo *et al.*, 1999). Metals such as iron and zinc that bind to p97 have been shown to be able to nucleate the formation of insoluble β-amyloid from soluble amyloid (Bush *et al.*, 1994).

The soluble form of p97 can cross the BBB and deliver iron across the BBB more efficiently than Tf, if both are injected into the tail vein of the mouse (Moroo *et al.*, 2002). These results may be an indication that p97 functions in shuttling iron across the BBB from the blood to the neuropil, transporting the iron needed for normal brain function. How p97 is regulated in reactive microglia and how its function in metal

transcytosis interplays with its elevation in bodily fluids of Alzheimer disease patients is currently being investigated.

IV. Proteins involved in iron uptake

A. Transferrin receptor 1

The transferrin receptor 1 (TfR1) is a protein that functions to uptake iron into cells through a tightly regulated process. The TfR1 gene is found on chromosome 3q26.2 and consists of 19 exons (Evans and Kemp, 1997). It is highly expressed on rapidly dividing cells including immature erythroid cells and placental tissue. Many nonproliferating cell types also express TfR1, including hepatocytes, endothelial cells of the BBB, reticulocytes and sertoli cells (Jefferies *et al.*, 1984; Kuhn *et al.*, 1990).

Transferrin receptor 1 is a Type II membrane protein with a 61 residue N-terminal cytoplasmic domain, a 28 residue domain that crosses the membrane once, and a 671 amino acid extracellular C-terminal domain. The TfR1 possesses three domains called the apical domain, protease-like domain, and helical domain (Lawrence *et al.*, 1999) (See Figure 1.2). Electron cryomicroscopy studies have shown that the binding domain is separated from the membrane by a stalk of about 2.9 nm while the dimensions of the globular binding domains are approximately 6.4 nm high, 10.5 nm across the homodimer, and 7.5 nm deep (see Figure 1.2) (Fuchs *et al.*, 1998). The receptor undergoes post-

Figure 1.2: Model of the transferrin receptor 1 complex. The TfR1 complex is shown with transferrin (Tf) bound to one lobe of the TfR1 homodimer. HFE and β2 microglobulin (β) interact with one half of the TfR1 homodimer. Each half of the TfR1 has three domains, labeled H, A, and P for helical, apical, and protease-like, respectively. HFE has three domains termed α1, α2, and α3. The TfR1 has three sites of N-linked glycosylation (n) at N251, N317, and N727, and one O-linked site (o) at T104 (Lawrence *et al.*, 1999; Lebron *et al.*, 1998).

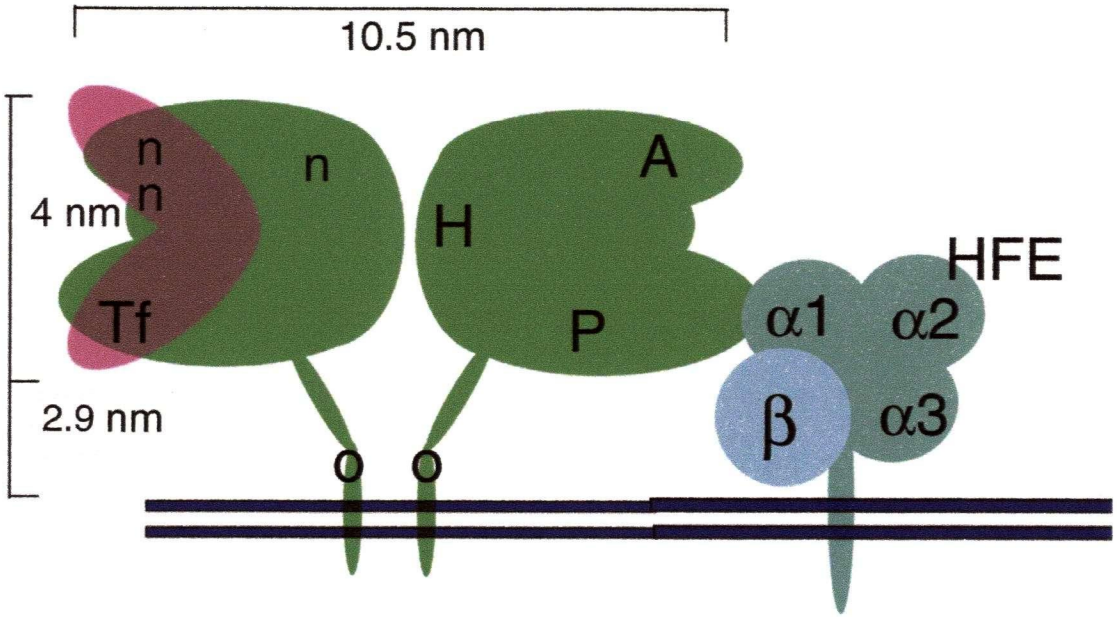
10.5 nm
4 nm
2.9 nm
n
n
n
Tf
H
A
P
HFE
α1
α2
β
α3

translational modifications including N and O-linked glycosylation as well as phosphorylation. Recombinant receptors lacking all three asparagine-linked (N-linked) glycosylation sites show decreased transferrin binding, while mutations that eliminate phosphorylation of the cytoplasmic serine residue do not seem to have any effect on receptor internalization efficiency (Rothenberger *et al.*, 1987b; Williams and Enns, 1991). A tyrosine based internalization motif (tyrosine, threonine, arginine, and phenylalanine at positions 20 - 23) is present in the cytoplasmic portion of the protein. Through mutational studies, this motif has been demonstrated necessary for endocytosis of the receptor (Collawn *et al.*, 1993).

The TfR1 functions as a homodimer with two disulfide bonds formed between the cysteines at positions 89 and 98 (Jing and Trowbridge, 1987). Each of the two C-terminal lobes of one TfR1 homodimer can bind one Tf protein in a pH-dependent manner. The binding affinity of the TfR1 for Tf is dependent on the iron binding state of the Tf: the highest affinity at physiological pH is seen between diferric Tf and TfR1, and the lowest for apo-Tf (Young *et al.*, 1984). The residues involved in Tf binding to the TfR1 have not been fully characterized, although Lawrence and associates have produced a model based on crystal structure analysis that proposes that Tf interacts with all three domains of the TfR1 (apical, protease-like and helical) (see Figure 1.2) (Lawrence *et al.*, 1999). The interaction of the TfR1 with HFE also seems to have an impact on Tf binding. Studies are underway in the Bjorkman laboratory to try to identify residues that are important for either binding to HFE or binding to Tf, but not both, in order to better understand the binding interactions (personal correspondence).

Mutational studies have shown that pH-dependent binding is a key component in the Tf /TfR1 recycling pathway, as the TfR1 strongly binds Tf saturated with iron at the pH of plasma (Kd ~ 10^{-7} to 10^{-9} mol/litre). The complex is then internalized via receptor mediated endocytosis in a clathrin coated pit and routed to the endosome, where the lower pH allows Tf to release iron. In fact, iron is released from Tf at a low pH faster and more efficiently when the Tf is complexed with the TfR1 than if Tf is unbound, demonstrating that the interaction with the TfR1 enhances iron release (Bali *et al.*, 1991; Sipe and Murphy, 1991). Following iron release, the complex is recycled back to the cell surface, where the apo-Tf is released and replaced by holo-Tf.

In order to study the physiological role of the TfR1, Levy and associates have created a knockout mouse lacking the TfR1 (Levy *et al.*, 1999). Transferrin receptor 1 -/- mice die by embryonic day 12.5. Moreover, embryos from embryonic day 8.5 to 12.5 demonstrate growth retardation, pericardial effusions, and severe pallor, while histological analysis shows edema and diffuse necrosis throughout the tissues (Levy *et al.*, 1999). As late as embryonic day 10.5, however, some TfR1 -/- mice are indistinguishable from wild-type mice, and do not show visible signs of anemia although they do not survive past day embryonic day 12.5. Both the anemic and non-anemic TfR1 -/- mice have defective erythropoiesis and abnormal development of the nervous system, exhibiting kinking of neural tubes. Levy and associates speculate that the reason the observed phenotype for the TfR1 knock-out mice is more severe than that of the hypotransferrinemic mice (mice with little or no transferrin) is that if Tf is missing from serum, unchelated iron is present and available for use in cells via an alternate iron uptake system. In the TfR1 knockout mice, in contrast, the vast majority of iron is bound to

serum Tf, making it unavailable for use because the receptor is not present to internalize the Tf.

Regulation of TfR1 expression is complicated and occurs at both the transcriptional and post-transcriptional levels. A region of 100 base pairs upstream of the transcriptional start site is involved in driving basal and serum/mitogenic stimulation of the *TfR1* promoter activity via an "AP-1 like" site (Casey *et al.*, 1988; Miskimins *et al.*, 1986; Owen and Kuhn, 1987). "AP-1/CREB like" (cyclic adenosine monophosphate response element binding protein) factors have been shown to bind to the "AP-1 like" site of TfR1 (Beard *et al.*, 1991; Lok *et al.*, 1996). The TfR transcriptional control element specific complex (TRAC), which is a nuclear protein that co-purifies with the Ku autoantigen, binds specifically to the transcriptional control element TRA (TfR transcriptional control element) of the *TfR1* gene (located at nucleotides –77 to –70 and necessary for increased expression in proliferation) (Roberts *et al.*, 1994). Differentiating erythroid cells exhibit specific up regulation of TfR1 transcription linked to both the Ets-binding site (transforming-specific protein produced by the *ets* gene, first discovered in the E26 avian erythrobastosis virus) and the AP-1 (activator protein-1) binding site in the 5' flanking region of the transcription start site (Sieweke *et al.*, 1996). Lok and Ponka have shown that a region (–118 to +14) of the *TfR1* promoter is necessary for erythroid differentiation induced promoter activity, and that mutation of EBS or the "AP-1/CREB-like" motif inhibit this inducible promoter activity (Lok and Ponka, 2000). Furthermore, they found that "CREB/ATF-like" factors and "Ets-like" factors bind to the identified element. Lok and Ponka also describe an element in the promoter region of the TfR1 that is responsive to hypoxia. This region contains a binding site for hypoxia inducible factor

1 and the motif organization is similar to that of many hypoxia inducible genes such as erythropoietin and ceruloplasmin (Lok and Ponka, 1999).

Post-transcriptional regulation of the TfR1 is mediated by the binding of iron regulatory proteins to the five IREs in the 3' untranslated region of the TfR1 mRNA. When cellular iron levels are low, the IRPs can bind to the IREs, thus stabilizing the transcript and allowing more TfR1 to be translated (Mullner and Kuhn, 1988). This elegant system regulates several of the proteins involved in iron metabolism, allowing coordinated expression of the proteins involved in the pathway. Another post-transcriptional control of TfR1 expression has recently been identified. Koeffler and associates have carried out experiments on cells with TfR1 without the 3' untranslated region (Tong *et al.*, 2002). The level TfR1 in these cells is increased when the cells are treated with desferroxamine (an iron chelator), even though the iron regulatory proteins can not bind to the transcript to stabilize it and increase protein expression level. The amount of transcript was not elevated, and the stability of the protein was unchanged. Transferrin receptor 2, which does not show iron-sensitive expression, was engineered with its 3' untranslated region replaced with that of TfR1. The addition of the transcript with the iron responsive elements made the expression increase about two-fold with the addition of desferroxamine. With TfR1, the observed increase is five-fold, indicating that the difference in responses is likely due to some RNA-independent method of regulation of TfR1 expression. This new method of iron dependent regulation of TfR1 expression needs to be examined further.

Transferrin receptor 1 is also detectable as a soluble protein in serum, and is measured clinically to help differentiate between iron deficiency anemia and chronic

disease anemia. The amount of soluble TfR1 in the blood correlates with the amount of erythropoiesis, thus indicating that the cleavage of TfR1 may be the method for reducing the amount of TfR1 when the red blood cell precursors differentiate into mature cells (Cook *et al.*, 1993; Nair *et al.*, 1990). The soluble form of the TfR1 is the result of a proteolytic cleavage at the arginine at amino acid position 100 near the transmembrane domain in the extracellular portion of the protein, which occurs during transit through the endosomal pathway, after presentation at the cell surface (Rutledge *et al.*, 1994; Shih *et al.*, 1990). The receptor is found in the serum as a homodimer that is lacking the disulfide bonds of the cell surface form.

B. HFE

HFE is a protein that seems to have a substantial impact on the regulation of iron absorption and the uptake of iron into cells. The *HFE* gene was identified by Feder and associates in 1996 and maps approximately 4 megabases telomeric to the *HLA-A* gene on chromosome 6 (Feder *et al.*, 1996). HFE, a major histocompatibility complex class I-like protein, was originally found expressed in the gastrointestinal tract and placenta (Parkkila *et al.*, 1997a; Parkkila *et al.*, 1997b). More recently, it has been found in tissue macrophages as well as circulating monocytes and granulocytes (Parkkila *et al.*, 2000). In the duodenum, HFE is expressed primarily in crypt cells, but there is very little HFE expressed in villus enterocytes (Parkkila *et al.*, 1997b).

The HFE protein forms a heterodimer with beta 2 microglobulin (β_2m) and the two proteins together form a complex with the TfR1 at the cell surface (See Figure 1.2) (Feder *et al.*, 1997; Lebron *et al.*, 1998; Parkkila *et al.*, 1997a; Waheed *et al.*, 1997). The

wild type HFE protein seems to have a significant effect on the uptake of Tf and iron by the TfR1 endocytosis pathway. Over-expression of HFE in transfected human hepatoma cells results in an approximately 50% decrease in receptor mediated Tf-iron uptake (Ikuta *et al.*, 2000; Roy *et al.*, 1999). An increase in the dissociation constant from 1.9 to 4.3 nM is also observed, indicating a decrease in the affinity of TfR1 for Tf in the presence of HFE (Ikuta *et al.*, 2000). It is not clear what the physiological significance of this decrease in affinity would be as the concentration of diferric Tf in blood is high enough to saturate all TfR1s, despite the presence of HFE (Ikuta *et al.*, 2000). The overexpression of HFE also seems to slow the rate at which the TfR1 complex recycles to the cell surface (in hepatoma cells), and this may lead to a decrease in iron uptake by the cell (Ikuta *et al.*, 2000). Expression of HFE in HeLa cells has been associated with a decrease in the intracellular iron pool, a decrease in the amount of ferritin translated due to a 5 fold increase in IRP binding, and a shift in the ratio of IRP1 to IRP2 in the cells (Roy *et al.*, 2002).

HFE, through the analysis of the knockout mouse phenotype, has been shown to be responsible for the most common type of hereditary hemochromatosis (HH) (Zhou *et al.*, 1998). Hereditary hemochromatosis is a disease of iron overload, and is the most common autosomal recessive disorder in persons of European descent. The prevalence of HH has been estimated at 1 in 200 to 1 in 400, with a carrier rate of between 1 in 7 to 1 in 10 in Caucasian populations (Bulaj *et al.*, 1996; Burke *et al.*, 1998; Crawford *et al.*, 1998; George *et al.*, 1998; Goldwurm and Powell, 1997; Jazwinska and Powell, 1997; Ramm *et al.*, 1997). The disease is characterized by a 2- to 3-fold increase in dietary iron absorption that leads to iron deposition in parenchymal cells of the liver, joints, pancreas,

heart, skin and pituitary gland. Prolonged iron deposition may lead to fibrosis and organ failure, frequently including hepatic cirrhosis, diabetes mellitus, cardiac dysfunction, arthritis and hypogonadism (Adams and Chakrabarti, 1998; Bacon *et al.*, 1999; Burke *et al.*, 1998; Cullen *et al.*, 1997; Niederau *et al.*, 1996; Niederau *et al.*, 1985).

The majority of patients with HH are homozygous for a cysteine to tyrosine mutation at amino acid residue 282 in the HFE protein (Feder *et al.*, 1996). This mutation has been shown to prevent β_2m from associating with the HFE protein, thus HFE is not expressed at the cell surface or associated with the TfR1. The mutant form of the protein is localized intracellularly, and colocalizes with calnexin, indicating that the protein may be retained in the endoplasmic reticulum and golgi due to improper folding (Ramalingam *et al.*, 2000). The mechanism by which this *HFE* mutation leads to deregulation of controls on iron absorption and thus a large increase in dietary iron uptake is under debate. Presumably, HFE must play a significant role in the iron absorption pathway, possibly in the "programming" of crypt cells. *HFE -/-* mice show increased expression of duodenal DMT-1, which supports the idea that *HFE* mutations in HH may lead to a decreased level of crypt cell iron. The crypt cell senses a decreased level of body iron and this prompts the cell, once it matures into a villus cell, to express increased levels of DMT-1 leading to increased dietary iron absorption (Fleming *et al.*, 1999). If the crypt cell originally senses abundant iron, then the level of DMT-1 expressed by the mature villus cell will be low.

In a recent publication, Townsend and Drakesmith hypothesized that the main role of HFE may be in programming of crypt cells through inhibiting the export of iron, rather than slowing the uptake of iron (Townsend and Drakesmith, 2002). In this theory,

they suggest that the binding of HFE to TfR1 is competed for by holo-Tf, so that when there is an abundance of iron loaded serum Tf, the HFE is displaced from the TfR1 complex and is available to interact with the iron export protein ferroportin. This interaction then inhibits the release of iron from the crypt cells (thus increasing overall iron stores within the cell). In effect this programs these cells to absorb less iron from the diet. This theory has yet to be proven experimentally.

Levy and associates have created HFE knockout mice and bred them with other strains of mice that have mutations in their iron uptake or metabolism (Levy *et al.*, 2000). One interesting mouse cross was between the *HFE -/-* and *β_2m -/-* mice. The absence of β_2m and HFE lead to a more severe iron overload phenotype than in the *HFE* knockout mice alone. A possible explanation is that the compromising of the immune system that results from the absence of *β_2m -/-* itself leads to a more severe iron overload phenotype.

Another set of crosses demonstrated that the iron overload observed in HH due to an *HFE* mutation is mediated through the DMT-1/ hephaestin pathway. When *HFE* knockout mice were crossed with *mk* (microcytic anemia) mice, which are characterized by a loss of function in DMT-1, the mice resembled the *mk* phenotype rather than the iron overload phenotype characteristic of the HFE knockout, resulting in extremely low iron stores (Levy *et al.*, 2000). This indicates that iron uptake in HH is probably mediated through a pathway involving DMT-1. Mice bred to possess a loss of function mutation in both *HFE* and hephaestin, a protein necessary for basolateral iron transport out of intestinal microvilli cells, also exhibit a decrease in iron loading in the liver. However, this did not lead to a complete block in iron transfer from enterocytes.

When *HFE* knockout mice are bred with *TfR1* heterozygotic mice, the animals have a more severe iron loading phenotype in hepatocytes than the *HFE* mutants alone. Levy and associates have hypothesized that this apparent contradiction occurs because the *TfR1* +/- mice have small erythrocytes with less hemoglobin than normal due to a decreased level of TfR1 (Levy *et al.*, 2000). This leads to an even greater increase in dietary iron absorption, possibly via an "erythroid signal", which leads to an increase in dietary iron absorption and compensates for the erythroid iron deficiency. Much work has yet to be done in order to discover what role HFE plays in iron absorption regulation, and to further illuminate the effect HFE has on the Tf /TfR1 pathway.

C. Transferrin receptor 2

Transferrin receptor 2 (TfR2) is a recently identified member of the transferrin receptor family (published first by Kawabata et. al., but simultaneously identified by others including this investigator.) The extracellular portion of this type II membrane protein shares 45% identity and 66% similarity with the TfR1 (Kawabata *et al.*, 1999). Two splice forms have been discovered: the α form which has a transcript size of approximately 2.9 kb, and a shorter (2.5 kb) β form which lacks the N-terminal portion of the protein. The shorter transcript probably encodes an intracellular protein as both the transmembrane and signal sequences are missing. Transferrin receptor 2 has a putative tyrosine based internalization motif (tyrosine, glutamine, arginine, and valine) similar, although not identical to that of the classical TfR1 (tyrosine, threonine, arginine, and phenylalanine) (Kawabata *et al.*, 1999). As well, two cysteine residues are present (109 and 112) in approximately the same location as those of the TfR1 (89 and 98) that may

allow the formation of disulfide bridges, however, this remains to be demonstrated experimentally. West and associates have shown that a recombinant TfR2 binds iron loaded Tf with a 25-fold lower affinity than TfR1, and that HFE can not be co-immunoprecipitated with TfR2 as it can with the TfR1 (West *et al.*, 2000).

As with HFE, a form of HH has been linked to the *TfR2* gene. Camaschella and associates found a cytosine to guanosine transversion in exon 6 of TfR2 (position 750 of the cDNA) causes a truncation of the extracellular portion of the protein (a stop codon replaces a tyrosine at residue 250) (Camaschella *et al.*, 2000). It is unclear why this particular truncation, in which the Tf binding portion of the TfR2 protein is removed, should lead to an iron overload phenotype. Further characterization of the role of TfR2 in iron metabolism is needed.

Fleming and associates have demonstrated that the 3' untranslated region of the murine TfR2 is significantly shorter than that of TfR1, and does not contain any regions similar to the consensus sequences of iron responsive elements (Fleming *et al.*, 2000). An examination of the hepatic expression of mouse TfR1 and TfR2 in iron overload supports this lack of iron regulation. A mouse model of HH shows down-regulation of mouse TfR1 mRNA in the HH model mice, while no such down regulation occurs with mouse TfR2 (Fleming *et al.*, 2000). It was recently demonstrated that Chinese Hamster Ovary (CHO) cells transfected with TfR2 are resistant to the iron deprivation effects of desferroxamine (an iron chelator), which suggests that TfR2 has the ability to increase the cellular iron pool and support cell growth, in the same manner as TfR1 does (Kawabata *et al.*, 2000). In addition, it was speculated that perhaps TfR2 is a lower affinity form of the

TfR1, and could in fact be a more primitive form, as TfR2 seems to be more closely related to the prostate specific membrane antigen than TfR1.

D. Stimulator of iron transport

The stimulator of iron transport (SFT) protein is a Tf-independent iron transporter that was originally identified using *Xenopus laevis* oocytes (Gutierrez *et al.*, 1997). The SFT protein is a 338 amino acid integral membrane protein with at least six membrane spanning regions (Yu and Wessling-Resnick, 1998). It is able to form a dimer, suggesting similarity to the 12 membrane spanning domains of DMT-1, and is localized to the plasma membrane and endosomal vesicles. The transcript for SFT is expressed in a number of tissues including spleen, duodenum, colon, liver, kidney, heart, brain, and peripheral blood leukocytes (Gutierrez *et al.*, 1997; Knutson *et al.*, 2001). The SFT contains an REXXE motif that is similar to the iron binding motif of ferritin, and it has been shown in HeLa cells to stimulate both Tf-dependent and independent iron uptake (Gutierrez *et al.*, 1997).

The mechanism of iron transport utilized by SFT remains unknown, however the expression of the protein does seem to be dependent upon intracellular iron levels. For instance, treatment of HeLa cells with desferroxamine, which depletes iron from the cell, leads to an increase in the SFT transcript (Yu *et al.*, 1998). The mechanism for this iron dependent-response is unknown, since no IRE has been identified. Furthermore, liver samples from patients with HH have a 5-fold higher level of the SFT transcript, compared to liver samples from control subjects (Yu *et al.*, 1998). In contrast, *HFE* knock-out mice do not show increased levels of the SFT mRNA (Knutson *et al.*, 2001).

V. Hypothesis and general approach

This research aims at identifying and characterizing a receptor for the soluble form of the p97 iron transport protein. The guiding hypothesis is that the soluble p97 binds specifically to a receptor and this receptor-ligand interaction leads to iron delivery to cells. A function has not yet been established for p97, although it is known that the GPI-linked, cell surface expressed form binds and internalizes iron, and can deliver that iron to the iron storage protein ferritin (Kennard *et al.*, 1995; Tiong, 2001). It should be noted that the soluble form of p97 is not a cleavage product of the GPI-form, but likely a splice variant (Food *et al.*, 1994). Since p97 resembles many of the other members of the Tf family, and as many of these members are in fact ligands for receptors, it seems reasonable that the soluble version of p97 also has a receptor and functions as a ligand. To determine the identity of this receptor, the most reasonable place to begin was with an examination of the receptor for Tf, the closest homologue of p97. Transferrin receptor 1 is located in many tissues throughout the body and is able to bind and internalize Tf with high affinity, as well as enable the iron carried by the Tf to remain in the cell while Tf itself is recycled back to the cell surface and released.

The first results chapter examines the hypothesis that soluble human p97 binds to the human TfR1, and that iron bound to the p97 can be delivered to the cell via this receptor-mediated mechanism. Initially, the general approach was to compare binding of the human p97 protein in two cell lines: one without TfR1, and one expressing human TfR1 on the cell surface. The difference in binding and iron uptake between the two cell lines is thus assumed to be due to p97 binding to the receptor. Various assays were performed to examine cell surface binding, including iodination of the p97, and

immunofluorescent labeling and Pandex assay. In addition, binding between soluble human TfR1 and p97 was measured in a surface plasmon resonance study (or BIAcore). For all of these assays, human Tf binding to TfR1 was measured as a positive control for the assays. To examine uptake of iron via p97, the total amount of radioactive iron taken up by the two cell lines was compared, as well as the amount of ^{55}Fe associated with immunoprecipitated ferritin in the two cell lines and measured using a scintillation counter.

A second hypothesis in the chapter 3 is that a different type of receptor exists for p97, namely integrin $\alpha V\beta 3$. This interaction was examined because p97 has a three amino acid motif, consisting of an arginine, glycine, and aspartate (referred to as an RGD motif). The RGD motif has been identified as an essential part of the recognition motif for a family of integrins. By comparing the p97 sequence to the available crystal structure of Tf, the RGD motif is likely exposed on the surface of p97. One prominent member of this heterodimeric family is integrin $\alpha V\beta 3$, which also binds the widest variety of ligands (Xiong *et al.*, 2001). For this reason, the interaction between the soluble p97 and a soluble engineered version of the heterodimeric integrin was measured by BIAcore.

To identify other receptors that may bind p97, homologues of the TfR1 were pursued. Database searches for proteins similar to the TfR1 led to the discovery of TfR2. This novel receptor, which was simultaneously discovered by Kawabata and associates, is extremely similar to the classical TfR1, with the mouse version sharing 40% identity with the mouse TfR1. The second results chapter begins with experiments aimed at characterizing a number of features of the TfR2, including the sequence, the expression

during development, as well as subcellular and tissue localization. Some features of the two receptors are similar, though TfR2 is in many ways unique from TfR1. Specifically, the endocytosis and subcellular localization of the transferrin receptors are similar, but the tissue expression patterns are distinct. To examine some characteristics of the TfR2 that complement the published data, many approaches were utilized. First the entire mouse sequence of TfR2 was obtained through the technique of "primer walking". Northern blot analysis was employed to examine both embryological expression in the developing mouse, and adult tissue expression in the human. To examine brain microvascular expression, the reverse-transcriptase polymerase chain reaction was carried out on RNA isolated from primary brain microvasculature. In addition, to study subcellular localization, immunofluorescence and confocal microscopy were used. The two receptors were also examined in the context of a cell line that expresses both TfR1 and TfR2, through immunoprecipitation and Western blotting, to see if they interact to form heterodimers.

Finally, the second results chapter also examines the hypothesis that p97 binds to TfR2 and that ^{55}Fe bound to p97 is transported into cells via TfR2. To examine this hypothesis, the approach was similar to that of results chapter 1. Cells transfected with mouse TfR2 were incubated with radioactive-iron loaded p97 and then the amount of iron within the cells compared. The difference in iron uptake between the two cell lines is deemed to be due to TfR2 mediated uptake. The model of p97 binding to the TfR2 and depositing iron within cells via this receptor was developed based on these results.

As a whole, the results substantially advance our understanding of the new iron transport receptor TfR2, and support a possible explanation for an additional iron uptake pathway via p97 in certain cells.

Chapter 2: Materials and methods

I. Cells and antibodies

Many different cell lines were used during the experiments contained in this thesis. The main group of cells is derived from Chinese Hamster Ovary (or CHO) cells. The parental CHO line was obtained from American Tissue Type Culture Collection (ATCC, Manassas, VA). TRVb cells are a CHO line that does not internalize Tf and thus has no functional transferrin receptors expressed (McGraw *et al.*, 1987). The phenotype arose as a spontaneous mutation and was selected with ricin A conjugated to transferrin. TRVb cells were then transfected with the constructs pCDTR1 and pSV3Neo (to confer G418 resistance) to produce TRVb-1 that expresses functional human TfR1. These cells were the kind gift of Dr. F. Maxfield from New York University. For clarity, TRVb cells from this point on will be referred to as transferrin receptor minus, or TfR-, and TRVb-1 cells will be labeled transferrin receptor plus or TfR1+. The TRVb cells were also transfected with a pcDNA3.1 vector containing a *myc* tag and mouse TfR2 (alpha form) using FuGENE 6 (Gibco). This cell line will be referred to as mTfR2+. Some experiments also use a parental CHO cell line transfected with the same mTfR2 vector (CHO-mTR2). The media used to grow the mTfR2+ and the CHO-mTfR2 cells also contained 1000 μg/ml G418 to maintain the expression of the TfR2. The TRVb transfected with human TfR2 (TfR2+), and TRVb-1 transfected with human TfR2 (TfR1,2+ respectively) were a gift from Dr. Caroline Enns, of the University of Oregon.

All the CHO derived cell lines are maintained in Ham's F12 media (Invitrogen Life Technologies Inc., Burlington, ON) with 10% (v/v) fetal bovine serum (Invitrogen

Life Technologies Inc.), 2 mM glutamine (Invitrogen Life Technologies Inc.), 20 mM HEPES (Sigma-Aldrich Canada Ltd), pH 7.4, at 37 ° C in a 5% CO_2 humidified incubator.

A human melanoma cell line called SK-MEL 28 (from ATCC) was transfected with the mTfR2 *myc*-tagged construct pcDNA3.1 in order to examine TfR2 localization in a human cell line. The SK-MEL 28 cells were grown in DMEM medium (Invitrogen Life Technologies Inc.), supplemented with the same conditions as above for Hams F12. The human erythroid leukemia cell line K562 (ATCC), which naturally expresses high levels of human TfR2, was also maintained in this DMEM media.

Primary human brain endothelial cells were obtained as a kind gift from Dr. Dorovini-Zis (Vancouver General Hospital). They were cultured in M199 medium (Invitrogen Life Technologies Inc.) supplemented with 10% heat inactivated horse serum (Sigma Chemical Co., St. Louis, MO), 10 μg/ml endothelial cell growth supplement (Collaborative Biomedical Products, Bedford, MA), 5 μg/ml insulin, 5 μg/ml Tf and 5 ng/ml selenium (ITS Premix, Collaborative Biomedical Products), and 600 USP units/l of heparin (Sigma).

The primary and secondary antibodies used in this thesis are listed in Table 2.1 and 2.2 respectively.

II. Binding of ^{125}I-p97 and ^{125}I-transferrin to transferrin receptors 1 and 2

A. Iodination of proteins

The iodination of the proteins was carried out using the Chloramine T (Sigma Aldrich) method. Equal volumes of p97 (provided by Synapse Technologies Inc.,

Table 2.1: Primary antibodies

Antibody	Antigen	Host	Isotype	Concentration	Source
Hyb C	p97	mouse	IgG1	1 mg/ml	Dr. Shuen-Kuei Liau, McMaster
L235	p97	mouse	IgG1	15 mg/ml	ATCC
Transferrin-FITC	Human transferrin	sheep	IgG	9.7 mg/ml	ICN Biomedicals
Transferrin	Human transferrin	mouse	IgG1	35 mg/ml	Cedarlane Laboratories
OKT9	Human TfR	mouse	IgG1	12 mg/ml	ATCC
Anti-Transferrin receptor	Transferrin receptor (for Western blotting)	rabbit	-	-	Gift from Dr. I. Trowbridge, Salk Institute
Anti-c-myc clone 9E10	Residues 410-419 of human c-myc	mouse	IgG1	-	Sigma
EEA-1	Amino terminal human EEA-1	Goat	-	200 μg/ml	Santa Cruz Biotechnology
Clathrin HC	Carboxy terminal of human clathrin heavy chain	rabbit	-	200 μg/ml	Santa Cruz Biotechnology
Anti-FLAG M2	Flag sequence	mouse	IgG	3.5 mg/ml	Sigma
Anti-FLAG M5	N-terminal Met-FLAG fusion proteins	mouse	IgG	3.5 mg/ml	Sigma
Ferritin	Human ferritin L-chain	rabbit	-	1.3 mg/ml	DAKO, Carpinteria CA.

Table 2.2: Secondary antibodies

Antibody	Concentration	Dilution Used	Source
Goat anti-mouse FITC	1 mg/ml	1:1000	Jackson Immunoresearch Laboratories Inc., West Grove, PA.
Alexa 488 nm conjugated Goat anti-mouse IgG	2 mg/ml	1:1000	Molecular Probes Inc., Eugene, OR
Alexa 488 nm conjugated rabbit anti-mouse IgG	2 mg/ml	1:500	Molecular Probes Inc.
Alexa 568 nm conjugated rabbit anti-goat IgG	2 mg/ml	1:500	Molecular Probes Inc.
Alexa 568 nm conjugated goat anti rabbit IgG	2 mg/ml	1:500	Molecular Probes Inc.
Peroxidase conjugated goat anti-mouse IgG	0.8 mg/ml	1:10,000	Jackson Laboratories Inc.
Peroxidase conjugated goat anti-rabbit IgG	0.8 mg/ml	1:10,000	Jackson Laboratories Inc.

Vancouver, BC) or human Tf (Sigma) and 0.5 M phosphate buffer at pH 7.4 (20 μl) were mixed together followed by 1 mCi NaI^{125} (10μl). To this mixture, 20 μl of freshly prepared Chloramine T (2.25 mg/ml in phosphate buffer) was added and kept at room temperature for one minute. Next, 20 μl of sodium-metabisulfate (7mg/ml sodium metabisulfate in 0.5M phosphate buffer) was added and again allowed to sit for one minute. Finally, 100 μl of NaI (15 mM) was added, and the entire mixture was passed with 20 ml PBS + 1% bovine serum albumin (BSA) through a Sephadex G-25 column (Amersham). The eluate was collected in 1 ml fractions.

A TCA (trichloroacetic acid) precipitation was carried out to determine the amount of labeling of the proteins as follows: Two microlitres of the labeled solution was added to 200 μl of 1% BSA in PBS. To this, 200 μl of 10% TCA was added and mixed, followed by centrifugation in a microfuge at maximum speed for 10 minutes. The supernatant was then transferred to a new eppendorf tube and both the supernatant and the pellet tubes were counted in the gamma counter. The counts per minute of the supernatants represent the non-TCA precipitable counts (or non-protein bound counts), while the counts per minute of the tubes with the pellets represent the TCA precipitable counts (or the counts bound to p97 or Tf).

B. Binding to transferrin receptors

The binding experiment was carried out in the following manner: TfR positive (TfR+) and TfR negative (TfR-) cells were harvested from tissue culture plates with Versene (5.37 mM disodium EDTA, 1.37 M NaCl, 26.83 mM KCl, 81,01 mM Na_2HPO_4, 14.7 mM KH_2PO_4, 11.1 M glucose). The cells were counted with a hemocytometer and

aliquoted into BSA-treated tubes at one million cells per tube. The 5 ml polystyrene tubes were first coated with a PBS solution containing 5% BSA to reduce the amount of protein binding to the tubes, and thus reduce background counts. Following this step the cells were briefly acid washed with a mixture of 2.6 ml 0.1 M glycine buffer (0.1 M glycine, 0.05 N HCl, 10 mM NaCl), 5 ml DMEM serum free tissue culture media, and 182 μl 1 M NaCl. Each tube of cells was kept on ice and washed three times with 1 ml of the acid wash, followed by three washes with PBS. The radioactive protein was then added to the serum free media mixture and incubated with the cells for one hour at 4°C, followed by two washes with ice-cold PBS+ 1% BSA. The cell bound counts were then determined in the gamma counter. The pH of the incubation mix was monitored and adjusted with 1 N HCl to be either pH 6.0 or pH 7.0. When competition experiments were carried out, the iodinated protein was first mixed with the unlabeled protein, then added to the cells, thus the cells were exposed to the radioactive and non-radioactive protein at the same time.

III. Pandex experiments

For the non-radioactive experiments, a Pandex Fluorescence Concentration Analyzer (Idexx, Westbrook, Maine) was used to measure the fluorescence of the cells in a specialized 96 well plate. The plate has a 0.22 μm cellulose acetate membrane rather than a solid bottom, to allow the wells to be drained under vacuum. This enables the washing of the cells to take place rapidly without removing the cells from the plate, and allows removal of the supernatant without centrifugation.

For these experiments, the cells were washed three times in serum free Hams F12 media (with 2 mM glutamine, 20 mM HEPES, pH 7.4) and placed at 37°C in a 5% CO_2 humidified incubator for 20 minutes. The cells were then harvested with Versene, counted with a hemocytometer, and resuspended at 1.25 million cells per tube in 1 ml Pandex buffer (serum free DMEM media with 0.1% sodium azide and 1% BSA). The cells were then incubated for 45 minutes at 4°C with either 1 ml of Pandex buffer, 1 ml of 30 μg/ml human Tf in Pandex buffer, or 1 ml of 30 μg/ml human p97 in Pandex buffer. The tubes were then centrifuged for 5 minutes at 4°C at 1200 revolutions per minute in a Sorval benchtop centrifuge. The cells were placed on ice and washed with the addition of 1 ml of cold PBS with 0.1% sodium azide and 2 mg/ml BSA, and centrifuged as before. The final incubation involved the addition of fluorescein isothiocyanate (FITC) conjugated L235 or anti-Tf at a 1 in 75 dilution, for 45 minutes at 4°C followed by deposition of 40 μl of cells (approximately 250, 000 cells) into the wells of the Pandex plate. The Pandex plate was then placed in the Pandex reader where the cells were washed 3 times, with fluorescent readings taken between each wash.

For the FITC labeling of the antibodies, FITC was added at 1 mg/ml to phosphate buffer at pH 9.5 (0.15 M Na2HPO4) and then 0.5 ml of the antibody at 4 mg/ml was added to 0.15 ml of the FITC solution at 1 mg/ml, and incubated overnight at room temperature in the dark.

IV. Protein dialysis and iron loading

Both p97 (Synapse Technologies, Inc., Vancouver) and Tf (Sigma) were supplied with iron partially bound to the protein. A dialysis protocol developed by Aisen and

Leibman was employed (Aisen and Leibman, 1968; Aisen and Leibman, 1972) in order to rid the protein of this tightly held ligand, and produce apo-p97 or apo-Tf. In this procedure, the solublized protein was injected into a Pierce 10,000 MW dialysis cassette and dialyzed in 1 L of 0.1M sodium citrate buffer (pH 6.0) at 4°C for three hours, with buffer changes after each hour. Following this, the protein was transferred to a new cassette and then dialyzed for four hours (with three buffer changes) in 0.1 M sodium perchlorate, and 25 mM HEPES at pH 7.4 at 4°C. Finally, the protein (using the same cassette) was dialyzed for three hours (with two buffer changes) in 25 mM HEPES at pH 7.4 at 4°C. The protein was then removed from the dialysis cassette and concentrated in a Centricon-TM10 (Millipore, Bedford, MA), and the protein concentration was measured either by spectrophotometer readings at 280 nm (with an extinction coefficient of 1.214 for p97) or by BCA (bicinchoninic acid) protein assay (Pierce).

To load the protein with iron, the iron chloride (either radioactive or not) was first mixed at a ratio of 1:1 with nitrilotriacetate (1 M each) for 10 minutes at room temperature. Then the dialyzed apo-p97 or apo-Tf was mixed with the ferric nitrilotriacetate at 2 moles iron per mole of protein. The pH for this step must be around pH 7.4 for proper iron loading, so the protein may need to be diluted in HEPES buffer to compensate for the low pH of the ferric nitrilotriacetate solution, especially for ^{55}Fe, as it is supplied in concentrated HCl. The mixture was allowed to sit at room temperature for one hour before the excess iron was dialyzed out of solution in three changes of 25 mM HEPES for 3 hours at ph 7.4, at 4°C. The iron-loaded proteins undergo a color change, from colorless in the apo-form to slightly pink in the iron-loaded form.

V. Iron uptake studies

The method for radioactive iron uptake *in vitro* involved measuring the internalized radioactivity of the various TRVb cell lines transfected with the TfR1 or TfR2. The cells were grown in six well tissue culture plates (Nunclon) until approximately 80 to 90% confluence was reached. The plates were then washed three times, each for 30 minutes at 37°C with 5% CO_2 and humidity, with Hams F-12 serum free media plus 1% (w/v) BSA. After washing, the incubation mix containing either ^{55}Fe-loaded Tf or p97 in Hams F-12 serum free media with 1% BSA was added to the cells. After incubation at 37°C with 5% CO_2 and humidity for the appropriate amount of time, the cells were washed three times (on ice) with 4°C wash buffer (PBS with 1% BSA) and then harvested with Versene. Finally, the amount of ^{55}Fe was counted in the Beckman LS6000IS Liquid Scintillation counter.

VI. Immunoprecipitations

Immunoprecipitations were carried out on TRVb cells, with and without the TfR1. The cells were grown to approximately 90% confluence in tissue culture plates. The adherent cells were incubated three times for 20 minutes each time at 37°C with serum free Hams F12 media (with 2 mM glutamine, 20 mM HEPES, and 1% BSA at pH 7.4) in a 5% CO_2 humidified incubator. This step was designed to remove any residual bound bovine Tf, and to slightly iron starve the cells. The cells were then incubated with 1 ml ^{55}Fe-loaded p97 or Tf in serum free media for four hours at 37°C in a 5% CO_2 humidified incubator. After the incubation, the incubation mix was removed, the plates were washed with PBS, and the cells were lysed in 1 ml 1% (v/v) Nonidet-P40 (NP-40)

(ICN Pharmaceuticals Inc., Costa Mesa, CA) in lysis buffer (20 mM Tris-Cl pH 7.4, 150 mM NaCl, 2 mM EDTA and 1 tablet protease inhibitor cocktail (Roche)) for 30 minutes on ice. The lysate was then collected in an eppendorf tube and centrifuged in a Biofuge B microcentrifuge (VWR Canlab Mississauga, ON) at 11,000 rpm at 4°C for 10 minutes. The supernatant was then collected and 3 μl of normal rabbit serum was added. The tube was rotated at 4°C for an hour. Next, 30 μl of protein G sepharose (50% (v/v) slurry) (Amersham-Pharmacia Biotech, Piscataway, NJ) was added, followed by additional rotation at 4°C for an hour. The samples were then centrifuged at 11,000 rpm for 5 minutes at 4°C, and the supernatant transferred to a new eppendorf tube. The lysate was then divided into the appropriate number of samples, and the primary antibody added. Antibodies used were L235 (against human p97), polyclonal anti-human TfR1 (against classical tranferrin receptor), and anti-ferritin (against ferritin) (See Table 1). After an incubation at 4°C for at least one hour (up to overnight) the immuno-complexes were precipitated with protein G sepharose (30 μl), for up to one hour at 4°C with rotation. The protein G immuno-complexes were washed twice in ice cold buffer B (0.2% (w/v) NP-40, 10 mM Tris-Cl pH 7.5, 150 mM NaCl, 2 mM EDTA), each time followed by centrifugation at 4°C and suction of the supernatant. Next, the samples were washed once as above with Buffer C (0.2% (w/v) NP-40, 10 mM Tris-Cl pH 7.5, 500 mM NaCl, 2 mM EDTA) and once with Buffer D (10 mM Tris-Cl pH 7.5) before resuspension in 1 ml of PBS and transfer to scintillation vials. The vials had 5 ml of ReadySafe scintillation counting fluid (Beckman Coulter Inc., Fullerton, CA) added, and the disintigrations per minute were determined on a Beckman LS6000IS Liquid Scintillation counter.

The variation to this protocol involves the co-immunoprecipitation of the TfR 1 and 2 from the TRVb3 cells. In this case, no radioactivity was used. Instead, the cells were simply washed with PBS, then harvested as above. The protocol is the same as that above until the final step. Here, instead of placing the lysate in PBS and adding scintillation fluid, the beads were solubilized for an SDS-PAGE gel by adding 40 μl of Mix II (1 ml of Bromo Mix (36% (w/v) sucrose, 0.01% (w/v) bromophenolblue, 0.1 M Tris-Cl pH 8.8), and 200 μl Mix I (18% (w/v) SDS, 0.05 M dithiothreitol (DTT) (Roche)). The beads in Mix II were heated at 95 °C for 2 minutes, then cooled to room temperature for 5 minutes, followed by a brief spin. Then, 5 μl of 0.5 M iodoacetamide (IAA) (Sigma-Aldrich Canada Ltd.) was added and the samples were allowed to sit for 15 minutes before being loaded on a standard 10% (w/v) SDS-PAGE gel and electrophoresed at 150 V for 1 hour. Next, the gel was transferred to a nitrocellulose membrane (Bio-Rad Laboratories, Hercules, CA) by electroblotting. Following the transfer, the blotted membrane was blocked with a 5% (w/v) skim milk and 0.1% (v/v) Tween 20 (Biorad) in PBS for 1 hour (to overnight) and then the proteins were detected using antibodies against the TfR1 (1:100) or against the flag-tag on TfR2 (1:100). The blotted membrane was incubated with the antibody for 1 hour at room temperature or overnight at 4°C (both with shaking) and then washed for 3 times 30 minutes with the 5% (w/v) skim milk wash buffer. After the washes, the blotted membrane was incubated in peroxidase-conjugated goat anti-mouse or peroxidase-conjugated goat anti-rabbit (both at 1:10,000 dilution) in the skim milk buffer, followed by the same wash protocol used for the primary. The blots were then treated with the chemiluminescence ECL Western blotting detection system (Amersham Pharmacia Biotech) and exposed to x-ray film.

VII. Surface plasmon resonance (BIAcore) experiments

A BIAcore 2000 biosensor system (Pharmacia Biosensor, Uppsala, Sweden) was used to assay the interaction of p97 with $\alpha_v\beta_3$ integrin (kind gift of Alistair Henry of Celltech), vascular endothelial growth factor receptor 2 (VEGFR-2) (R&D Systems), and the TfR1 (kind gift of Pamela Bjorkman, California Institute of Technology). The extracellular domains of the α_v and β_3 subunits were linked at the C-terminal end to the Fc of mouse IgG1 to enforce heterodimerization .(Stephens *et al.*, 2000) The soluble version of the human TfR1 was generated through truncation at the C-terminal end, to remove the intracellular and transmembrane domains (Lebron *et al.*, 1998). The soluble TfR1was purified in the Bjorkman lab from supernatants of baculovirus-infected High 5 cells using Ni-NTA chromatography (Ni-NTA superflow; Qiagen) and followed by gel filtration chromatography with a Superdex-200 FPLC column (Pharmacia).

On the BIAcore sensor chip carboxymethylated dextran matrix (Sensor Chip CM5, Research Grade, BIAcore) was preactivated with N-hydroxysuccinimide/ N-ethyl-N'-[3-(diethylamino)propyl] carbodiimide according to the manufacturer's recommendations. All steps were carried out at room temperature.

For the experiments, random amine coupling of the p97 and $\alpha_v\beta_3$ integrin to the chip was achieved by subsequent injection of 10 μg/ml p97 in 10 mM sodium acetate at pH 4.5, and $\alpha_v\beta_3$ integrin at 50 μg/ml at pH 4.5. One cell on the chip was left blank to serve as a control, and the sensorgram generated was subtracted as a baseline from the experimental sensorgrams. To perform binding assays, samples of p97, $\alpha_v\beta_3$ integrin, or VEGFR2 were injected in Hepes buffer (10 mM Hepes, 150 mM NaCl, 0.005% polysorbate 20, 2 mM $MgCl_2$, 0.6 mM $CaCl_2$, pH 7.4). To regenerate the chip for the

experiments (between injections) a wash step was performed with 0.01 M Hepes at pH 7.4 with 3 mM EDTA.

For the TfR1 experiments, the TfR1 protein was coupled to the chip by flowing a 0.1 mg/ml solution in 3.46 mM maleate buffer at pH6.0 across the flow cell for various amounts of time. This yielded three flow cells with increasing amounts of protein coupling, and one blank flow cell with no bound protein. The iron-loaded p97 in this experiment was injected at 10 μl and 50 μl at pH 7.4, and the apo-p97 was injected at 50 μl at pH 6.0.

VIII. Northern blot analysis

The northern blots of multiple human tissues and mouse embryos, were both commercially prepared by Clontech Laboratories. The probes used were both prepared through polymerase chain reaction, followed by labeling with ^{32}P. The primers used to generate the cDNA that was labeled to make the probe are listed in Table 2.3. For probe labeling, 5 μl of gel-purified DNA probe (QIAEX II Gel Extraction Kit, Qiagen Inc., Mississauga, ON) was added to 4 μl sterile distilled water. This mixture was denatured by heating on a heat block to 100°C for five to ten minutes, followed by a quick chill in ice. Next, 1 μl each of dATP, dGTP, and dTTP was added, followed by 2 μl of reaction mixture (solution 6) (Random Primed DNA Labeling Kit, Roche). Finally, 5 μl of ^{32}P-dCTP and 1 μl Klenow enzyme was added and mixed by pipetting. The mixture was incubated at 37°C for 30 minutes. After the incubation, the unincorporated label was removed by eluting the probe through a G50 sephadex spin column. The ExpressHyb solution was prewarmed to 68°C, and the membrane was prehybridized in at least 5 ml of

warmed ExpressHyb solution (Clontech) for 30 minutes at 68°C with rotation. The probe was then added to the pre-warmed solution and incubated with the blot for at least 1 hr (to overnight) at 68°C with continuous rotation. After incubation, the membrane was rinsed in wash solution 1 (0.3 M NaCl, 0.03 M sodium citrate pH 7.0, 0.05% (w/v) sodium dodecyl sulfate) several times at room temperature, then washed for 30-40 minutes with constant shaking, and several solution changes. Next, the blot was washed with wash solution 2 (15 mM NaCl, 1.5 mM sodium citrate pH 7.0, 0.1% (w/v) sodium dodecyl sulfate) for about 30 minutes. The blot was shaken to remove excess liquid, then wrapped in plastic wrap without allowing the blot to dry (so that it could be stripped and reprobed). The blot was then exposed to x-ray film or a phosphoimager and developed.

To strip the blot, a solution of 0.5% (w/v) sodium dodecyl sulfate was heated to 90–100°C, then the membrane was added and incubated for 10 minutes with shaking. The solution was then allowed to cool for 10 minutes before removing the blot. The membrane was air-dried slightly before it was put in a plastic bag for storage.

IX. Reverse transcriptase and polymerase chain reaction

The RNA from various cell lines used for these experiments was isolated using the RNeasy Mini Kit (QIAGEN, Inc.) according to the manufacturer's instructions. To make the complementary DNA (cDNA), 5 μg of total RNA was used, along with 1 μl of oligo dT_{18}, and RNAse-free distilled water to make the volume 12 μl. This solution was heated to 70°C for 10 minutes, followed by a quick chill and centrifugation. Next, 4 μl of 5x first strand buffer, 2 μl 0.1 M dithiothreitol, and 1 μl 10 mM dNTP mix (10 mM of each dATP, dCTP, dGTP, dTTP) was added (Gibco). This was mixed gently at 42°C for

2 minutes. Finally, 1 μl Superscript II (Gibco) was added, the mixture was mixed up and down by pipetting, and then incubated at 42°C for 50 minutes. After incubating, the reaction was inactivated by heating to 70°C for 15 minutes, followed by the addition of 1 μl of RNase H (Gibco) and incubation at 37°C for 20 minutes.

The polymerase chain reactions to create probes and to ascertain experession in brain endothelial cells were carried out in a UNOII or Tgradient thermocycler (Biometra), using primers made by Sigma (see Table 2.3).

X. Immunofluorescence staining and confocal laser scanning microscopy

The adherent cells were grown on sterile coverslips (No. 1, 18 mm, Fisher Scientific Inc.) to approximately 60 to 80% confluence. The coverslips were washed gently twice with PBS, then blocked for 1 hour in 2% (w/v) BSA in PBS. The cells were then fixed for 20 minutes in 2% (w/v) paraformaldehyde in PBS, and permeabolized with 0.1% (w/v) saponin in PBS with 2% (w/v) BSA. The coverslips were stained with 200 μl primary antibody, diluted in the appropriate amount of PBS with 2% (w/v) BSA (see Table 2.1) for 30 minutes at room temperature with gentle shaking. Control coverslips were incubated with no first antibody. When double labeling was carried out, both antibodies were mixed together in the PBS then added simultaneously to the coverslips. Following the 30 minute incubation, the coverslips were washed five times (for two minutes each time) with 0.1% (w/v) saponin in PBS with 2% BSA. The cells were then incubated with the appropriate secondary antibody conjugated to either Alexa 488 or 568

Table 2.3: Primers

Template	Primer Name	Sequence	Application
mTfR2 α	FL3+1	CTT CTG CTC TAA AAG CTG CG	Sequencing
mTfR2 α	Sep 13-2	CAG AAG GAT GGA AGT CCC	Sequencing
mTfR2 α	FFS1	ACC CTG GTC CAA GAT ATC CTC G	Sequencing
mTfR2 α	FFS2	TGC GAG TTG GAA TTA CTA GCT TCG	Sequencing
mTfR2 α	FFS3	CAC CTC TCA GGC TCT CCT TAT CG	Sequencing
mTfR2 α	FFS4	ACC TCA AAG CTG TTG TGT ACG TG	Sequencing
mTfR2 α	FFS5	CCT GCC AGG CGT GTG GGG AC	Sequencing
mTfR2 α	FFS6	CAG TGG CTC AGC TCG CGG	Sequencing
mTfR2 α	FFS7	GCC CTG GTA GAC CAC CTG CG	Sequencing
mTfR2 α	FFS8	GCC GTT GCT TAC CCA GAA AGC	Sequencing
HTfR1	Probe +	CTC AAA AAG ATG AAA ATC TTG CG	Northern/ RT PCR
HTfR1	Probe -	CCA AAG AAT GAA AGT TCT GCG	Northern/ RT PCR
Actin	Probe +	TGA AGT CTG ACG TGG ACA TC	Northern/ RT PCR
Actin	Probe -	ACT CGT CAT ACT CCT GCT TG	Northern/ RT PCR
MTfR2	Probe +	CAA CGT TGG GGT CTA CTT CGG	Northern
MTfR2	Probe -	GAT CAG GGA CCA GAT AGG GGG	Northern
MTfR1	Probe +	CTA CCT GGG CTA TTG TAA GCG	Northern
MTfR1	Probe -	GGT CTG CCT CAA CAA CGG G	Northern
HTfR2	Probe A	CGT GGT CCA GCT TCT GGC GGG	Northern/ RT PCR
HTfR2	Probe E	GTA GCT GGG TCA CGT CCC	Northern/ RT PCR
HTfR2	Probe F	CCT GGA TTT CCA CCA GGG C	Northern/ RT PCR
HTfR2	Probe G	GGC CAT GTT CCT GCA GTT C	Northern/ RT PCR

(see Table 2.2) diluted in PBS with 2% (w/v) BSA for 30 minutes at room temperature, followed by washes as above. After washing, the coverslips were equilibrated with 6 drops of Slow Fade Equilibration buffer Component C (Molecular Probes, Eugene, OR) for 10 minutes at room temperature. After the 10 minutes, all the liquid was suctioned from the coverslip, and the coverslips were mounted on a slide with 5 μl of an equal mixture of 50% glycerol in PBS and Molecular Probe Slow Fade Component A. The coverslips were then sealed onto the slide with nailpolish. The BioRad Radiance Plus confocal laser scanning microscope was used to capture the images of the cells, and an NIH imaging system was used to analyze the images produced.

XI. Statistical analysis

The difference between the means of experimental groups and control groups was compared with the use of the Student's t-test, which compares the size of the difference between means with the standard error of that difference (Motulsky, 1995).

Null hypothesis = no average difference between the two means

Alternate hypothesis = there is a significant difference between the two means

t = difference between means / Standard Error of difference

SE of difference (equal N) = square root ($SEM_a^2 + SEM_b^2$)

$$\text{Pooled SD} = \sqrt{\frac{(N_a-1)*SD_a^2 + (N_b-1)*SD_b^2}{N_a + N_b - 2}}$$

$$\text{SE of difference} = \text{pooled SD} \sqrt{1/N_a + 1/N_b}$$

Chapter 3: Interaction of soluble p97 with transferrin receptor 1 and integrin $\alpha_v\beta_3$

I. Cellular based assays to examine p97 binding to the transferrin receptor 1

A. Rationale

Melanotransferrin (p97) is a protein expressed as two distinct forms: the GPI-linked cell surface form and a soluble form found in serum and cerebral spinal fluid (Alemany *et al.*, 1993; Brown *et al.*, 1981; Food *et al.*, 1994; Kennard *et al.*, 1996). The presence of a soluble form produced by a splice variant rather than as a cleavage product released from the cell surface raises the possibility that soluble p97 has a distinct function from that of the GPI-linked version (Hsu, 1997; McNagny *et al.*, 1996). As it has been established that GPI-linked p97 binds iron and can transport the bound iron into cells, the search for a physiological function of soluble p97 in this thesis began by examining possible receptors for soluble p97. Considering that p97 has a 39% homology to Tf (Rose *et al.*, 1986), possible binding and internalization of p97 by TfR1 was examined, and is detailed in the first section of this chapter (see model in Figure 3.1).

Prior to the cloning and generation of recombinant forms of receptors through molecular biology techniques, the characterization of receptor interactions can be very difficult. Evaluating binding of a radioligand to tissue or cells is complicated if more than one receptor on a cell binds to the ligand or when a cell line that does not bind the ligand of interest is unavailable. Even with the receptor cloned and expressed in cells, characterization of receptor interactions is not trivial. Often, one goal of receptor-ligand

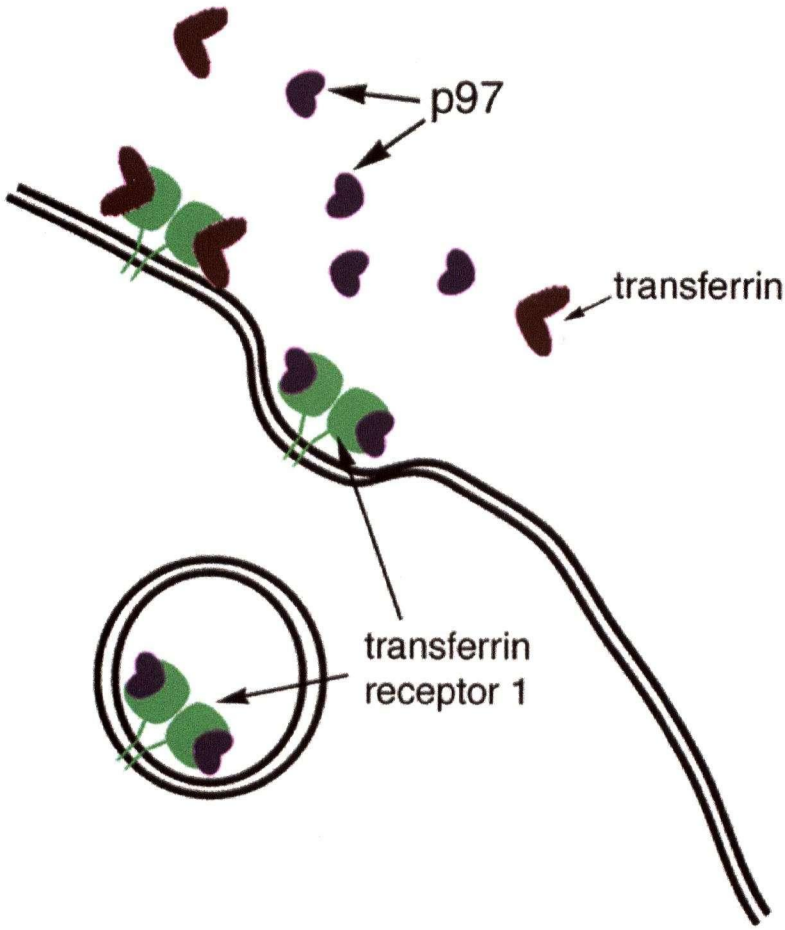

Figure 3.1: Model of internalization of p97 via transferrin receptor 1. In this model, soluble p97 and Tf are present in the blood stream. The TfR1s on the cell surface can bind either p97 or Tf, and internalize either ligand. The complex is then present in the endosomes, and recycled to the cell surface after iron is dissociated from the p97 or Tf.

binding studies is to calculate a binding affinity for the interaction. Scatchard experiments, performed to generate these numbers, rely on a number of assumptions in order for the results to be accurate. These assumptions are that the receptors are equally accessible to ligands, that there is no partial binding, that neither the ligand nor receptor is altered by binding, and that the interaction is reversible. Often, not all of these assumptions apply, which can render the results very difficult to interpret and lead to incorrect binding affinities. These experiments also require substantial amounts of radioligand with high specificity.

Alternatives to these types of studies exist. One of the more powerful techniques that can be used after a receptor is cloned is to create two cell lines that can be compared directly: a "negative" cell line that does not express the protein of interest, and a "positive" cell line which consists of the negative cell line transfected with the protein of interest. Under various experimental conditions, differences measured between the two cell lines can reasonably be assumed to be due to the presence of the transfected protein. In the case of the human TfR1, a cell line for these types of assays was created in 1987, when a Chinese hamster ovary (CHO) cell line was isolated through repeated rounds of mutagenesis with ricin A chain conjugated Tf (McGraw *et al.*, 1987). The cells that internalized Tf through the TfR were poisoned by the ricin through its ability to act at ribosomal target sites and inhibit cellular protein synthesis (Sundan *et al.*, 1982). The isolated mutant cell line (called TRVb, referred to hereafter as TfR-) does not bind detectable amounts of Tf and was characterized to lack functional TfRs. A human TfR1 construct was then transfected into these cells to produce a cell line that can bind and internalize Tf, called TRVb-1 (for clarity in this thesis TRVb-1 will be termed TfR1+).

To test the hypothesis that soluble p97 specifically binds to human TfR1, two different cell-based assay systems were utilized. The first assay system uses iodinated p97, and examines cell surface binding of the protein at 4°C. This is carried out either in the presence or absence of excess unlabeled p97, to compete for binding sites. This assay also compares binding at the acidic pH of 6.0 to binding at the neutral pH of 7.0 to determine if pH has an effect on binding. The second assay uses a particle concentration fluorescent immuno-assay (or Pandex assay) to measure the amount of fluorescence on the surface of a fixed number of cells in a specialized 96 well plate. This approach uses antibodies raised against p97 rather than radioactively labeled protein, followed by a FITC-labeled secondary antibody to detect p97 binding to TfR1.

B. Results I: ^{125}I p97 binding to the human transferrin receptor in cells

Iodination is a common protein labeling technique, and was the method used successfully to examine uptake of ^{125}I labeled Tf by Maxfield and associates in the primary characterization of the TfR1+ cell line (McGraw *et al.*, 1987). Transferrin receptor 1 deficient CHO cells (TfR-) and those transfected with the human TfR1 construct pCDTR1 (TfR1+) were harvested with versene. Following the harvest, the cells were briefly acid washed with glycine buffer at pH 4.0 to remove any bound bovine Tf from the tissue culture medium, washed with PBS, and aliquoted into tubes. The cells were then incubated with iodinated protein (or iodinated protein plus 100 times unlabeled protein) for 1 hour at 4°C. Finally, the cells were washed and the bound radioactivity associated with both the TfR- and TfR1+ cells was measured in a gamma counter. The difference in bound counts between the cell lines (TfR- and TfR1+) was plotted (Figure

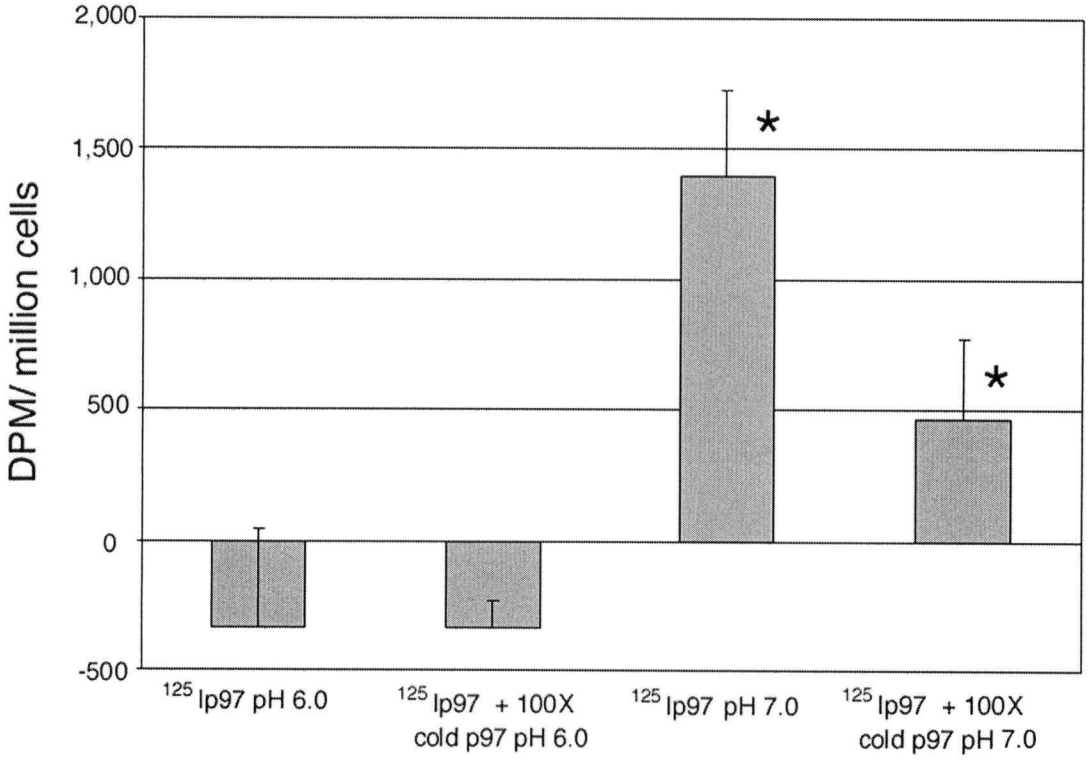

Figure 3.2: ^{125}Ip97 binding to transferrin receptor 1, with unlabeled p97 competition. ^{125}Ip97 and ^{125}Ip97 with 100x unlabeled p97, incubated with TfR- and TfR1+ cells at either pH 6.0 or 7.0. Represents the mean +/- standard error for a representative experiment performed in triplicate, n=4.
* Statistical significance was assessed with the use of a Student's t-test ($p<0.005$).

3.2). Therefore, the amount of bound radioactivity plotted per million cells represents the amount of iodinated protein bound specifically to the TfR1.

Figure 3.2 shows that, at pH 6.0, there is no significant binding of ^{125}I p97 to the TfR1, and the addition of 100 times unlabeled protein has no effect on the amount of radioactivity bound to the cells. The reason that the plotted results are less than zero is that, although the two cell lines did not have significantly different amounts of bound radioactivity, the "background binding" or the binding measured on the TfR- cells was slightly higher than the binding on the TfR1+ cells. At pH 7.0 the amount of binding on the cells with TfR1 is significantly higher (assessed with Student's t-test, $p<0.005$) than the amount bound to the cells without the TfR1, with the difference being approximately 1,400 disintegrations per minute (DPM) per million cells. Furthermore, when unlabeled p97 is included to compete with the ^{125}I p97 (at a ratio of 100:1, unlabeled p97: ^{125}I p97) the bound radioactivity decreases to approximately 500 DPM, which is significantly lower than the amount bound in the absence of the cold competition (assessed by a Student's t-test, $p<0.005$).

C. Results II: Particle concentration fluorescent immunoassay study of p97 binding to transferrin receptor 1

The Pandex (particle concentration fluorescent immunoassay) is a technique that allows measurement of the bound fluorescence-labeled antibody on a pre-determined number of cells. In some instances, when examining lower affinity or transient protein-protein interactions, the Pandex can be more sensitive than flow cytometry, as bound fluorescence in the flow cytometer is measured one cell at a time in a FACS buffer

solution. This can lead to some interactions being lost with flow cytometry, as the ligand is highly diluted by FACS buffer, and thus can dissociate under the conditions present. In the Pandex, specialized 96-well plates are used that have wells with filtered bottoms to allow for incubation of the cells with antibodies within the wells. This is followed by rapid washing and draining steps, all performed within the context of the Pandex fluorescence concentration analyzer (Idexx, Westbrook, Maine) (Jolley *et al.*, 1984).

Figure 3.3 shows the results of an experiment in which TfR- and TfR1+ cells were harvested with versene, briefly acid washed to remove any bound bovine Tf, and aliquoted at 1.25 million cells per tube. The cells were then incubated with either Pandex buffer alone (serum free DMEM medium with 0.1% w/v sodium azide and 1% w/v BSA) or Pandex buffer with 0.3 μg/ml soluble iron-loaded p97 for 45 minutes at 4°C. The cells were washed with cold Pandex buffer, then incubated with 200 μl of anti-p97 antibody (hyb-C-FITC) for 45 minutes at 4°C. After the incubation, 800 μl of Pandex buffer was added to the tubes and the cells were loaded into the wells at 40 μl per well (thus approximately 50,000 cells per well). The wells were then drained and washed three times, and the bound fluorescence was read by the Pandex reader.

In Figure 3.3, the difference between bound fluorescence from the cells incubated in the first step with 0.3 μg/ml p97 in Pandex buffer, and those incubated in Pandex buffer without p97 (as a measure of background fluorescence) was plotted as a representation of the p97 bound to the cells. There was no bound fluorescence detected over background on the TfR- cells, but about 1,400 fluorescent units were measured bound to the TfR1+ cells. The fluorescence bound to the TfR1+ is assumed to represent the p97 bound to the TfR1. The mean fluorescence measured on the TfR1+ cells is

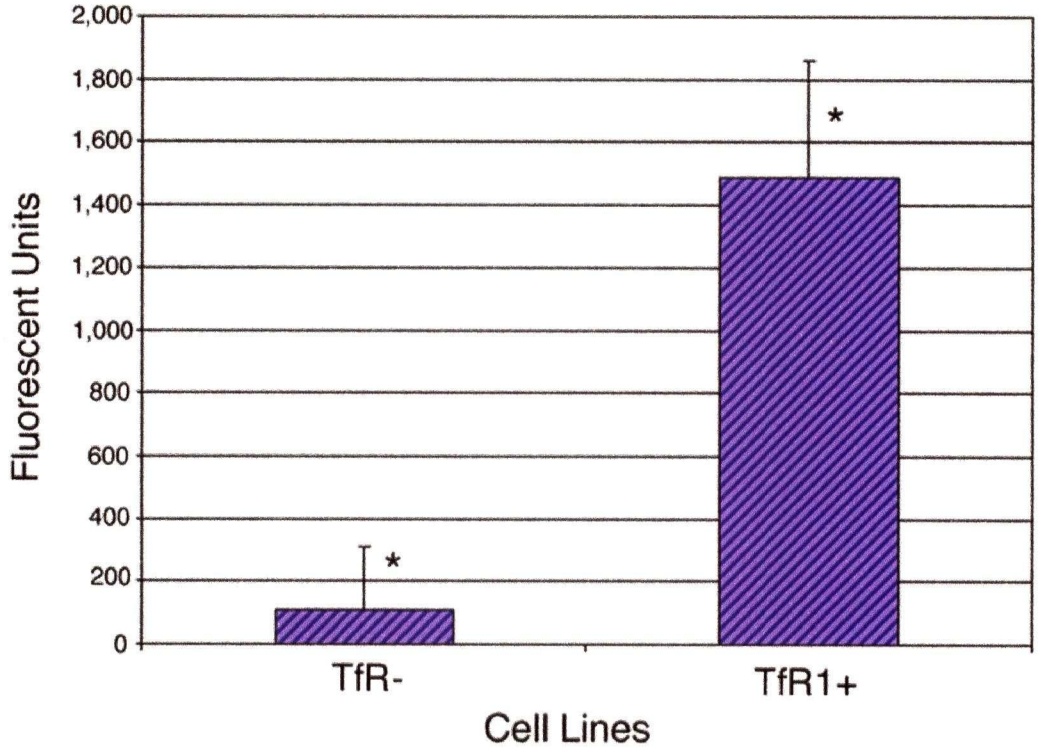

Figure 3.3: Binding of soluble p97 to transferrin receptor 1, detected with the p97 antibody Hyb-C-FITC. TfR- and TfR1+ cells incubated with p97 and the anti-p97 antibody Hyb-C-FITC, and bound fluorescence determined in a Pandex reader. Fluorescent units bound to the cells are plotted after subtraction of measured background fluorescence due to antibody alone. Represents the mean +/- standard error for a representative experiment, n=7. Statistical significance was assessed with the use of Student's t-test ($p<0.005$).

significantly higher than that measured for the TfR- cell line, as assessed by the Students's t-test ($p<0.005$).

D. Results III: p97 can compete with transferrin for binding to the transferrin receptor 1

The model that p97 binds to TfR1 is based in part on the high homology between p97 and the main ligand of the TfR1, Tf. Using this model, it is assumed that p97 and Tf use the same or a very similar binding pocket on TfR1. If this is true, p97 should be able to compete with Tf for binding to that area, and excess p97 will interfere with Tf binding to TfR1.

In Figure 3.4, a Pandex experiment is depicted that demonstrates p97 competition with Tf. The experiment was performed as described in section C above, except that the primary protein incubation was Pandex buffer alone (as the negative control), 0.3 μg/ml Tf, or 0.3 μg/ml Tf with 30 μg/ml p97 as a specific competitor. The first two columns in Figure 3.4 show that on TfR- cells (with no TfR1) there is very little binding of Tf over background levels, and the presence of excess p97 does not have an effect on the bound fluorescence measured. In this graph, the bars represent fluorescence due to the antibody alone subtracted from the fluorescence measured in the wells where the cells were initially incubated with protein. In this way the graph depicts only the fluorescent units measured above background. The third column in Figure 3.4 shows the fluorescent units bound to the TfR1+ cells, which is approximately 24,500 fluorescent units. The Tf clearly binds to the TfR1, as can be determined by comparing column 1 with column 3. The final column shows that, in the presence of a 100 fold excess of p97 (30 μg/ml of

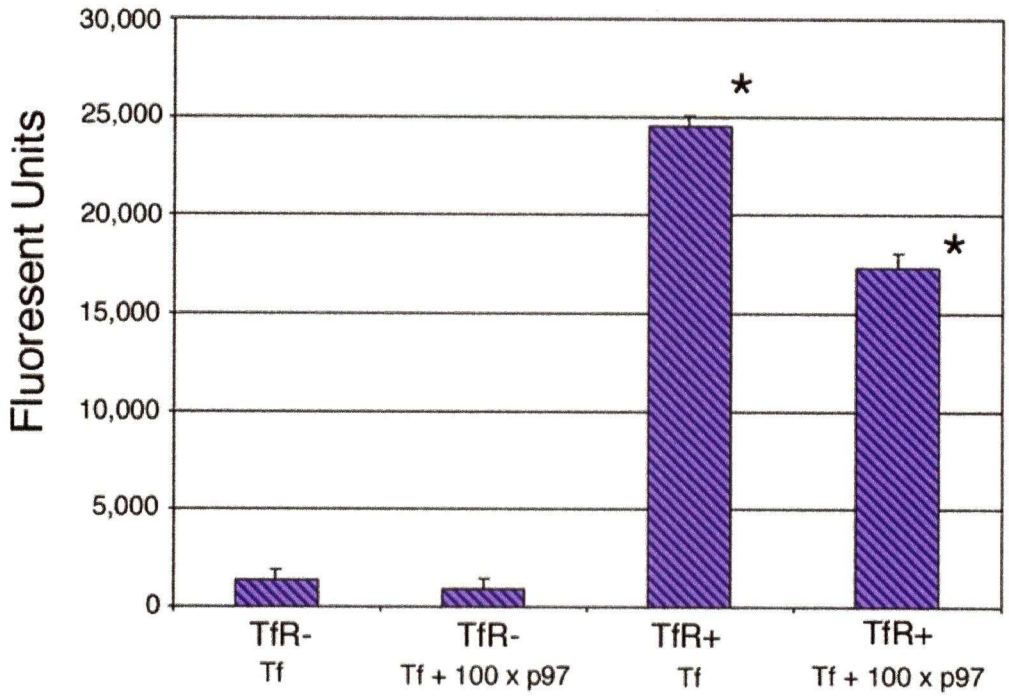

Figure 3.4: Binding of transferrin to transferrin receptor 1, with and without competition by excess p97. TfR- and TfR1+ cells were incubated with Tf, or Tf and 100x concentration of p97, then Tf binding to the cells was measured with an anti-Tf antibody in a Pandex reader. Fluorescence is plotted after subtraction of background fluorescence due to antibody alone. Represents the mean +/- standard error for a representative experiment, n=8. Statistical significance was assessed with the use of a Student's t-test ($p<0.005$).

p97 with 0.3 μg/ml Tf), the amount of bound Tf is significantly reduced. The difference between binding measured in the presence of Tf alone and binding of Tf with excess p97 present is significant when analyzed with the Student's t-test ($p<0.005$).

E. Discussion

The results from the binding experiments support the hypothesis that p97 can bind to TfR1, under the *in vitro* conditions used for these experiments. As outlined in Figure 3.2 it is clear that a significantly greater amount of radioactively labeled p97 is able to bind to the cells with TfR1 compared to the cells without TfR1, and that this binding is pH dependent. The pH dependence of Tf binding to TfR1 and of iron binding to Tf has been well documented in a study by Dautry-Varsat and associates (Dautry-Varsat *et al.*, 1983). This study demonstrated that diferric Tf binds strongly to TfR1 at pH 7.0, and that as the pH lowers to that approximating the endosome (about pH 5.0) the Tf loses its bound iron. At the lower pH, apo-Tf remains bound to the TfR1. Apo-transferrin has a high affinity for TfR1 at the pH of approximately 5.5, but rapid dissociation of apo-Tf occurs at pH 7.3. This may be similar to the situation occurring with p97. The iron loaded p97 does not show any measurable binding affinity for TfR1 at the lower pH of 6.0 used in this experiment, while significant binding was measured at the neutral pH. Consistent with this, Figure 3.2 also demonstrates that the iodinated p97 seems to bind to the TfR1 at pH 7.0 in a specific manner, in that it can be inhibited by the inclusion of excess unlabeled p97.

The Pandex experiments (depicted in Figures 3.3 and 3.4) use a technique that allows the incubation of cells with protein and antibody followed by wash steps that are

carried out very rapidly to help minimize the effects of dilution on the dissociation of the ligand-receptor interaction. Prior to using the Pandex assay, multiple attempts to measure p97 binding to TfR1 under various conditions with flow cytometry were not able to demonstrate measurable binding. Perhaps the period of time the cells are diluted in FACS buffer causes p97 to dissociate from the receptor, due to the low affinity nature of the interaction. Thus, the Pandex analysis is a more powerful technique than FACS because the wash steps are minimized and the cells are not in solution for long periods after the antibody solution is washed away.

Using the Pandex it was clearly demonstrated that the p97 associates with the TfR1+ cells and not the TfR- cells (Figure 3.3). These experiments were carried out at neutral pH, and confirm the cell surface binding observed with the iodinated p97 in Figure 3.2. Further, the presence of excess p97, but not excess BSA in the Pandex buffer, is able to compete for binding with the Tf, and thus decreases the binding of Tf to TfR1+ cells (Figure 3.4). Together with the data shown in Figure 3.2, this demonstrates that p97 is binding specifically to the TfR1. It is important to note that the difference in fluorescence units for p97 and Tf (shown in Figures 3.3 and 3.4 respectively) does not reflect relative binding affinities of Tf and p97 for TfR1, but rather it is a measure of the amount of fluorescent labeling on the antibody. Another contributing factor is that the anti-Tf antibody is a polyclonal antibody while the anti-p97 antibody is monoclonal. This could also increase the fluorescent units observed in Figure 3.4, as more antibody may bind to the Tf than to the p97 because the polyclonal Tf antibody can bind multiple antigen sites on the Tf, possibly allowing greater amplification of the fluorescent signal. The fact that the presence of 100 times p97 only reduces Tf binding to the TfR1 by 30%

indicates that the affinity of p97 for the TfR1 is much lower than the affinity of Tf, under the conditions of this experiment.

The three experiments described above all measure p97 binding to the surface of cells, and were carried out at 4°C to ensure that internalization of the receptors from the cell surface did not take place (Dautry-Varsat *et al.*, 1983). The Pandex assay is not designed to measure uptake and intracellular accumulation of ligand. The iodinated protein assay is often used to measure endocytosis in this way, but despite many attempts, uptake of the ^{125}I p97 at 37°C could not be conclusively shown to occur above the level of background, while uptake of ^{125}I Tf was clear (data not shown). This may indicate that the binding of p97 to the TfR1 has very low affinity or does not lead to protein internalization through endocytosis, but it may also be a problem with the iodination of the protein. Transferrin iodinates easily and the modification does not adversely affect the ability of Tf to bind to the TfR1 (Klausner *et al.*, 1983). Lactoferrin, another iron binding protein that shares high homology with p97 and Tf (Metz-Boutigue *et al.*, 1984), does sustain damage to its monomeric form during iodination, and is prone to formation of tetramers after the modification (Rosenmund *et al.*, 1986). Iodination does not seem to cause excessive polymer formation in p97, and iodinated p97 is able to bind iron after iodination, which is demonstrated through the color change of the solution from colorless to pink. It is not possible to test what proportion of the iodinated p97 is altered after iodination, since no functional assay exists. If the percentage of functionally labeled p97 that is present after iodination is very small, higher background may occur, and this would make the internalization assay very difficult to measure over non-specific counts. This may also explain why, despite many attempts and various protocols, kinetic data on

the interaction of p97 and TfR1 was not obtainable. Future experiments using metabolically labeled p97 (such as ^{35}S) or iodination through other techniques that produce less incorporation might be able to address these problems.

II. Uptake of radioactive iron bound p97 by transferrin receptor 1

A. Rationale

It has been established that GPI-linked p97 expressed on the surface of cells is capable of internalizing bound iron and delivering it to ferritin (Kennard *et al.*, 1995; Tiong, 2001). If the soluble form of p97 binds to the TfR1 in a manner similar to Tf, perhaps the function of this interaction is to allow additional iron delivery to the cells, or iron delivery under certain specialized conditions. The ability of p97 to bind to TfR1 under controlled tissue culture conditions has limited application to identifying and understanding the function of the interaction. To understand if p97 is actually functioning in a manner similar to that of Tf, an examination of net iron uptake is necessary.

To test the hypothesis that iron bound to p97 is delivered to cells via the interaction between p97 and the TfR1, and that the internalized iron is delivered to the iron storage protein ferritin two cell lines (TfR- and TfR1+) were compared in an assay similar to those of section I.A.. In addition, the p97 was loaded with radioactive ^{55}Fe, and the accumulation of the ^{55}Fe within the cells over time was determined. To measure if the iron from the p97 is delivered into the classical iron storage pathway of the cell (namely to the storage protein ferritin) an immunoprecipitation experiment was

performed. This allows the tracking of the radioactive iron through p97, TfR1, and ferritin.

B. Results I: ^{55}Fe-p97 uptake by cells expressing transferrin receptor 1

In the iron uptake experiment, the TfR- and TfR1+ cells were grown in 6 well tissue culture plates. Upon reaching approximately 80% confluence, the plates were washed with PBS, then incubated with serum free Hams F12 media three times, for 30 minutes each to remove bound bovine Tf and to slightly iron starve the cells. Following the washes the cells were incubated with the serum free Hams F12 medium with 1% BSA and the radioactive iron-loaded p97 for 2 hours at 37°C, washed at 4°C and then harvested. The DPM of the internalized ^{55}Fe was determined in a scintillation counter. Figure 3.5 shows that the internalized ^{55}Fe was not significantly different between the two cell lines (as measured by Student's t-test analysis).

C. Results II: Immunoprecipitation of p97, transferrin receptor 1, and ferritin

If soluble p97 were to deliver its iron ligand to cells, then iron may enter the regular iron storage pathway of the cell. If the iron follows the same path as that released from Tf, excess iron brought into the cells by p97 should be shuttled to the iron storage protein ferritin. In order to assess the contribution of iron loaded p97 to the standard iron storage pathway, the amount of radioactive iron bound to ferritin was measured.

In this experiment, the TfR- and TfR1+ cells were incubated with ^{55}Fe-loaded p97 and ^{55}Fe-loaded Tf for 2 hours at 37°C. Following this incubation, the cells were washed, harvested, and an immunoprecipitation was carried out using antibodies against

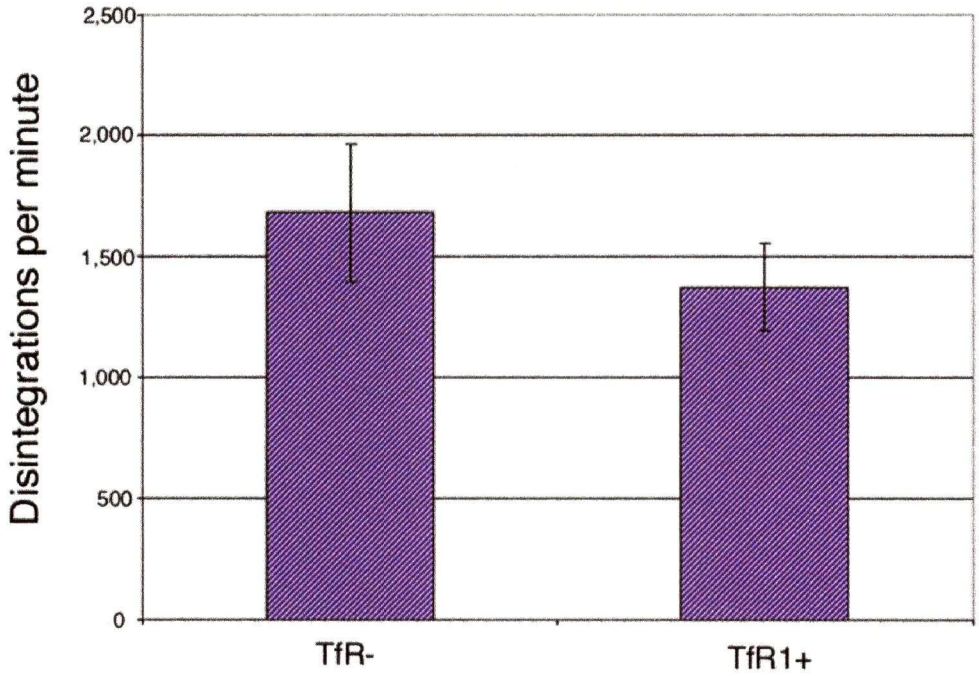

Figure 3.5: Uptake of ^{55}Fe-p97 by cells with and without transferrin receptor 1. The TfR- and TfR1+ cells were allowed to internalize ^{55}Fe-loaded p97 for 2 hours and the internalized counts measured in a scintillation counter. Represents the mean +/- standard deviation for a representative experiment, n=6.

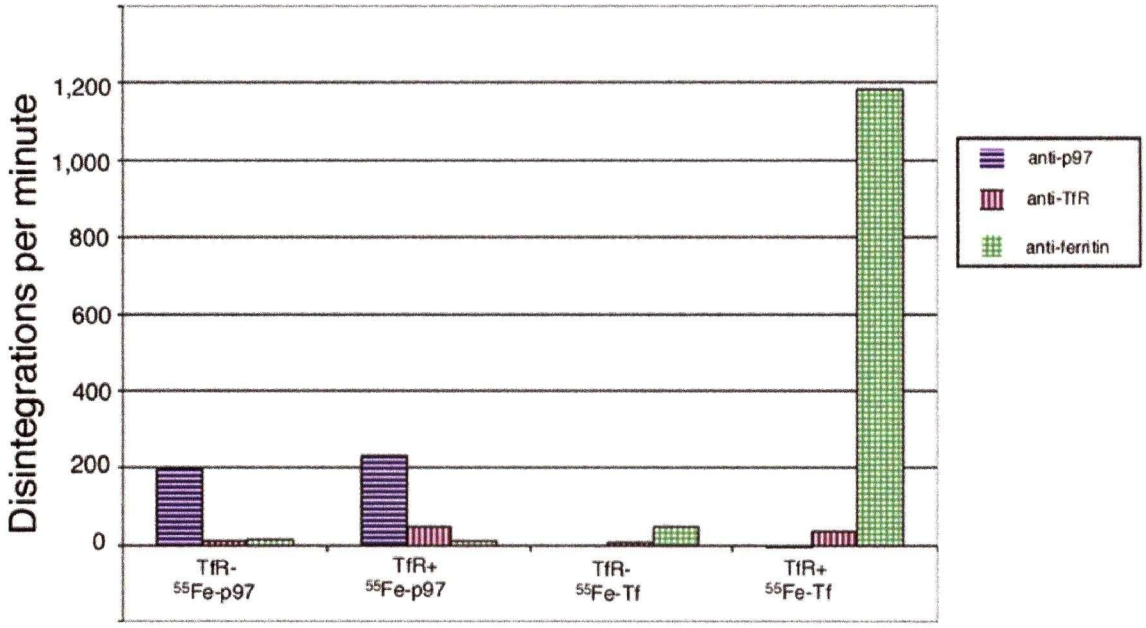

Figure 3.6: Immunoprecipitation of ferritin, p97 and transferrin receptor 1 from cells after incubation with ^{55}Fe-loaded p97 or transferrin. The TfR- and TfR1+ cells were incubated with ^{55}Fe-loaded protein for 2 hours, then immunoprecipitated with antibody against ferritin, p97 or TfR1. The immunoprecipitated counts were measured in a scintillation counter. A representative experiment is shown.

p97, Tf and ferritin. The results shown in Figure 3.6 depict that significant amounts of radioactive iron are measured in conjunction with the iron storage protein ferritin only in the case of the TfR1 positive cells incubated with ^{55}Fe-loaded Tf, but not p97. Higher levels of ^{55}Fe remain associated with the p97 immunoprecipitated from both TfR- and TfR1+ cell lines compared to Tf, which seems to retain almost no radioactive iron.

D. Discussion

Under the experimental conditions outlined above, it has been determined that ^{55}Fe-loaded p97 does not deliver a significant amount of iron to the cells examined via the TfR1, therefore the null hypothesis is supported. Indeed, in Figure 3.6 it is clear that the amount of iron, while very similar between the two cell lines, may be slightly higher for the cell line without the TfR1 (although the iron uptake is not statistically different between the two cell lines). Further, as shown in Figure 3.6, the iron that does get internalized into the cells via iron-loaded soluble p97 is not delivered to the iron storage protein ferritin. In addition, the iron that enters the cells when the TfR- cells are incubated with ^{55}Fe-loaded Tf also does not get delivered to ferritin. This may indicate that in these cases the iron that is being measured may be background binding to the cell surface, or may be entering a different pathway within the cell. The amount of ^{55}Fe associated with ferritin in the TfR1+ cells incubated with ^{55}Fe-Tf is substantially higher than the amount measured in any other case. This result is consistent with the published data on holo-Tf iron delivery via TfR1. Bottomley and associates found that in K562 (erythroid leukemia) cells, 85% of the iron taken up via this pathway is delivered to

ferritin (Bottomley *et al.*, 1985). It seems clear that holo-p97 is not functioning here in the same manner as holo-Tf.

In Figure 3.6, the amount of iron associated with p97 after the immunoprecipitation of both cell lines is higher than that associated with Tf. The fact that the Tf immunoprecipitated from the TfR- cell line does not have iron associated with it indicates either that very little Tf associates with the cells if the TfR1 is not present, or that the Tf that is non-specifically associated with the cells allows its iron to dissociate. From the known dissociation behavior of iron from Tf the former explanation seems more plausible: that Tf does not bind measurably to the TfR- cells and is thus not present to be immunoprecipitated after the wash steps. Unlike Tf, p97 shows a high degree of non-specific binding to the cells. This is apparent as only a small increase in bound counts are present in the immunoprecipitation from the TfR1+ cells compared to the TfR- control cells. This association with both cell types may indicate that p97 has a much higher propensity for non-specific binding than Tf, or that an as yet unidentified specific receptor for p97 exists on both cell types. This phenomenon should be investigated further.

III. Surface plasmon resonance studies to measure binding of soluble p97 to soluble transferrin receptor 1 and the integrin $\alpha_v\beta_3$

A. Rationale

While cell based assays can be a powerful technique for examining interactions between proteins, sometimes the results can be difficult to interpret due to the presence of many factors that can not be controlled in complex biological systems. For this reason,

biosensors to detect the interaction between isolated proteins can be a useful tool to supplement information gained in other ways. One biosensor, called BIAcore, measures biomolecular interactions in real time (Nice and Catimel, 1999). The system utilizes a sensor chip with a gold film to which a ligand (protein, peptide, oligonucleotide, or carbohydrate of interest) is immobilized, allowing measurement of analyte binding to a ligand. Unlike in the field of biological receptors, in BIAcore terminology, the ligand is the stationary substrate, fixed on the BIAcore chip. The analyte is the substance in solution, flowing over the BIAcore chip.

The surface of the BIAcore chip has a dextran matrix (see Figure 3.7) that is covalently linked to the gold film (Hashimoto, 2000). Before the ligand can be bound to the chip, the surface of the chip is first activated by using a mixture of N-ethyl-N'-(dimethyl-aminopropyl)carbodiimide hydrochloride (EDC) and N-hydroxysuccinimide (NHS). Once activated, the NHS-ester groups react with amino groups in the ligand molecules and thus immobilize the ligand. Following this immobilization, the rest of the active groups in the matrix are deactivated by injecting 1 M ethanolamine-HCL through the flow cells. In the BIAcore 2000, four flow cells can be used on the chip, so three different ligands, or three concentrations of the same ligand can be loaded onto the cells, and the fourth is maintained as a blank cell to monitor background binding interactions. One chip can be used multiple times with regeneration steps between experiments, as long as the ligand-analyte interaction is reversible. Some interactions, such as many between an antibody and antigen, are of such high affinity that the treatments required to separate the two binding partners are very stringent, and damage the ligand or the chip in the attempt to regenerate the chip.

Figure 3.7: Diagram of Surface Plasmon Resonance detection system.

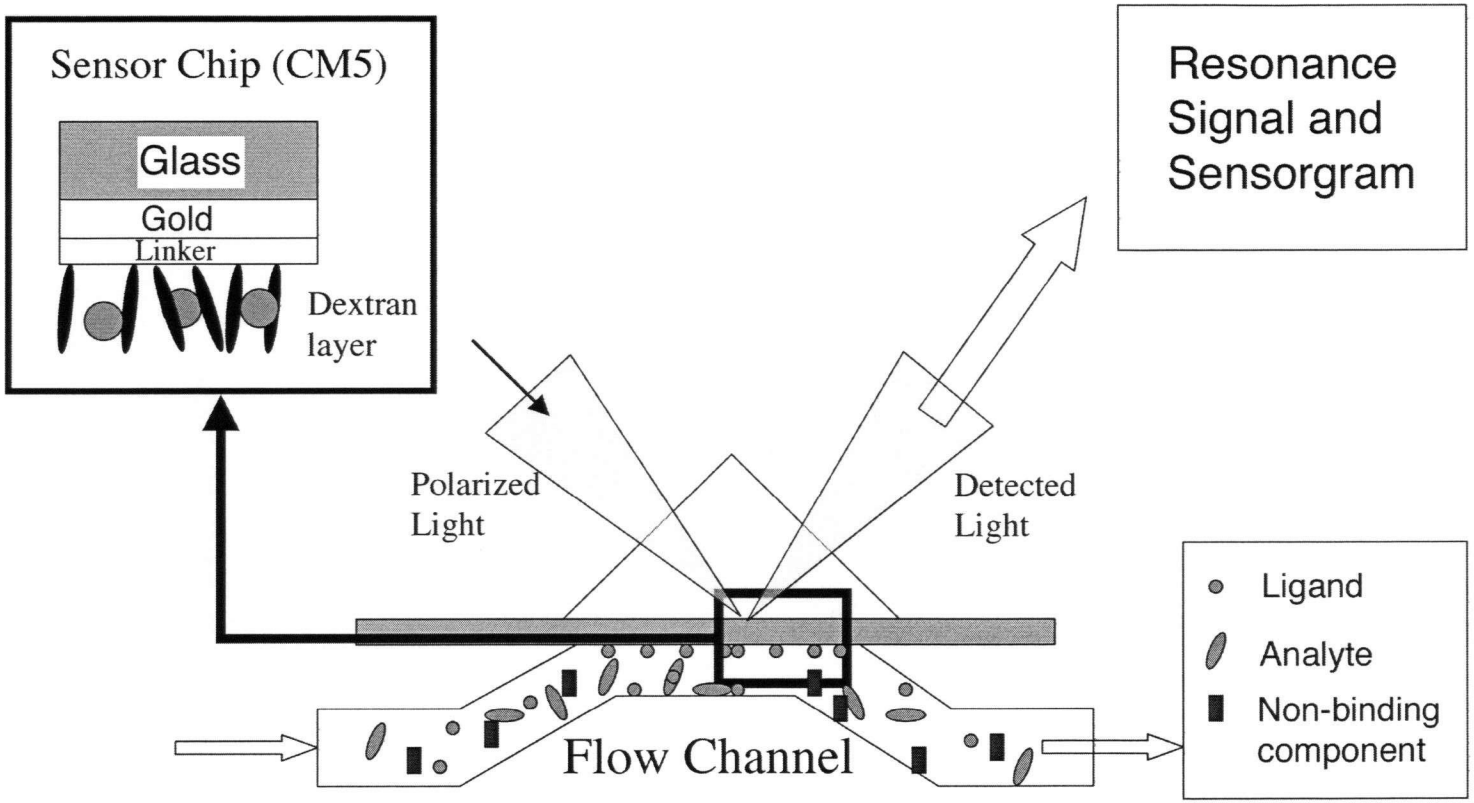

(Adapted from Hashimoto et al., 2000)

Once the chip is prepared, the analyte can be injected and allowed to flow over the chip. The BIAcore measures the change in surface plasmon resonance that occurs due to the change in molecular mass near the gold film when the analyte binds to the ligand on the chip. Specifically, a polarized light is focused onto the gold surface of the chip, and while much of the light is reflected, some of the energy is transferred to electrons in the gold (plasmons), thus causing a drop in the amount of reflected light.

The binding of the analyte to the ligand causes a change in mass, and thus a change in the refractive index of the gold. This is measured as a drop in the intensity of the reflected light at a specific angle of reflection. The changes in refractive index that are measured represent the change in mass that occurs as the ligand binds to or dissociates from the analyte. The information is formulated into a sensorgram that graphically depicts the association and dissociation phases of the binding interaction. The sensorgram shows resonance signal versus time, with the units of the resonance signal being the resonance unit. A shift in the resonance angle of 0.1° is represented by 1000 resonance units (RU) (Hashimoto, 2000). With proper controls, including measurements at various concentrations of bound ligand on the chip and analyte, as well as proper analysis, the BIAcore can generate a dissociation constant that is comparable to those generated through older methods, such as a Scatchard analysis. In a Scatchard experiment, binding experiments are carried out to equilibrium, and then bound ligand is plotted vs. free in a Scatchard plot (Rovati, 1993; Rovati, 1998).

Two hypotheses were tested using this method: 1) p97 binding to TfR1 and 2) p97 binding to the integrin $\alpha_V\beta_3$. Although the first major effort towards revealing a functional receptor for p97 focused on a role in iron transport and thus the TfR1,

homology to Tf is only one model that can be applied to predict possible interactions for p97. A second model is that p97 may bind to an integrin. The family of related heterodimeric receptors which integrate the intracellular cytoskeleton with the extracellular matrix in order to achieve migration and adhesion of the cells was first termed integrin in a review article (Hynes, 1987). The receptors are made up of two subunits, an α subunit (one of eighteen individual α subunits) and a β subunit (one of eight in mammals) (Plow *et al.*, 2000). Individual receptors are often capable of binding multiple ligands. Integrins containing an α_4, α_5, α_8, α_{IIb}, or α_V component recognize the RGD motif (arginine, glycine, and aspartate amino acids) in their respective ligands (van der Flier and Sonnenberg, 2001). p97 has an RGD motif at residues 190-192. Through comparison of the p97 sequence to the sequence and crystal structure of Tf, it is likely that the RGD motif is exposed on the surface of p97, and may be available for integrin binding. The RGD motif is known to be an important component of the recognition motif of ligands for a family of integrins. The significance of the RGD was first identified through the determination that the fibronectin receptor ($\alpha5\beta1$) binds to fibronectin in a manner dependent upon the RGD motif of fibronectin (Pytela *et al.*, 1985). It was subsequently determined that a related receptor binds vitronectin in the same RGD dependent manner (Pytela *et al.*, 1985). Integrin $\alpha_V\beta_3$ is a good choice to study not only because it binds ligands through an RGD motif, but because p97 is an angiogenic protein (Sala *et al.*, 2002), in that it leads to the formation of blood vessels in chorioallantoic assays, and the integrin $\alpha_V\beta_3$ has been linked to angiogenesis in tumors (Brooks *et al.*, 1994a; Brooks *et al.*, 1994b). For this reason, integrin $\alpha_V\beta_3$, which has been described as a "promiscuous" integrin and binds to many different ligands including

vitronectin, angiostatin and osteopontin (Xiong *et al.*, 2001), was examined for its ability to bind p97.

B. Results I: p97 binding to soluble transferrin receptor 1 measured by BIAcore

The data from the cellular studies suggest that p97 may bind to the TfR1 under certain conditions, but kinetic data to determine binding constants were not obtainable through the traditional methods already employed. To determine if soluble p97 binds to the soluble TfR1, and to measure this interaction, a series of BIAcore experiments were carried out. The soluble TfR1was prepared and purified in Dr. Pamela Bjorkman's lab, as outlined in Chapter 2. The CM5 sensor ship was prepared with TfR1 coupled to the chip by direct amine coupling.

The coupling densities of the TfR1 on the chip were varied, with the first cell blank (acting as the negative control), the second with 110 response units bound, the third with 309 response units, and the fourth with 670 response units. The Tf injection did show binding to the TfR1, and the level of binding with the three flow cells corresponded to the amount of TfR1 loaded onto each cell (see Figure 3.8a). The flow cell with the lowest amount of bound TfR1 (shown as the bottom curve in figure 3.8a, just above the line indicating the blank flow cell), shows the least amount of association when the Tf flows over. The upper-most curve, which is flow cell 4 with 670 response units of TfR1 bound, shows the highest amount of association of Tf. There was, however, no binding observed with different concentrations of holo-p97 at pH 7.4 (Figure 3.8b shows 50 μM p97, 10 μM p97 not shown), or with apo-p97 at pH 6.0 (see Figure 3.8c). In both cases, with the blank flow cell used as a negative control and subtracted from the other flow

Figure 3.8: Sensorgram of transferrin and p97 binding to soluble transferrin receptor 1. The sensor chip is loaded with 110, 309, and 670 response units of soluble TfR1 on flow cells 2, 3, and 4. a) 1 μM holo-Tf binding to three concentrations of TfR1 bound to the BIAcore chip. b) 50 μM holo-p97 at pH 7.4 binding to TfR1. c) 50 μM apo-p97 at pH 6.0 binding to TfR1. The bars above the sensorgrams indicate time of protein injection.

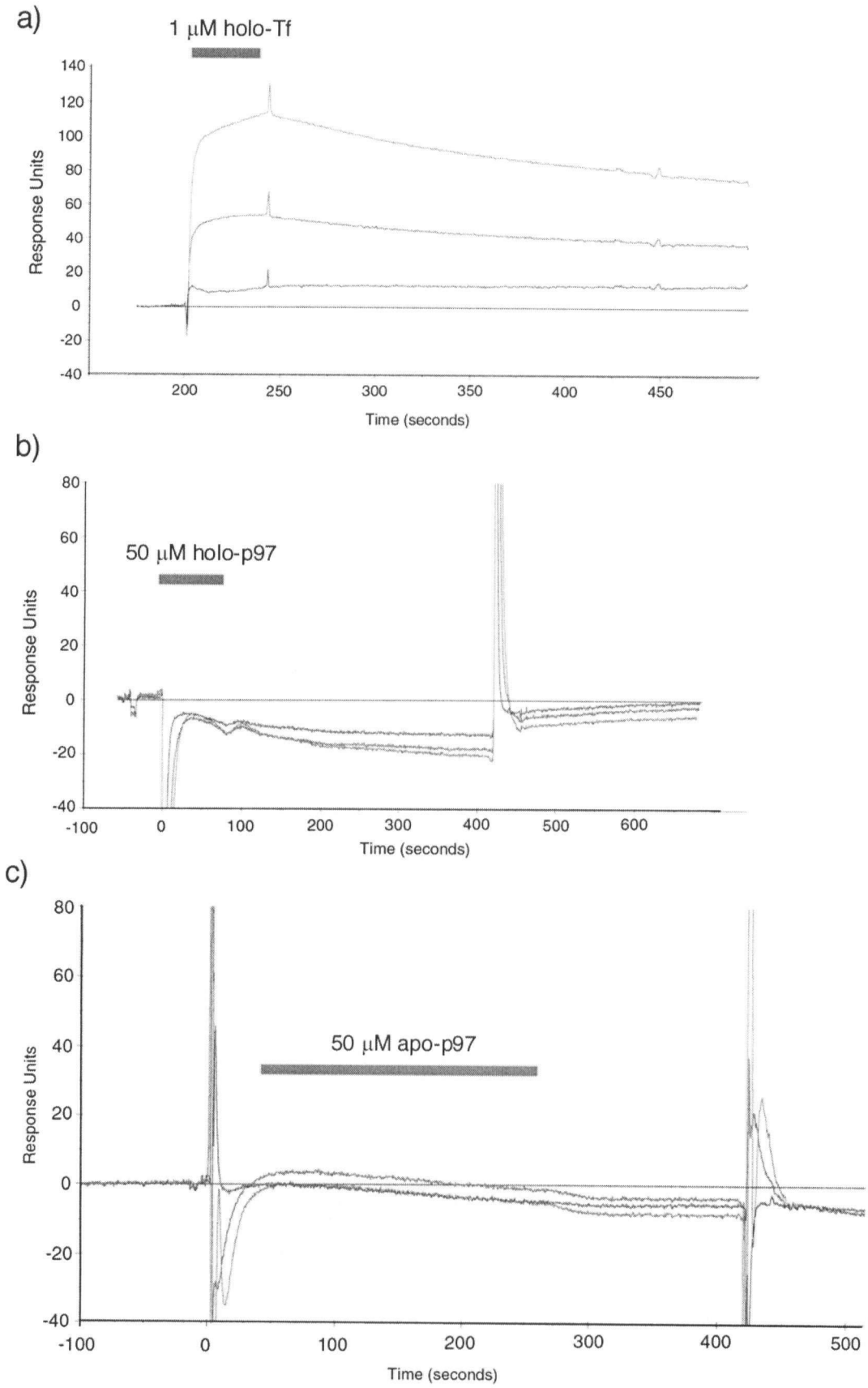
a)
1 μM holo-Tf
Response Units
140
120
100
80
60
40
20
0
-20
-40
200
250
300
350
400
450
Time (seconds)
b)
50 μM holo-p97
Response Units
80
60
40
20
0
-20
-40
-100
0
100
200
300
400
500
600
Time (seconds)
c)
50 μM apo-p97
Response Units
80
60
40
20
0
-20
-40
-100
0
100
200
300
400
500
Time (seconds)

cells to zero the response units, the amount of binding is at zero or just above zero response units. No rise in signal indicating an association rate or down slope indicating a dissociation rate is observed for p97. The length of injection is indicated on the sensorgram as a bar.

C. Results II: p97 binding to soluble integrin $\alpha_V\beta_3$

A BIAcore 2000 biosensor system was used to assay the interaction of p97 with $\alpha_v\beta_3$ integrin (the kind gift of Alistair Henry of Celltech plc) at 25°C. The extracellular domains of the α_v and β_3 subunits were linked at the C-terminal end to the Fc of mouse IgG1 to enforce heterodimerization (Stephens *et al.*, 2000).

The carboxymethylated dextran matrix was preactivated with NHS according to the manufacturer's recommendations. Random amine coupling of the p97 or $\alpha_v\beta_3$ integrin to the chip was achieved by subsequent injection of 10 μg/ml p97 in 10 mM sodium acetate at pH 4.5, and $\alpha_v\beta_3$ integrin at 50 μg/ml at pH 4.5. One cell on the chip was left blank to serve as a control, and the sensorgram generated from the control cell was subtracted as a baseline from the experimental sensorgrams. To perform binding assays, samples of p97 or $\alpha_v\beta_3$ integrin were injected in Hepes buffer (10 mM Hepes, 150 mM NaCl, 0,005% polysorbate 20, 2 mM $MgCl_2$, 0.6 mM $CaCl_2$, pH 7.4).

In Figure 3.9a) the integrin $\alpha_v\beta_3$ was bound to the chip, and fibronectin was injected over the flow cell at 50 μg/ml as a positive control. The sensorgram is shown with the blank subtracted. The binding of the fibronectin to the integrin is clear from the shape of the rising curve during the injection and the decreasing curve after the injection.

Figure 3.9: Sensorgram of fibronectin and p97 binding to the integrin $\alpha_v\beta_3$. The sensor chip in a) through e) is loaded with the heterodimer $\alpha_v\beta_3$, while the flow cell in f) is loaded with p97. a) 50 μg/ml fibronectin is injected over a flow cell with integrin $\alpha_v\beta_3$. b) 50 μg/ml of apo-p97 injected over integrin $\alpha_v\beta_3$. c) 50 μg/ml of holo-p97 injected over integrin $\alpha_v\beta_3$. d) 1 mg/ml of holo-p97 injected over integrin $\alpha_v\beta_3$. e) 1 mg/ml of holo-p97 with 1 mM manganese injected over integrin $\alpha_v\beta_3$. f) 400 μg/ml integrin $\alpha_v\beta_3$ with 1 mM manganese injected over flow cell with p97 loaded. Bars above the sensorgrams indicate time of protein injection.

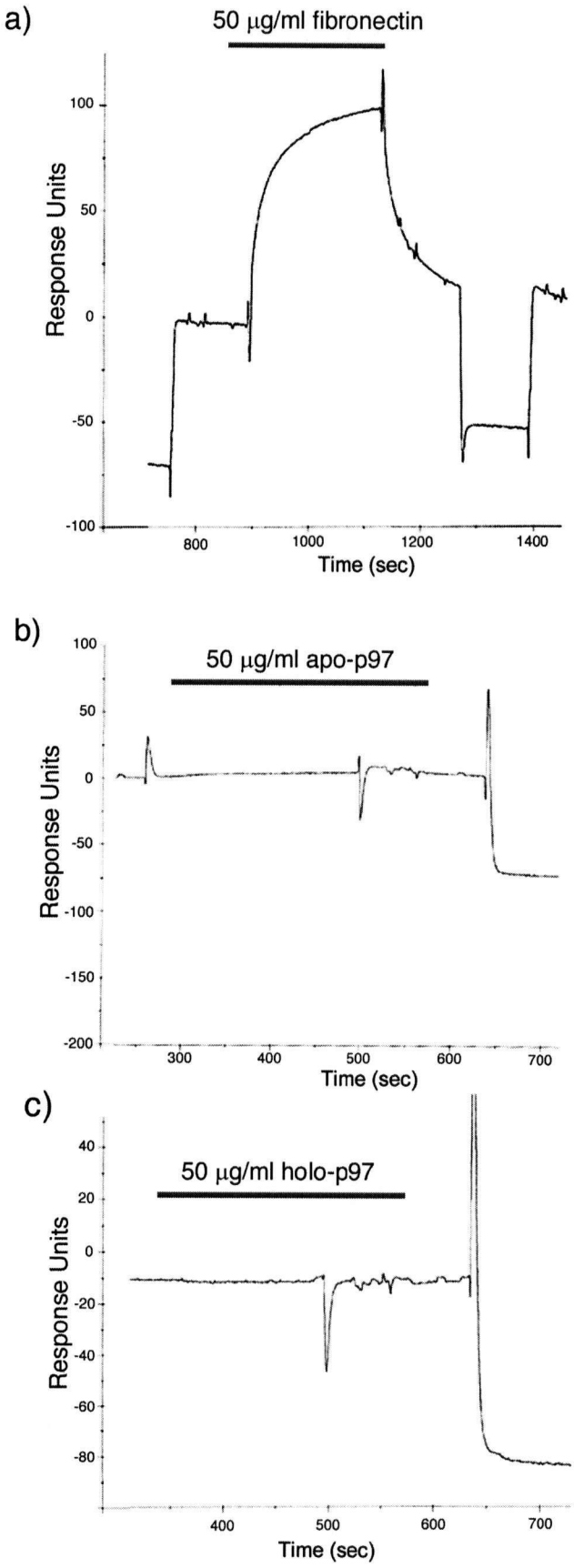
a)
50 μg/ml fibronectin
Response Units
100
50
0
-50
-100
800
1000
1200
1400
Time (sec)
b)
50 μg/ml apo-p97
Response Units
100
50
0
-50
-100
-150
-200
300
400
500
600
700
Time (sec)
c)
50 μg/ml holo-p97
Response Units
40
20
0
-20
-40
-60
-80
400
500
600
700
Time (sec)

d)

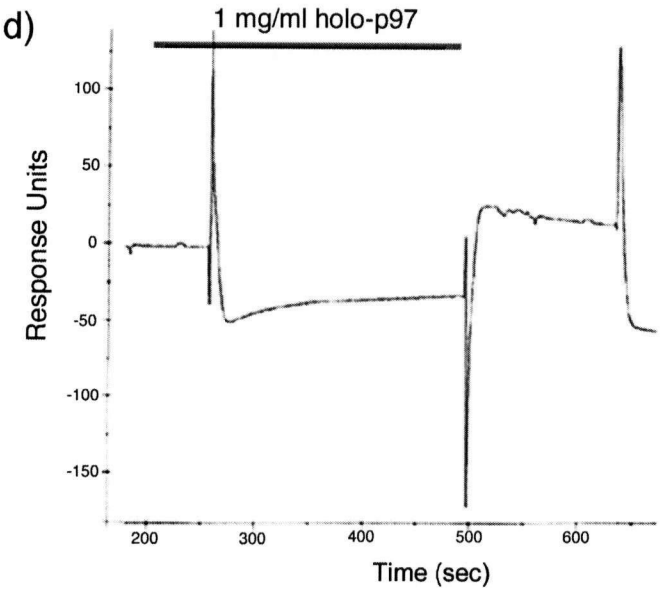
1 mg/ml holo-p97
Response Units
100
50
0
-50
-100
-150
200
300
400
500
600
Time (sec)

e)

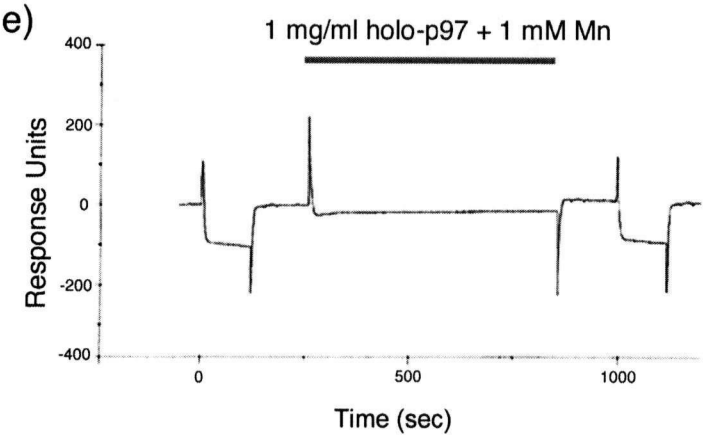
1 mg/ml holo-p97 + 1 mM Mn
Response Units
400
200
0
-200
-400
0
500
1000
Time (sec)

f)

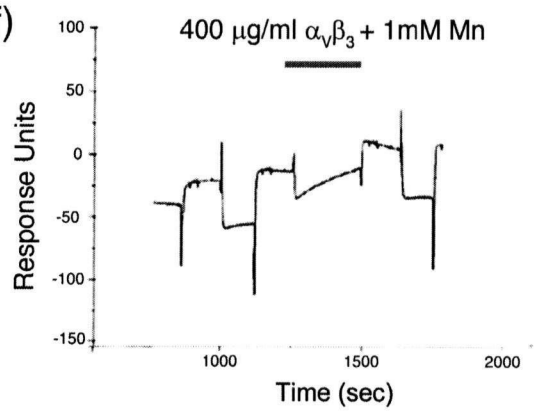
400 μg/ml $\alpha_V\beta_3$ + 1mM Mn
Response Units
100
50
0
-50
-100
-150
1000
1500
2000
Time (sec)

Approximately 100 response units difference are measured. Figures 3.9b)- e) also show the integrin $\alpha_v\beta_3$ bound to the chip, now with various concentrations of injected p97 as the analyte. Figure 3.9b) shows the injection of 50 μg/ml of iron-free (apo) p97, while Figure 3.9c) shows the same concentration of iron-loaded (holo) p97 injected over the integrin. In Figure 3.9 d) a much greater concentration (1 mg/ml holo-p97) is injected, and in Figure 3.9e) the same 1 mg/ml holo-p97 is injected, but with the addition of 1 mM manganese. The manganese is included as a known activator of integrins (Diamond and Springer, 1994). In all these cases, no difference from the baseline is observed in the sensorgrams. (All graphs are shown with the blank flow cell subtracted.) Figure 3.9f) shows the injection of the integrin $\alpha_v\beta_3$ at 400 μg/ml in buffer with 1 mM manganese over the chip bound with holo-p97. The binding of the analyte to the ligand was lower than the binding observed to the blank. No binding above background was observed in any of the conditions except the positive control. The length of the injections into the flow cells is indicated in Figure 3.9 by the gray bar over the sensorgram.

D. Discussion

In both BIAcore experiments, the null hypothesis is supported. p97 does not show measurable binding to the TfR1 or integrin $\alpha_v\beta_3$. The positive controls bound in both series of BIAcore experiments, which indicates that the loading of the chips was successful and that the ligands are functioning properly in terms of binding ability. The fact that no binding was observed in the experimental injections, where the binding of p97 to the TfR1 or the integrin $\alpha_v\beta_3$ was assessed, indicates that there is no measurable binding under the tested conditions. While this is strong evidence that no high affinity

interaction occurs between the two proteins, it does not rule out the possibility of biological interactions between the two proteins in very specific situations, or under particular conditions required for binding that have not been determined and tested.

The level of sensitivity of the BIAcore 2000 approaches the low ng/ml concentration level, which enables the system to measure interactions at physiologically relevant concentrations (Nice and Catimel, 1999). The real sensitivity of the BIAcore, however, depends on a number of factors. These include the relative masses of the ligand and analyte, the level of immobilisation on the chip as well as the orientation of the ligand on the chip, the rates of both association and dissociation, and the volume and concentration of the injection (Nice and Catimel, 1999). For example, if the analyte is of much smaller molecular mass than the ligand, the change in refractive index when the analyte molecule binds will be very small, creating an extremely low signal. This, however, should not be a major problem in these experiments, as both the ligands and analyte molecules are fairly large.

In addition, while the immobilisation of the ligand to the chip seems to have been quite successful, there is no way to determine definitively how much of the ligand is oriented correctly. Direct amine coupling which was used in both experiments has the disadvantage of being orientationally non-specific, in that the protein of interest can be affixed to the matrix via any reactive amine group. Thus, this method does not guarantee that the majority of the bound ligand will be oriented in a way that promotes binding by the analyte. An alternative to this method would be to attach a linker molecule, such as a ligand-specific antibody covalently to the matrix, and then attach the ligand to the antibody (although the binding of the ligand to the chip may be slightly less stable under

these conditions). In this way, all the bound ligand should be oriented in a similar fashion, and as long as the antibody of interest does not obscure the binding site of the analyte, this method may lead to better BIAcore results. This coupling method was attempted, as the TfR1 was cloned with a 6 histidine tag on the C-terminus (Lebron *et al.*, 1998), thus creating a protein that can be correctly and uniformly oriented on the chip with the use of an anti-his antibody. Unfortunately, the analyte (p97) bound very strongly to the anti-his antibody, thus making this fixation method untenable. The problem of orientation is complicated even more with the integrin $\alpha_v\beta_3$, as the heterodimer has to be assembled correctly in order for the interaction with the ligand to occur. In this case, however, the fact that the positive control proteins (Tf and fibronectin) were able to bind to the immobilized ligands indicates that at least some of the ligand must be oriented in a position that favors binding. There was a rather smaller signal than expected generated for the positive controls, which might indicate that some of the ligand was not oriented correctly on the chip (West *et al.*, 2000). If a greater signal (i.e. more response units) could have been measured for both Tf binding to TfR1 and fibronectin binding to the integrin $\alpha_v\beta_3$, this would provide more confidence that the assay could measure a very small binding affinity interaction. Finally, if the dissociation rate of the binding interaction is very fast, it may also be difficult to observe binding with the BIAcore technology.

It seems clear that under the conditions examined in these BIAcore experiments, there is no strong interaction between p97 and TfR1. The results shown earlier in this chapter point to a binding interaction occurring between these two proteins. This apparent discrepancy may be explained by noting that many factors are present in the cell

binding studies that are absent in the surface plasmon resonance assay, such as additional proteins, media, and different solute and pH conditions. As well, the TfR1 used in the BIAcore experiments is truncated so that the membrane-spanning and intracellular domains are not present. The construct used to produce the soluble TfR1 was expressed in a lytic baculovirus/insect cell expression system. The human TfR1 gene with the first 120 amino acid residues deleted, was fused 3' to a gene segment that encodes the hydrophobic leader peptide from the baculovirus protein gp67, plus a his tag and factor Xa site, and then inserted into a modified pAcGP67a vector (West *et al.*, 2000). In experiments used to examine the effect of point mutations on the binding of Tf and HFE to the TfR1, Bjorkman and associates have found that some amino acid residues near the site of truncation of the TfR1 are very important for high affinity Tf binding (unpublished observations). If p97 and Tf do not bind in exactly the same spot, or if p97 binds with lower affinity than Tf (which seems likely), then perhaps the truncation of the TfR1 would lower binding of p97 to a level that is not detectable by the BIAcore. It does seem, from all the results in this chapter, that any interaction between p97 and the TfR1 is of low affinity. For this interaction to be physiologically relevant it would likely have to take place in specialized circumstances to be useful (because in the bloodstream p97 is unlikely to compete with Tf for binding to the TfR1). These specialized circumstances may include places like transport across the blood-brain barrier (discussed in the following chapter).

Furthermore, no interaction could be measured between p97 and the integrin $\alpha_v\beta_3$ by BIAcore. It is not possible as yet to rule out p97 binding to integrin $\alpha_v\beta_3$, because ligand binding to integrins is a complex phenomenon. For example, the β_3 integrins have

been shown to have two classes of ion binding sites within them, one that must have an ion present for the ligand to bind and a second that inhibits ligand binding when the ion is bound (Hu *et al.*, 1996). The binding of ligand is regulated by the coordination between these two ligand binding pockets. It is also quite possible that p97 may bind to a different integrin via the RGD peptide, as we have only tested the binding to one possible receptor. There have been eight to twelve identified integrins that recognize the RGD motif (Ruoslahti, 1996).

The binding studies of p97 to various receptors lead to the conclusion that while p97 may bind to TfR1, another receptor may be important in the physiological role of p97, as the measured interaction between p97 and TfR1 is of low affinity. Given the high level of Tf in the blood, p97 would have to be acting in a very specialized area for this interaction to have a physiological role in the body. The examination of p97 and integrins will have to be continued before this possible mode of action can be ruled out.

Chapter 4: Characterization of the novel receptor transferrin receptor 2, including interaction with p97

The results of the binding of p97 to the TfR1 did not produce clear and convincing evidence that TfR1 is the main receptor for the soluble form of p97, so a search was initiated for other likely receptors. The first step in this process was to search databases to find proteins closely related to TfR1. Transferrin receptor homologues were initially targeted in this search for the same reason that TfR1was examined for binding to p97: p97 is very similar in sequence and structure to Tf, and the TfR1 binds Tf with a very high affinity. This avenue was pursued further due to the evidence shown in Chapter 3, that p97 does interact to some degree with TfR1. Using the expressed sequence tag (EST) database of the National Center for Biotechnology Information, a homologue of the TfR1 was identified first in human and then in mouse tissues (Boguski *et al.*, 1993). The EST database contains short cDNA segments generated by researchers that are sequenced once and added to the public domain without further sequence conformation. They represent a survey of the cDNA of a tissue or organism, and have been useful in the past for applications including identification of new members of gene families and for discovering orthologues of genes (Boguski, 1995).

After analyzing three EST clones of human and mouse each (all from American Type Culture Collection) and determining in each case that they were from the same gene, the longest cDNA of each species was used to pursue a full length clone. Several rounds of screening were carried out on a human liver library with a short probe made from the EST (ATCC # 363316) derived from human infant brain. A longer fragment of

the novel cDNA was successfully isolated from the liver library. Before a full-length cDNA could be isolated, Kawabata and associates (Kawabata *et al.*, 1999) independently published the full length human TfR2 protein, so attention was turned instead to the mouse EST of TfR2.

I. Tissue expression of transferrin receptor 2

A. Rationale

The identification of a new member of the TfR family, and potentially important protein in iron uptake and transport, has raised many questions in the field of iron transport. Comparing this new receptor to the classical receptor in terms of its expression in adult and fetal tissue is one method of gaining some important information about the new receptor. For example, differential expression of the two related receptors may lead to some insight into the nature of TfR2's physiological role.

Often the expression and function of a protein can be quite different when comparing adult tissue with embryonic tissue. For this reason, two Northern blots of adult and fetal organs were examined for TfR2 expression. First, a Northern blot analysis was carried out representing multiple human adult organs. These included heart, brain, placenta, lung, liver, skeletal muscle, kidney and pancreas. As well, a second Northern blot was completed to determine the level of expression in a mouse embryo at different stages of development, beginning with embryo day 7 (E7) and culminating at E17. These various stages represent quite disparate occurrences in the development of the mouse. The hypothesis in these studies is that TfR1 and TfR2 have distinct expression patterns, both in the adult and the developing organism.

The brain is an organ with a high requirement for iron, and the route by which iron is specifically delivered to the brain is not thoroughly understood. It has been proposed that the major route for iron transport to the brain is via Tf, but in a hypotransferrinemic mouse model that possesses less than 1% of the normal serum Tf levels, brain iron uptake is quite adequate (Dickinson *et al.*, 1996; Malecki *et al.*, 1999b). This indicates that an additional route of iron uptake besides the Tf/TfR1 system may be involved. With this in mind, an experiment was designed to determine if TfR2 is present in cells that compose the blood-brain barrier (BBB). The BBB consists of endothelial cells of the cerebral microvessels with tight junctions. The blood is thus prevented from diffusional contact with the brain, unlike most other areas of the body, and transport across the BBB is very tightly regulated (Abbott *et al.*, 1999). The endothelia of the brain capillaries is different from most non-brain capillaries in that they have a greatly reduced number of pinocytotic vesicles, no fenestrae, and the mitochondial volume is higher (Brightman, 1992). All these factors combine to produce a protective barrier that allows the microenvironment of the brain to be carefully regulated. In addition, p97 is able to traverse the BBB to a much greater degree than Tf, and thus it is possible that p97 may function in shuttling iron into or out of the brain. It is very likely that in order to facilitate the amount and rapidity of transport across the BBB observed with p97, a specific receptor is involved in this movement.

Kawabata and associates have previously reported that TfR2 is not expressed in brain tissue (Kawabata *et al.*, 1999). However, the brain capillary endothelial cells of the brain microvasculature make up such a small proportion of total brain material, a Northern blot or reverse transcription of the mRNA followed by polymerase chain

reaction (RT-PCR) (carried out to assess whether TfR2 is present in brain) may not necessarily be sensitive enough to detect any transcripts if the template material is drawn from whole brain homogenates. To examine for the presence of TfR2 in the BBB, cultured primary human brain capillary endothelial cells were harvested for their RNA in these experiments, and then the RT-PCR was performed.

B. Results I: Northern blot of multiple human organs

Figure 4.1 shows a multiple organ Northern blot probed with a ^{32}P-labeled cDNA probe of TfR2. The Northern blot was purchased from Clontech Laboratories, and was loaded with approximately 2 μg of poly A+ RNA per lane from eight different tissues: heart, brain, placenta, lung, liver, skeletal muscle, kidney, and pancreas. The probe was created by PCR with EST 363316 (ATCC) used as the template. The primers used are listed in Table 2.3. The hybridization was carried out as suggested by Clontech, with a one hour incubation of the probe in ExpressHyb solution followed by several washes, and development on the phosphoimager.

Figure 4.1 shows that the only band that can be visualized on the blot is in the liver at about 2.7 kb. The signal from the liver band is quite strong, and no other detectable signal was found in any other tissue lane, or at any other size on the blot. Following the hybridization with the probe of human TfR2, the blot was stripped and re-probed with a β-actin probe as a loading control. All lanes showed approximately equal β-actin signal (data not shown).

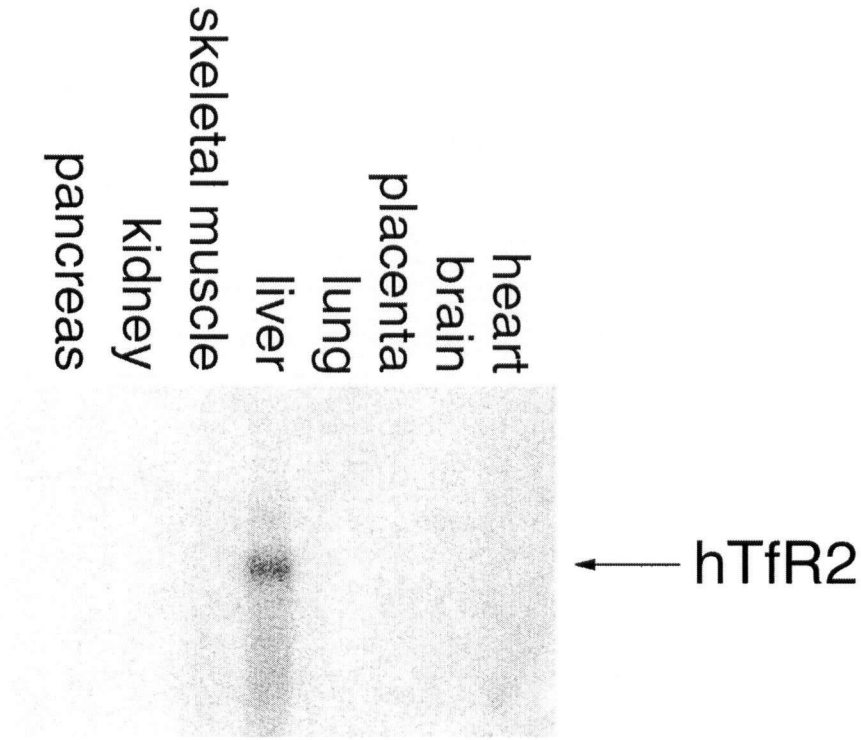

Figure 4.1: Human multiple tissue Northern blot of transferrin receptor 2. Northern blot with RNA from pancreas, kidney, skeletal muscle, liver, lung, placenta, brain and heart, hybridized with a ^{32}P-labeled human TfR2 cDNA probe.

C. Results II: Mouse embryo Northern

The mouse embryo Northern blot represents the poly A+ RNA from four different mouse embryos at days 7, 11, 15, and 17. It was commercially prepared with 2 μg of RNA per lane on a denaturing formaldehyde gel, transferred to a nylon membrane and fixed by ultraviolet radiation. The blot was first probed with a mouse TfR2 cDNA short probe according to the Clontech protocol. The probe was approximately 250 base pairs long, generated by PCR from the cloned full-length mouse TfR2, gel purified and labeled with ^{32}P. After the initial hybridization, the blot was stripped and re-hybridized with a cDNA probe against the TfR1 (approximately 640 base pairs, also generated by PCR and gel purification). Finally, it was stripped and re-hybridized with a cDNA probe from β-actin, to check that the loading of RNA on the blot was comparable between the various embryonic ages. The specific activity of all three probes was very similar.

In Figure 4.2a, the mouse TfR1 signal is clearly visible even in the youngest embryo at day E7. The signal increases through day E11 until it peaks at day E15. At day E17, the signal has markedly decreased. In contrast, in Figure 4.2b the signal for mouse TfR2 is only visible beginning with E15, and has increased by day E17. Figure 4.2c shows that all four lanes on the Northern blot have comparable levels of β-actin.

D. Results III: Transferrin receptor 2 on human blood-brain barrier endothelial cells

To determine if the transcript of the alpha, or transmembrane form, of TfR2 is found in human brain microvascular cells, primary human brain microvascular cells from two individuals were cultured, and the RNA was harvested. The RNA was then used in RT-PCR to amplify a transcript specific to the alpha form of the protein. Figure 4.3a

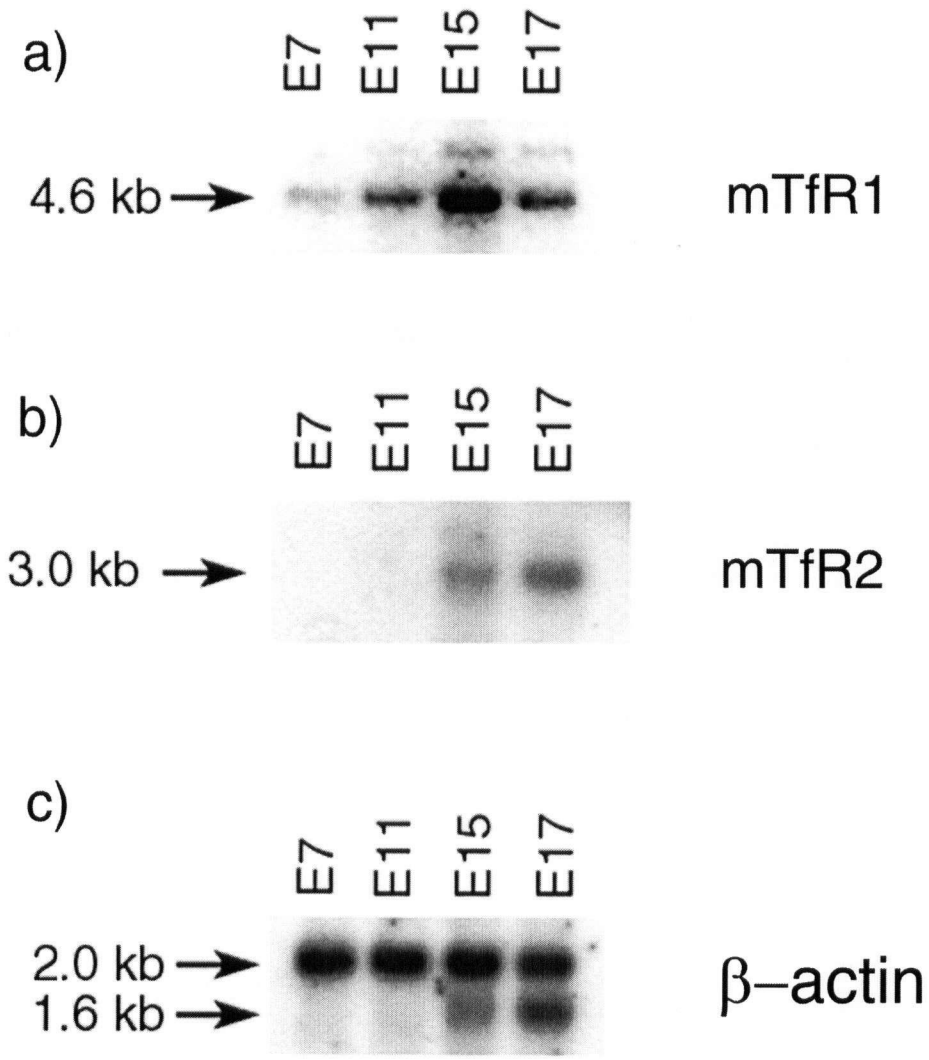

Figure 4.2: Mouse embryo Northern blot of transferrin receptor 1, transferrin receptor 2, and β-actin. The mouse embryo Northern blot contains RNA from four mouse embryo stages: day 7, 11, 15 and 17.
a) shows the embryo blot hybridized with a ^{32}P-labeled probe against TfR1.
b) embryo blot hybridized with a ^{32}P-labeled probe against TfR2.
c) embryo blot hybridized with a ^{32}P-labeled probe against β-actin.

a)

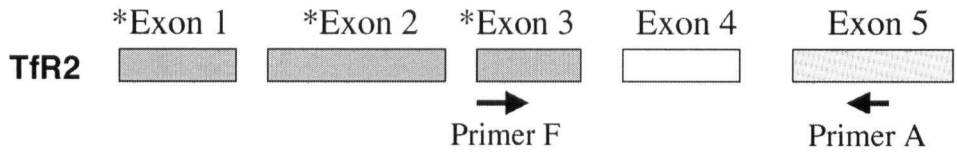

b)

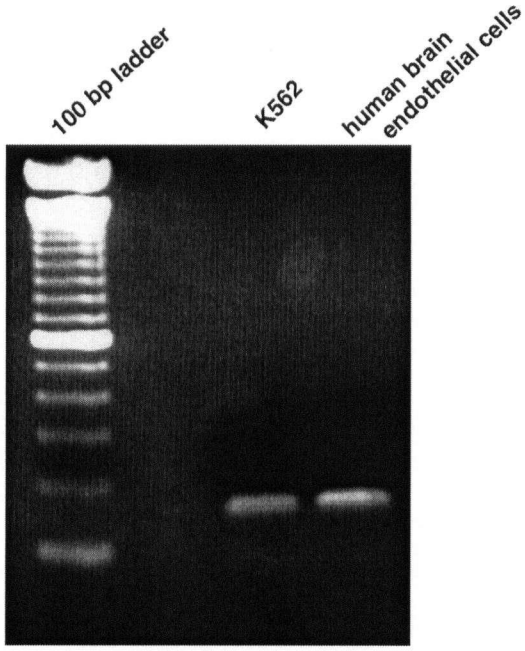

Figure 4.3: Transferrin receptor 2 in brain endothelial cells. a) Exon structure of TfR2 (Kawabata *et. al.*, 1999). Exons 1,2, and 3 are found only in the α–form of TfR2, while exon 4 is only found in the β–form. Exon 5 is common to both forms. Primer F is complementary to sequence within exon 3 and primer A is complementary to sequence in exon 5. b) Agarose gel of PCR product from K562 cells and human brain endothelial cells. PCR product generated with primers F and A.

shows the primers used for the amplification, and Figure 4.3b shows that both K562 cells (human erythroid leukemia) and the primary brain microvascular endothelial cells produce a band of approximately 200 bp, which is the predicted result. After the PCR reactions, the band was cut from the agarose gel, purified, and sequenced to confirm that the product was TfR2 α. This procedure was carried out on two separate samples of RNA, isolated from two sources of human brain microvascular cells, and confirmed by sequencing both times. As a negative control, the TfR2 and actin PCR was also carried out on cDNA from human heart tissue, which has previously been determined to be negative for TfR2α expression by RT-PCR (Kawabata *et al.*, 1999).

E. Discussion

The expression of the TfR2 in adult tissue is markedly different from that of the TfR1. In Figure 4.1, TfR2 can only be detected in the liver, while no detectable signal is observed for the pancreas, kidney, skeletal muscle, lung, placenta, brain or heart. This data agrees with that of Kawabata and associates, who subsequently published a Northern blot showing that the TfR2 α form can only be strongly detected in the liver, while a very weak signal was also detectable in the stomach, and that the band is of comparable size (Kawabata *et al.*, 1999). The expression of human TfR2 is similar to that observed for mouse TfR2 (Fleming *et al.*, 2000). A RT-PCR experiment also showed expression of the TfR2 α transcript in the liver derived cell line HepG2, and the erythroid leukemia cell line K562 (data not shown). This result was also confirmed by Kawabata (Kawabata *et al.*, 1999). The high degree of liver expression of TfR2 suggests that the primary role of TfR2 may be within this organ. Hepatocytes have a high requirement for iron as they

have a high rate of metabolic activity, and iron is essential as a cofactor for cytochromes a, b, and c, cytochrome oxidase and the iron sulfur complexes of the oxidative chain (all involved in adenosine triphosphatase, or ATP, production) (Connor *et al.*, 2001). This is likely one reason why TfR2 remains highly expressed in the liver throughout the life of the organism.

Transferrin receptor 1 expression is very low in the adult liver, both under normal physiological conditions, and in the case of iron overload (Fleming *et al.*, 2000). Thus, the iron loading of the liver that takes place early on in iron overload diseases such as hereditary hemochromatosis (HH) may be due to TfR2 on hepatocytes (Fleming *et al.*, 2000). Unlike TfR1, TfR2 expression is not regulated by the amount of iron in the cell through the iron response element system mentioned earlier (Kawabata *et al.*, 1999). This lack of regulation by cellular iron conditions may be advantageous under normal physiological conditions, as the liver is an organ with a constitutively high requirement for iron.

The difference between expression of TfR1 and TfR2 during embryogenesis is very distinct. Mouse TfR1 is clearly visible by Northern blot quite early in development, by day E7 (Figure 4.2). At this stage, the head process is forming, along with the foregut pocket and the first somites, but most organs are not distinguishable (Rugh, 1990). Transferrin mRNA is detectable in whole embryos by E6 (Plowman, 1986). It is initially produced in the visceral yolk sac, by endodermal cells (Meehan *et al.*, 1984), and the production of Tf mRNA is several fold higher in these cells than in the adult liver. Transferrin receptor 2 transcript is not detectable at this stage (Figure 4.2b). The fetal liver develops from the gut ectoderm at E9. Transferrin mRNA can be detected in fetal

liver as early as E11 (Ekblom and Thesleff, 1985). By E11, the TfR1 is expressed to a greater degree than at day E7 (Figure 4.2), but TfR2 is not yet discernable. At this point in development, organogenesis is occurring, but the organs are not completely formed. By E15, which is the first day TfR2 α transcript is detectable, organogenesis is complete, however rapid cell growth continues to take place. At this point, the liver is beginning to carry out some of its major functions and thus has a constitutive need for iron (discussed earlier). This situation continues through day E17 and beyond. The Northern blot shows that expression of TfR1 peaks around day E15, and is expressed to a lesser degree after that. This may be due to the high demand of the body for iron at early stages to support extremely high rates of cell division and growth. As well, during embryogenesis, the liver accounts for approximately 5% of the body weight and is an extremely active hematopoeitic organ. The rise and fall of TfR1 levels in the embryo roughly correspond to the proliferation of hematopoeitic stem cells in the liver (McNagny, 1990). Even after embryogenesis, the cells that continue to need high levels of iron, such as reticuloendothelial cells, continue to express high levels of TfR1.

The examination of TfR2 expression on cells of the BBB was undertaken to try to understand the relationship between p97 and brain iron transport. The microvessels within the brain consist of specialized endothelial cells that have tight junctions. These cells make up the barrier between the brain and the blood and maintain control over the ionic microenvironment of the brain for important processes such as synaptic processing (Abbott *et al.*, 1999). Therefore, specific transport systems exist to allow selective movement of specific compounds such as macromolecules and peptides that the brain requires for proper functioning.

The brain is an organ with high energy requirements, and thus a high demand for iron. While the brain weighs only 2% of total adult weight, it accounts for 25% of the body's oxygen consumption (Thompson and Thompson, 2001). As mentioned before, iron is essential for the production of ATP, and the brain requires ATP for such tasks as maintaining membrane ionic gradients, synthesizing neurotransmitters, and generating lipids and cholesterol for the synthesis of myelin (Beal, 1998; Connor and Menzies, 1996). The transport of iron into the brain is not clearly understood. Studies have demonstrated that serum Tf does not cross the BBB (Crowe and Morgan, 1992). Instead the brain produces its own Tf, which is located in the interstitial fluid of the brain and CSF at levels about 100 times lower than the amount normally found in serum (Rouault, 2001). Using a mouse model in which oligodendrocytes fail to thrive, it was shown that oligodendrocytes in the brain produce the bulk of the Tf transcripts (Bartlett *et al.*, 1991). The current theory of iron transport across the BBB is that iron en route to the brain is internalized via the regular Tf/TfR1 pathway, released within the endosomes, and transported across the cell to the brain parenchyma, where it is picked up by Tf in the CSF and transported to where it is needed within the CNS. One unexplained aspect of this system is that, while there is a molar excess of Tf in the blood stream to prevent free iron from causing cell damage through free radical formation, there is a molar excess of iron relative to the levels of Tf in the CSF (Bradbury, 1997; Moos and Morgan, 1998). Whether this iron is bound to proteins such as p97 is unknown. As well, this explanation of iron transport into the brain does not explain how iron can be successfully delivered to the brain in hypotransferrinemic mice (mice with extremely low serum Tf levels) (Dickinson *et al.*, 1996). Transferrin is required for correct distribution of iron within the

brain (Malecki *et al.*, 1999a), as the hypotransferrinemic mice display abnormal iron accumulation in the choroid plexus. Clearly, Tf plays an important role in this system, but pieces of the puzzle to make the picture complete are still missing.

In vivo studies involving injections of p97 and Tf into mice have shown that a much greater proportion of p97 is transported into the brain compared to Tf, after intravenous injection of the proteins (Moroo *et al.*, 2002). Figure 4.4 shows that the proportion of p97 transported into the brain is 7 times that of Tf (Moroo *et al.*, 2002). The proteins, labeled with radioactive ^{125}I were examined in the brain parenchyma fraction of brain homogenate one hour after injection, followed by perfusion and capillary depletion of the brain to remove the microvessels (Triguero *et al.*, 1990). While ^{125}I-Tf is not detectable in the parenchyma after this treatment, p97 can be recovered and appears to be intact, as shown by Western blot (Moroo *et al.*, 2002). Transport across the BBB has also been demonstrated through injection of fluorescently labeled proteins (p97, Tf, and BSA labeled with Alexa fluor 488) into the tail vein of a mouse. While all three proteins can be found in the brain microvessels very clearly, only p97 can be visualized in the brain parenchyma (see Figure 4.5) (Moroo *et al.*, 2002). The fact that p97 is transported across the BBB into the brain suggests that a specific receptor exists on the capillary endothelia to facilitate this transport.

Previous publications have shown by RT-PCR and Northern blot that TfR2 is not expressed in the brain (Kawabata *et al.*, 1999). The approach used for these experiments, however, was not sensitive enough to identify expression in certain lower frequency subsets of cells within the brain, as some of these specialized cells make up a very small proportion of the total cell mass of the brain. One of these specialized sub-types of cells

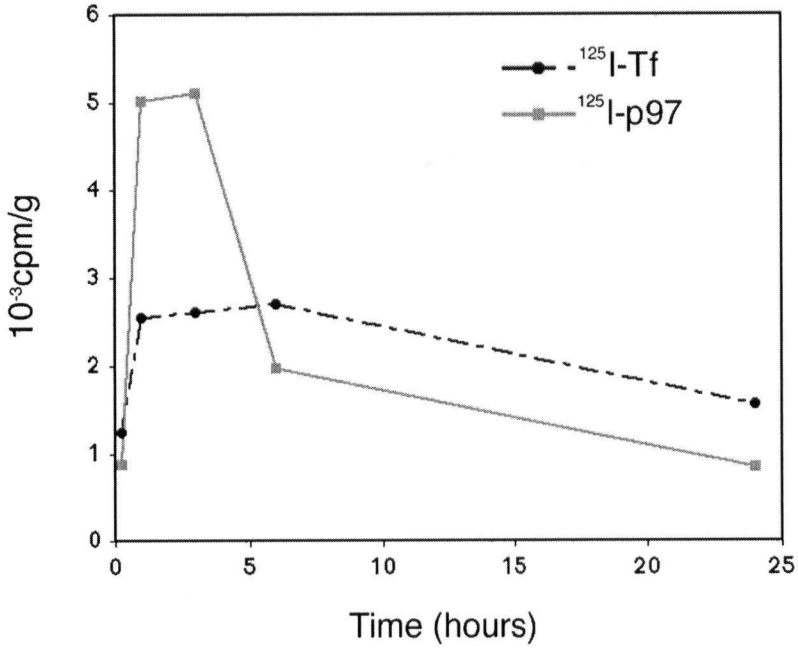

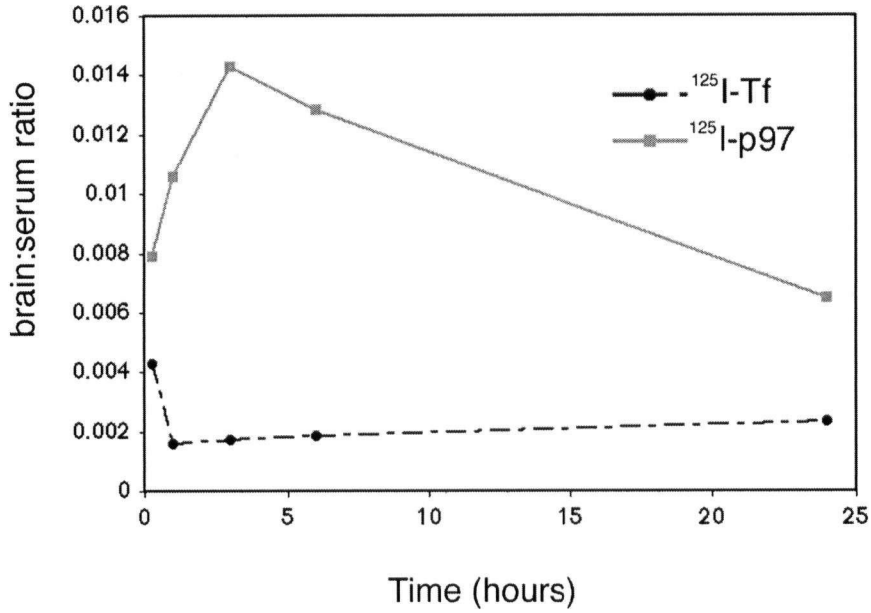

Figure 4.4: Uptake of ^{125}I-p97 and ^{125}I-Tf *in vivo*. a) The level of ^{125}I-p97 reaches a peak 3 hours after injection and is cleared from the brain within 5 hours. The maximum value of ^{125}I-p97 is approximately two fold higher than that of ^{125}I-Tf. b)Ratio of brain dpm: serum dpm for both ^{125}I-p97 and ^{125}I-Tf. (Moroo *et. al.* 2002)

Figure 4.5: Visualization of p97 and Tf uptake by the brain. Intraperitoneally injected **(a)** Alexa 488-p97 and **(b)** Alexa 488-Tf appear in the brain after one hr. Although p97 and Tf can be seen in the microvessels of respective mice (solid arrows), p97 appears to transcytose the BBB more efficiently than Tf and exhibits a punctate distribution in the cytoplasm of cerebral cortical cells (open arrows). Scale bar represents 10 μm. **(c)** After DIG-labeled p97 was injected into a mouse, the brain was harvested, sectioned, and the p97 localized with colloidal gold conjugated anti-DIG antibody and visualized by gold enhancement. Although parenchymal structures are weakly fixed, this electron micrograph shows that DIG conjugated p97 crosses the intact BBB and can be seen in the brain parenchyma. Scale bar represents 1 μm. (Moroo *et. al.,* 2002).

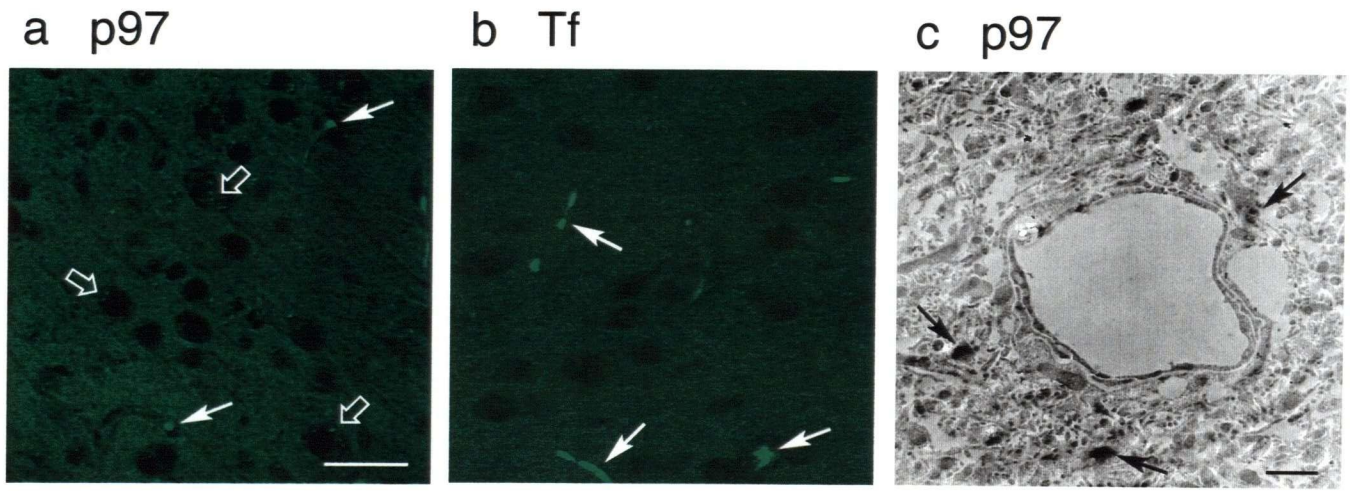
a p97
b Tf
c p97

is the endothelial cells of the brain microvascular system. When the RNA from these cells grown in culture was harvested and used in a RT-PCR reaction, the TfR2 α signal is clearly present (see Figure 4.3). Transferrin receptor 2 has 2 forms, due to alternate splicing events. One form is called the α form and includes exons 1, 2 and 3, and has both the full transmembrane domain and signal sequence, and is expressed on the surface of cells (Kawabata *et al.*, 1999). The second, or β form of TfR2 lacks exons 1, 2, and 3, which code for the transmembrane and intracellular portions of the protein, including the signal sequence, and is likely to be located intracellularly. This form is detected in small amounts in nearly all tissues and cell lines examined through RT-PCR (Kawabata *et al.*, 1999). To ensure that the form of the transcript present in the microvascular cells of the brain is the α form, primers were designed such that the forward primer is complementary to a sequence within exon 3, which is found in the transcript of the TfR2 α form, but not β form (Kawabata *et al.*, 1999) (Figure 4.3a).

The role of TfR2 in the cells of the BBB is not known. It has not been demonstrated if this protein is located luminally or abluminally, or if it is capable of undergoing transcytosis. Future experiments must be undertaken to examine the localization of TfR2 in various polarized cells. If the protein is expressed specifically on the apical surface of the polarized cells, this would suggest that it may be expressed on the luminal surface, or the surface facing the blood, in cerebral microvessels. This must also be confirmed with direct antibody staining once a good antibody is developed. It has been suggested that the high serum levels of p97 observed with Alzheimer disease may be due to an increased production of p97 in the brain, and that this p97 may be able to

cross the BBB from the brain to the serum via a receptor. More work will have to be done before one can conclude that TfR2 is involved in this process.

II. Subcellular localization

A. Rationale

To further characterize TfR2, and as an initial step toward eventual transcytosis experiments, it is important to examine where the receptor is located in the cell and what vesicles it travels through along the internalization pathway. The endocytosis pathway of TfR1 is very well studied, and has long been cited as a classical model of receptor mediated endocytosis. Endocytosis of the TfR1 has been shown to require the cytoplasmic domain of the receptor, specifically the YTRF motif (which conforms to the classical YXXO endocytosis signal that consists of an aromatic amino acid, often tyrosine, followed by two large hydrophobic residues) (Collawn *et al.*, 1990; Iacopetta *et al.*, 1988; Jing *et al.*, 1990; Rothenberger *et al.*, 1987a). The hypothesized endocytosis motif is also present in TfR2, with YQRV (tyrosine, glutamine, arginine, and valine) closely resembling the classical endocytosis motif (Kawabata *et al.*, 1999). To investigate the endocytosis of this protein, confocal microscopy was used to examine TfR2 expressing cells that were immunofluorescently labeled with markers of the endocytic vesicles. The hypothesis to be tested is that TfR2 follows a similar endocytosis pathway to TfR1, and that it is localized to the early endosome during receptor mediated endocytosis.

Another question that may increase the understanding of the function of TfR2 is whether TfR2 might function in tandem with TfR1. Transferrin receptor 1 exists at the

cell surface as a homodimer, with two disulphide bonds forming in the extracellular portion of the molecule to hold together the two monomers. TfR2 is also present as a homodimer (Kawabata *et al.*, 1999), and has cysteines in a similar position to those found in TfR1. The possibility that the two receptors can exist as heterodimers on cells that express both receptors is addressed in this section. The hypothesis is that TfR1 andTfR2 form heterodimers on the surface of cells.

B. Results I: Confocal immunofluorescence

Two sets of immunofluorescence experiments were carried out to assess which subcellular compartments TfR2 is found in. In the first experiment, shown in Figure 4.6a) the SK-Mel-28 human melanoma cells were transiently transfected with a myc-tagged mouse TfR2 construct. These cells were then double stained with antibody against the myc tag (9E10) and antibody against the early endosomal antigen (EEA1), which recognizes a membrane bound protein that is both specific to the early endosome and essential for fusion between early endocytic vesicles. The cells were grown on coverslips, washed and blocked with 1% BSA in PBS, and permeablized with saponin. This permeablization step allows the antibody to enter the cell, as both antigens are intracellular. In this experiment, the EEA1 antigen is shown in green (visualized with secondary antibody rabbit anti-goat Alexa 488), and is depicted alone in the first frame of the figure. Antibody against c-myc (the marker on the mTfR2) is shown in red (with secondary antibody rabbit anti-mouse Alexa 568), alone in the second frame. The

Figure 4.6: Subcellular localization of transferrin receptor 2 in transfected human melanoma cells, SK-mel-28. a) EEA1 is shown in green, in the first panel, visualized an anti-EEA1 antibody and with rabbit anti-goat Alexa 488 secondary antibody. Mouse TfR2 is stained with anti-myc antibody 9E10 in the center panel, and visualized with rabbit anti-mouse Alexa 568. The merged image is shown on the right. b) Anti-clathrin antibody staining the transfected human melanoma cell line is shown in green on the left, visualized with goat anti-rabbit Alexa 488. Mouse TfR2 is stained with 9E10, and visualized with the secondary goat anti-mouse Alexa 568. The right frame shows the merged image. In both a) and b) some yellow punctate staining indicating colocalization is indicated with large arrows, while the small arrows indicate no colocalization.
Scale bar=5μm

a)

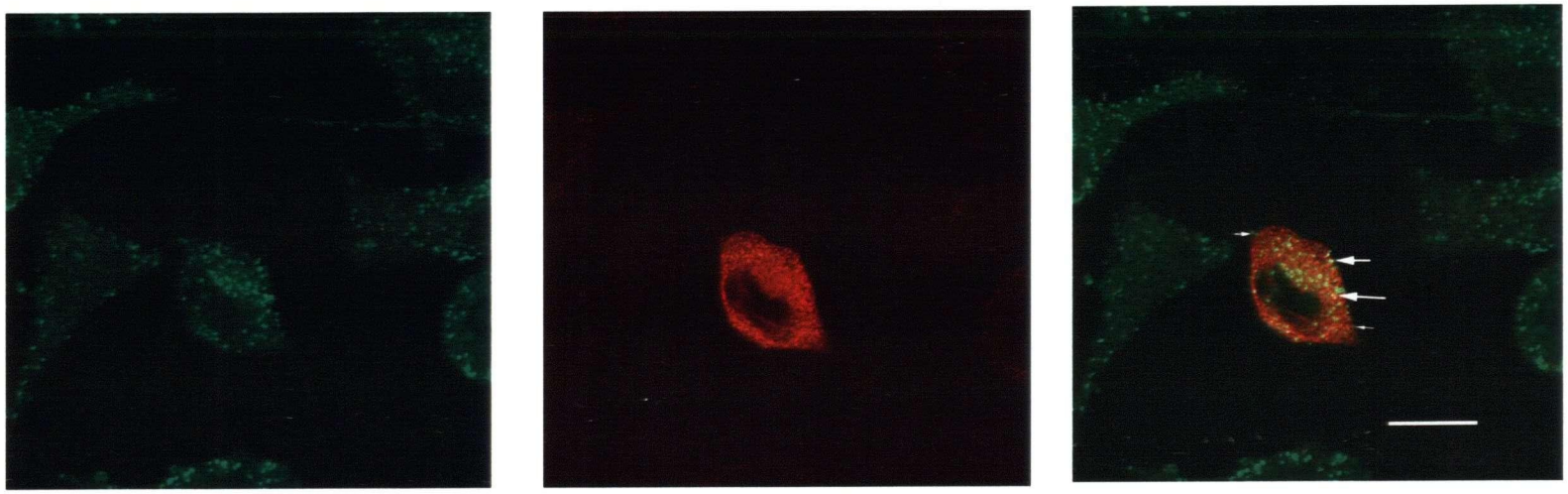

EEA-1 c-myc (mouseTfR2) merged image

b)

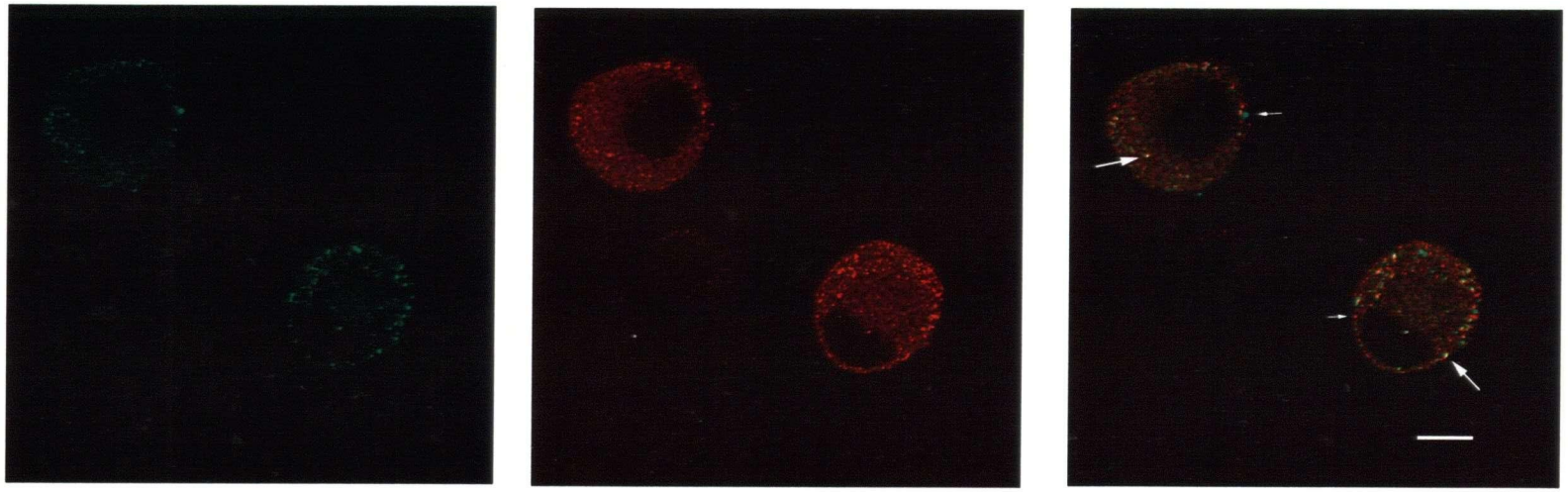

Clathrin c-myc (mouseTfR2) merged image

merged image is seen in the third frame. The areas where the EEA1 and TfR2 colocalize are visualized as yellow, and indicated with the larger arrows.

Another marker of endosomes is the clathrin heavy chain. Clathrin heavy chain is found in vesicles that have originated from both the plasma membrane and trans-golgi network (Robinson and Pearse, 1986). In receptor mediated endocytosis, the receptors are associated with clathrin coated vesicles (Mellman, 1996). In this double labeling experiment, antibodies against the myc tag and those against the clathrin heavy chain were used. In figure 4.6b), the left frame shows the antibody against the clathrin heavy chain (in green, detected with goat anti-rabbit Alexa fluor 488). The middle frame shows anti-c-myc, which recognizes the myc tag on the TfR2, and is visualized in red (with goat anti-mouse Alexa 568). The right frame is the merged image, with yellow representing the areas where the clathrin heavy chain and the TfR2 are colocalized. In both a) and b), areas of colocalization are shown with large arrows, whereas areas that show single staining are indicated for comparison with small arrows.

C. Results II: Western blot of heterodimers of transferrin receptors 1 and 2

To determine if TfR1 and 2 form heterodimers on the surface of the cells, cells without transferrin receptors, cells with TfR1 or TfR2, and cells with both TfR1 and TfR2 were examined. A FACs profile showing the level of expression of both proteins on the four cell lines is shown in Figure 4.7a and b. The cells were harvested with versene, counted and aliquoted to 2 million cells per tube. The cells were then incubated with anti-TfR1 antibody, normal rabbit serum, or no first antibody on ice, and washed to remove any unbound antibody. Next, the cells were solublized and immunoprecipitated

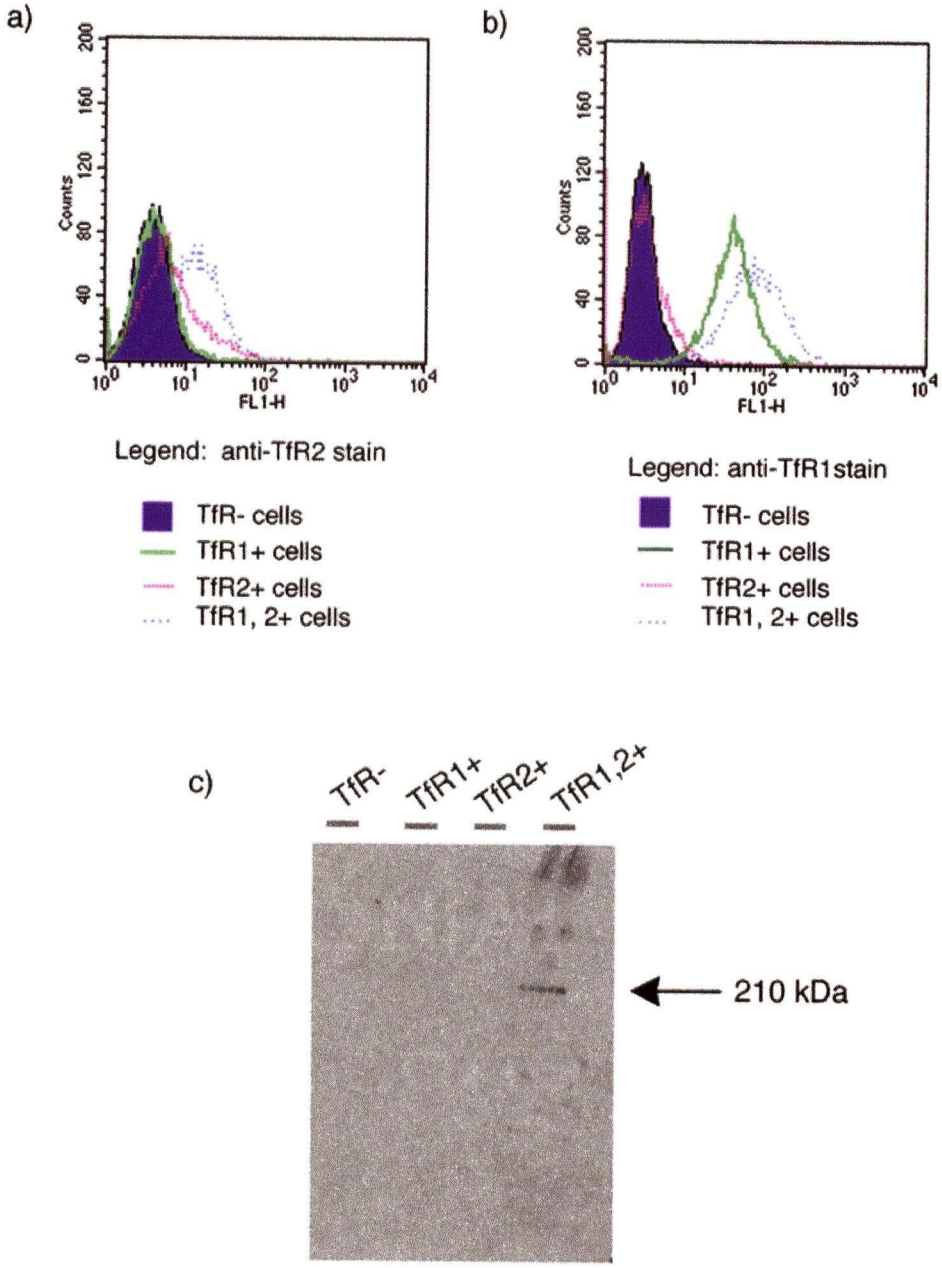

Figure 4.7: Western blot of heterodimers of transferrin receptors 1 and 2. a) FACS profile showing expression of TfR2 on TfR-, TfR1+, TfR2+, and TfR1,2+ cells. b) FACS profile showing expression of TfR1 on TfR-, TfR1+, TfR2+, and TfR1,2+ cells. c) Western blot showing TfR-, TfR1+, TfR2+, and TfR1,2+ cells immunoprecipitated with anti-TfR1 antibody and blotted with anti-FLAG antibody to detect TfR2.

with protein G sepharose beads. Finally, the lysates were run on an 8% SDS-PAGE gel and transferred to nitrocellulose. The lysates were not reduced with DTT, so the disulphide bonds between receptors were not broken. The membrane was then blotted with an antibody against the FLAG-tag of hTfR2. Figure 4.7c shows that a band at 210 kDa is present only in the lane loaded with lysate from cells that express both TfR1 and TfR2.

D. Discussion

Confocal immunofluorescence microscopy is a sensitive way to examine subcellular localization of proteins. With this technique, optical slices allow one to distinguish vesicles within the cell, and double labeling can determine if two proteins are co-localized within the same vesicle. The TfR2, shown in Figure 4.6a), co-localizes with a marker of early endosomes, EEA1, as well as with clathrin (Figure 4.6b), another marker of endosomes. This is shown by the punctate yellow staining pattern in the cells, indicated by a large arrow. This result supports the hypothesis that TfR2 follows the same endocytic pathway as TfR1 (Tiong, 2001). This is logical, as the endocytic signal present in the cytoplasmic portion of TfR2 is similar to that of TfR1. The endocytic recycling process of TfR1 is a very well studied phenomenon. The binding of ligand to receptor at the cell surface stimulates an accumulation of ligand-receptor complexes at clathrin-coated pits, which eventually bud off of the cell surface and become clathrin-coated vesicles. These vesicles lose their clathrin coats and fuse with early endosomes. The pH of endosomes is approximately 6-6.8, and this slightly acidic nature promotes the dissociation of many ligands from their complexes (Forgac, 1992; Robinson and Pearse,

1986). The receptors accumulate in the tubular extension regions of the early endosomes after the removal of ligand, and these extensions bud off to become recycling vesicles that transport the receptor back to the cell surface (Mellman, 1996). The ligands that remain accumulate within the vesicles and these early endosomes then fuse with late endosomes or lysosomes.

In the case of the TfR1, Tf does not dissociate at the pH of the endosome, but iron which is bound to Tf does dissociate. The apo-Tf at this pH remains bound to TfR1 and is recycled to the cell surface. With TfR2, Kawabata and associates have demonstrated that ^{55}Fe can accumulate in the TfR2+ cells after incubation with Tf-^{55}Fe (Kawabata *et al.*, 1999). The confocal results support the hypothesis that TfR2 follows a similar pathway to that of TfR1, but further research must be completed to confirm this. One experiment that is underway involves the mutation of the endocytic signal of TfR2 from 23YRRV26 to ARRV. In TfR1, this tyrosine to arginine mutation leads to an 80% decrease in internalization of the TfR1 (Collawn *et al.*, 1990). It will be interesting to see if TfR2 is affected in a similar way.

The Western blot experiment, shown in Figure 4.7 demonstrates that TfR1 and TfR2 form heterodimers on the cell surface. The flow cytometry data in 4.7a shows that only the TfR2+ and TfR1, 2+ cell lines express TfR2. The high background fluorescence is likely due to the fact that the TfR2 FLAG marker is an intracellular antigen. In Figure 4.7b it is clear that only the TfR1+ and TfR1,2+ cells stain positively for presence of TfR1. The immunoprecipitation experiment was performed by doing an identical immunoprecipitation on the four cells lines: TfR-, TfR1+, TfR2+, and TfR1,2+. Since the antibody for the immunoprecipitation was added to intact cells, the proteins being

immunoprecipitated are more likely to represent functional surface expressed receptors as opposed to those retained internally, such as in the endoplasmic reticulum. The Western blot was stained with an anti-FLAG antibody, which recognizes the FLAG tag of TfR2. The fact that no FLAG-tagged protein is seen in the third lane (that of TfR2+ cells) but is clearly present in the fourth lane (TfR1,2+ cells) indicates that the protein in lane 4 is present because it was immunoprecipitated in conjunction with TfR1, which was specifically immunoprecipitated by the anti-TfR1 antibody. The size of the protein on the Western blot closely corresponds with the known size of the TfR1 homodimer (~210 kDa), and once the gel was stripped and the blot detected with an anti-TfR1 antibody, the bands correspond in size (data not shown).

The presence of TfR1 and TfR2 as a heterodimeric complex leads to some interesting new questions about TfR2 function. If the two receptors function as one unit in some cells in which they are both expressed, such as erythroid cells (Kawabata *et al.*, 2000) and cells of the BBB (Jefferies *et al.*, 1984), perhaps the presence of the TfR1 confers some iron-responsiveness to the function of the heterodimer. Transferrin receptor 2 does not possess an iron response element (Kawabata *et al.*, 1999), and does not exhibit any modulation of expression due to iron levels (Fleming *et al.*, 2000). Transferrin receptor 1, on the other hand, is tightly regulated by the iron levels of the body, as discussed earlier. This iron-responsiveness is shared by many of the proteins involved in the iron uptake, transport and storage pathway, thus would seem very important for tight regulation of this system. When TfR1 expression is down-regulated due to high intracellular levels of iron, this may down-regulate the heterodimer, and curtail any function that it may have had. Some level of iron-responsiveness conferred on the

function of TfR2 may be advantageous in certain situations. Further experiments to determine if this heterodimerization occurs *in vivo*, rather than in transfected cell lines, will be important to carry out, as well as experiments designed to discover if this phenomenon has a specific function, and if it is actually iron-sensitive.

III. Cloning, constructs and transfections of mouse transferrin receptor 2

A. Rationale

In order to study this new protein, the full sequence of the cDNA had to be determined, followed by insertion into a cloning vector for manipulation. For ease of identification in the absence of a good antibody against the protein, the mouse TfR2 was expressed with a myc-tag on the C-terminal end of the protein and was transfected into cells. The myc tag represents a portion of the human *c-myc* oncogene product, and includes the epitope 410-419 of human *c-myc* recognized by the anti-c-myc monoclonal antibody, 9E10 (Campbell *et al.*, 1992).

B. Results I: Sequence of mouse transferrin receptor 2

The mouse EST, ATCC # 1978344 was originally derived from a 14 day *mus musculus* embryo. Through sequence analysis and comparison to the published human TfR2 sequence, it was confirmed that the EST was from mouse TfR2, and that the clone represented the full-length TfR2 cDNA. Figure 4.8 shows the full length TfR2 cDNA sequence derived from "primer walking", where additional primers are designed from the sequence already obtained to generate additional sequence until the entire cDNA

Figure 4.8: Sequence alignment of the transferrin receptors. Aligned sequences of mouse TfR2, mouse TfR1 (Stearne *et al.*, 1985), human TfR2 (Kawabata *et al.*, 1999), and human TfR1 (Schneider *et al.*, 1984). Shaded areas represent homologous sequence, while the boxed areas represent identical sequence.

```
mTfR2   1  MEQRWGLLRRVQQWSPRPSQTIYRRV---EGPQLEH  33
mTfR1   1  MMDQARSAFSNLFGGEPLS---YTRFSLARQVDGDN  33
hTfR2   1  MERLWGLFQRAQQLSPRSSQTVYQRV---EGPRKGH  33
hTfR1   1  MMDQARSAFSNLFGGEPLS---YTRFSLARQVDGDN  33

mTfR2  34  LEEE--DREEGAELPAQFCPMELKGPEHLGSCPGRS  67
mTfR1  34  SHVEMKLAADEEENADNNMKASVRKPKRFNGRLCFA  69
hTfR2  34  LEEEEEDGEEGAETLAHFCPMELRGPEPLGSRPRQP  69
hTfR1  34  SHVEMKLAVDEEENADNNTKANVTKPKRCSGSIC-Y  68

mTfR2  68  IPIPWAAAGRKAAPYLVLITLLIFTGAFLLGY----  99
mTfR1  70  AIALVI-FFLIGFMSGYLGYCKRVEQKEECVKL---  101
hTfR2  70  NLIPWAAAGRRAAPYLVLTALLIFTGAFLLGY----  101
hTfR1  69  GTIAVIVFFLIGFMIGYLGYCKGVEPKTECERLAGT  104

mTfR2 100  VAFRGSCQACGDSVLVVDEDVNPEDSGRTT----LY  131
mTfR1 102  --AETEETDK----------SETMETEDVPTSSRLY  125
hTfR2 102  VAFRGSCQACGDSVLVVSEDVNYEPDLDFHQGRLYW  137
hTfR1 105  ESPVRE----EPGEDFPAARRLYWDDLKRKLSEKLD  136

mTfR2 132  WSDLQAMFLRFLGEGRMEDTIRLTS-------LRER  160
mTfR1 126  WADLKTLLSEKLNSIEFADTIKQ----LSQNTYTPR  157
hTfR2 138  -SDLQAMFLQFLGEGRLEDTIR----QTSLRERVAG  168
hTfR1 137  STDFTSTIKLLNENSYVPREAGSQKDENLAL-----  167

mTfR2 161  VAGSARMATLVQDILDKLSRQKLDHVWTDTHYVGLQ  196
mTfR1 158  EAGSQKDESLAYYIENQFHEFKFSKVWRDEHYVKIQ  193
hTfR2 169  SAG---MAALTQDIRAALSRQKLDHVWTDTHYVGLQ  201
hTfR1 168  -------------YVENQFREFKLSKVWRDQHFVKIQ  191

mTfR2 197  FPDPAHANTLHWVDADGSVQEQLPLEDPEVYCPYSA  232
mTfR1 194  VKSSIGQNMVTIVQSNGNLD---PVESPEGYVAFSK  226
hTfR2 202  FPDPAHPNTLHWVDEAGKVGEQLPLEDPDVYCPYSA  237
hTfR1 192  VKDSA-QNSVIIVDKNGRL--VYLVENPGGYVAYSK  224

mTfR2 233  TGNATGKLVYAHYGRSEDLQDLKAKGVELAGSLLLV  268
mTfR1 227  PTEVSGKLVHANFGTKKDFEELS---YS-VNGSL-V  257
hTfR2 238  IGNVTGELVYAHYGRPEDLQDLRARGVDPVGRLLLV  273
hTfR1 225  AATVTGKLVHANFGTKKDFEDL----YTPVNGSIVI  256
```

```
mTfR2 269  RV--GITSFAQKVAVAQDFGAQGVLIYPDPSDFSQD  302
mTfR1 258  IVRAGEITFAEKVANAQSFNAIGVLIYMDKNKF---  290
hTfR2 274  RVGV--ISFAQKVTNAQDFGAQGVLIYPEPADFSQD  307
hTfR1 257  VRAGKIT-FAEKVANAESLNAIGVLIYMDQTKF---  288

mTfR2 303  PHKPGLSSHQAVYGHVHLGTGDPYTPGFPSFNQTQF  338
mTfR1 291  ---PVVEADLALFGHAHLGTGDPYTPGFPSFNHTQF  323
hTfR2 308  PPKPSLSSQQAVYGHVHLGTGDPYTPGFPSFNQTQ-  342
hTfR1 289  ---PIVNAELSFFGHAHLGTGDPYTPGFPSFNHTQF  321

mTfR2 339  PPVESSGLPSIPAQPISADIADQLLRKLTGPVAPQE  374
mTfR1 324  PPSQSSGLPNIPVQTISRAAAEKLFG-KMEGSC---  355
hTfR2 343  ----------------------KLKG----PVAPQE  352
hTfR1 322  PPSRSSGLPNIPVQTISRAAAEKLFGN-MEGDCPSD  356

mTfR2 375  WKGHLSGSPYRLGPGPDLRLVVNNHRVSTPIS--NI  408
mTfR1 356  PARWNIDSSCKLELSQNQNVKLIVKNVLKERRILNI  391
hTfR2 353  WQGSLLGSPYHLGPGPRLRLVVNNHRTSTPIN--NI  386
hTfR1 357  WKTDSTCRMVTSESK---NVKLTVSNVLKEIKILNI  389

mTfR2 409  FACIEGFAEPDHYVVIGAQRDAWGPG-AAKSAVGTA  443
mTfR1 392  FGVIKGYEEPDRYVVVGAQRDALGAGVAAKSSVGTG  427
hTfR2 387  FGCIEGRSEPDHYVVIGAQRDAWGPG-AAKSAVGTA  421
hTfR1 390  FGVIKGFVEPDHYVVVGAQRDAWGPG-AAKSGVGTA  424

mTfR2 444  ILLELVRTFSSMVSN--GFRPRRSLLFISWDGGDFG  477
mTfR1 428  LLLKLAQVFSDMIS-KDGFRPSRSIIFASWTAGDFG  462
hTfR2 422  ILLELVRTFSSMV-SN-GFRPRRSLLFISWDGGDFG  455
hTfR1 425  LLLKLAQMFSDMVL-KDGFQPSRSIIFASWSAGDFG  459

mTfR2 478  SVGATEWLEGYLSVLHLKAVVYVSLDNSVLGDGKFH  513
mTfR1 463  AVGATEWLEGYLSSLHLKAFTYINLDKVVLGTSNFK  498
hTfR2 456  SVGSTEWLEGYLSVLHLKAVVYVSLDNAVLGDDKFH  491
hTfR1 460  SVGATEWLEGYLSSLHLKAFTYINLDKAVLGTSNFK  495

mTfR2 514  AKTSPLLVSLIENILKQVDSPNHSGQTLYEQVALTH  549
mTfR1 499  VSASPLLYTLMGKIMQDVKHP-VDGKSLYRDSNWI-  532
hTfR2 492  AKTSPLLTSLIESVLKQVDSPNHSGQTLYEQVFTN  527
hTfR1 496  VSASPLLYTLIEKTMQNVKHP-VTGQFLYQDSNW-A  529
```

```
mTfR2 550  PSWDAEVIQPLPMDSSAYSFTAFAGVPAVEFSFMED  585
mTfR1 533  -SKV-EK---LSFDNAAYPFLAYSGIPAVSFCFCED  563
hTfR2 528  PSWDAEVIRPLPMDSSAYSFTAFVGVPAVEFSFMED  563
hTfR1 530  -SKV-EK---LTLDNAAFPFLAYSGIPAVSFCFCED  560

mTfR2 586  DRVYPFLHTEEDTYENLHKMLRGRLPAVVQAVAQLA  621
mTfR1 564  AD-YPYLGTRLDTYEALTQKVP-QLNQMVRTAAEVA  597
hTfR2 564  DQAYPFLHTKEDTYENLHKVLQGRLPAVAQAVAQLA  599
hTfR1 561  TD-YPYLGTTMDTYKELIERIP-ELNKVARAAAEVA  594

mTfR2 622  GQLLIRLSHDHLLPLDFGRYGDVVLRHIGNLNEFSG  657
mTfR1 598  GQLIIKLTHDVELNLDYEMYNSKLLSFMKDLNQFKT  633
hTfR2 600  GQLLIRLSHDRLLPLDFGRYGDVVLRHIGNLNEFSG  635
hTfR1 595  GQFVIKLTHDVELNLDYERYNSQLLSFVRDLNQYRA  630

mTfR2 658  DLKERGLTLQWVYSARGDYIRAAEKLRKEIYSSERN  693
mTfR1 634  DIRDMGLSLQWLYSARGDYFRATSRLTTDFHNAEKT  669
hTfR2 636  DLKARGLTLQWVYSARGDYIRAAEKLRQEIYSSEER  671
hTfR1 631  DIKEMGLSLQWLYSARGDFFRATSRLTTDFGNAEKT  666

mTfR2 694  DERLMRMYNVRIMR------VEFYFLSQYVSPADSP  723
mTfR1 670  NRFVMREINDRIMK------VEYHFLSPYVSPRESP  699
hTfR2 672  DERLTRMYNVRIMRIPLSAQVEFYFLSQYVSPADSP  707
hTfR1 667  DRFVMKKLNDRVMR------VEYHFLSPYVSPKESP  696

mTfR2 724  FRHIFLGQGDHTLGALVDHLRMLRADGSGAASSRLT  759
mTfR1 700  FRHIFWGSGSHTLSALVENLKL--------RQKNIT  727
hTfR2 708  FRHIFMGRGDHTLGALLDHLRLLRSNSSGTPGA--T  741
hTfR1 697  FRHVFWGSGSHTLPALLENLKLRK----------Q  721

mTfR2 760  AGLGFQESRFRRQLALLTWTLQGAANALSGDVWNID  795
mTfR1 728  A---FNETLFRNQLALATWTIQGVANALSGDIWNID  760
hTfR2 742  SSTGFQESRFRRQLALLTWTLQGAANALSGDVWNID  777
hTfR1 722  NNGAFNETLFRNQLALATWTIQGAANALSGDVWDID  757

mTfR2 796  NNF  798
mTfR1 761  NEF  763
hTfR2 778  NNF  780
hTfR1 758  NEF  760
```

sequence is known. The sequence in Figure 4.8 has been aligned to the human TfR2, as well as both human and mouse TfR1. The mouse TfR2 shares 40% amino acid identity with mouse TfR1, and 82% identity with its human orthologue. Through comparison to the human form of the protein, it was determined that the mouse TfR2 clone is the α-form of the TfR2, or the transmembrane (surface expressed) form of the protein.

Through sequence analysis it is clear that the newly discovered mouse TfR2 possesses an internalization signal at residues 23 to 26 that is very similar to that of the classical transferrin receptor. The mouse TfR2 internalization signal consists of a YRRV (tyrosine, arginine, arginine, and valine) which is very similar to the internalization signal of the mouse TfR1 and human TfR1 of YTRF (tyrosine, threonine, arginine, phenylalanine). In addition, the RGD sequence (arginine, glycine, and aspartate) located at amino acid residue 673 is completely conserved throughout all four proteins as shown in Figure 4.8. The RGD sequence is known to be critical to Tf binding to the TfR1 (Dubljevic *et al.*, 1999).

C. Results II: Myc-tagged mouse transferrin receptor 2 construct and transfections

Figure 4.9 depicts Chinese hamster ovary cells transfected with the vector containing the mouse TfR2 cDNA tagged with a human *c-myc* tag. As the antigen (*c-myc*) is located on the intracellular tail of the receptor, the cells were initially fixed with 2% paraformaldehyde then treated with 0.1 % saponin to permeablize the membrane and stained with anti-myc antibody. In Figure 4.9, the TfR2 can be seen on the cell surface of the four cells, as well as in vesicles within the cell, but is excluded from the nuclei. This

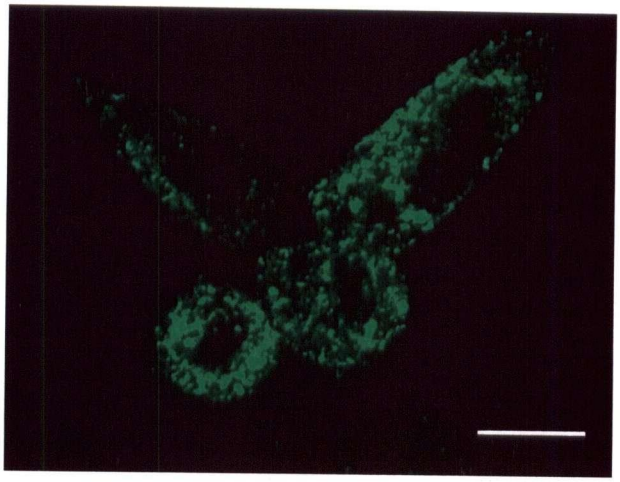

Figure 4.9: Chinese hamster ovary cells transfected with mouse transferrin receptor 2. Cells are permeablized and stained with the anti-c-myc antibody 9E10 followed by goat anti-mouse Alexa 488 to show subcellular localization of mouse TfR2. Scale bar = 5 μm

staining was performed to confirm the expression of the TfR2 and the presence of the mouse TfR2 on the cell surface prior to experiments to examine iron uptake.

D. Discussion

The full-length sequence of the mouse TfR2 reveals a 798 amino acid protein that shares 40% sequence identity with the classical mouse TfR1. It also shows 82% amino acid identity with its human orthologue. The proteins are very similar in many important aspects, including the internalization signals. The fact that the mouse TfR2 possesses an internalization signal that is very similar to that of the classical TfR1, and conforms to the typical format of an endocytosis signal, indicates that the receptor is probably able to internalize from the cell surface and targeted to the endosome in a manner similar to that of the classical receptor. This targeting was confirmed experimentally (Figure 4.6). The tyrosine-X-X-(hydrophobic residue) motif has been recognized as the motif involved in internalization of clathrin-coated pits by endocytosis, and is recognized by the μ2 subunit of AP2 adaptors (Owen and Evans, 1998). The AP2 subunit links the internalization signal to the clathrin coat through the μ2 subunit.

The putative transmembrane domain, determined through alignment of the mouse and human TfR2 proteins is 92% identical at the amino acid level to that of the human orthologue, with 22 of 24 amino acids shared between the two sequences. Overall, the level of cross species conservation is extremely high.

IV. Uptake of ^{55}Fe-loaded p97 by mouse transferrin receptor 2

A. Rationale

In order to determine if p97 is a ligand of TfR2, the ability of p97 to deliver its bound iron to cells via TfR2 was determined. This was accomplished by comparing the amount of iron taken up by TfR- and mouse TfR2+ cells. In chapter 3 it was shown that p97 does bind to the TfR1 in both radioligand studies and Pandex fluorescence studies. However, the ^{55}Fe uptake studies with p97 and TfR1 showed that p97 does not internalize iron via this method. For this reason, the more functional aspects of p97 uptake by mouse TfR2 were addressed initially. In addition, binding of p97 loaded with ^{55}Fe to the surface of cells at 4°C (therefore with no receptor internalization) was also examined. The hypothesis being tested is that ^{55}Fe-loaded p97 is able to both bind to cells via mouse TfR2, and internalize within the cells via the receptor.

B. Results I: ^{55}Fe-p97 uptake by mouse transferrin receptor 2

Figure 4.10 shows that significantly more radioactive iron ($p<0.005$ by Student's t-test) is internalized by the CHO-mouse TfR2+ cells than the cells transfected with vector alone. The cells were initially washed to remove any bound Tf, and blocked with BSA to try to minimize non-specific background binding of the protein to the cells. The cells were then incubated with ^{55}Fe-loaded p97 for 2 hours at 37°C, washed on ice and harvested for counting in the Beckman scintillation counter. The results are from a representative experiment, performed in triplicate.

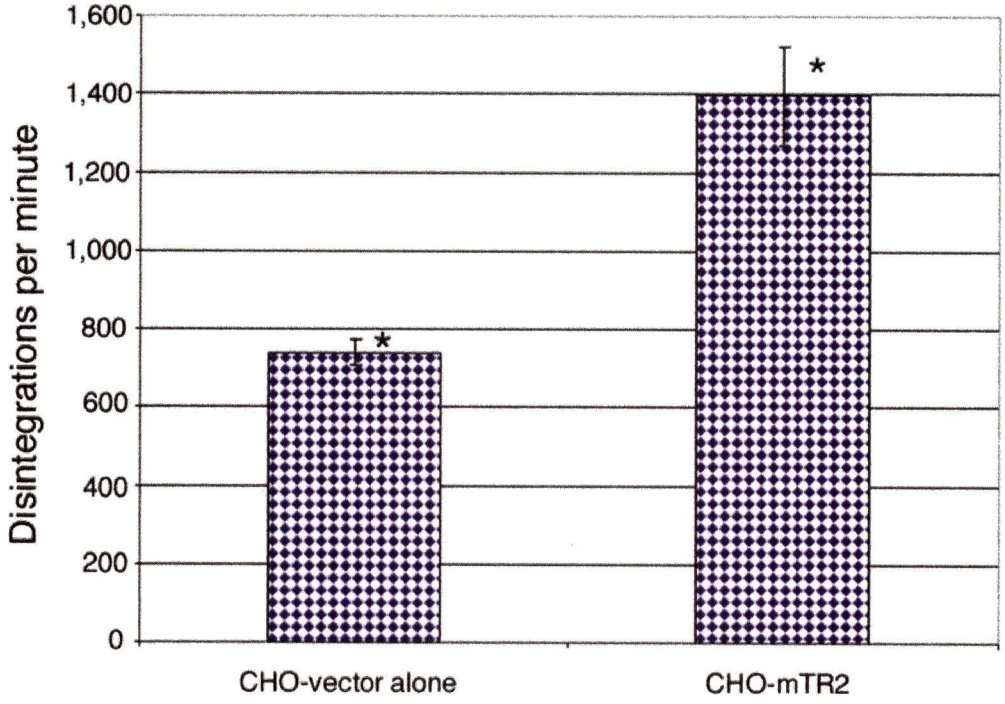

Figure 4.10: ^{55}Fe-loaded p97 uptake by Chinese hamster ovary cells and Chinese hamster ovary cells transfected with mouse transferrin receptor 2. The cells with and without the mouse TfR2 were allowed to internalize the ^{55}Fe-loaded p97 for 2 hours and the internalized counts were measured in a scintillation counter. Represents the mean +/- standard deviation for a representative experiment, n=6. *Statistical significance was assessed with the use of Student's t-test ($p<0.005$).

C. Results II: ^{55}Fe-p97 binding by mouse transferrin receptor 2

The cells in this experiment (TfR- and mouse TfR2+) were incubated with ^{55}Fe-loaded p97 at 4°C. The cells were then washed, harvested, and the DPM of the bound ^{55}Fe was determined in a scintillation counter. The TfR- cells in this experiment (Figure 4.11) have significantly less ^{55}Fe bound to the surface of the cells than the mouse TfR2+ cells, after being incubated with the iron loaded p97 (Student's t-test, $p<0.005$). The results are from a representative experiment, performed in triplicate.

D. Discussion

Two experiments were designed to show if p97 binds to TfR2, and if iron bound to p97 can be internalized by TfR2. These experiments both use human p97 and mouse TfR2. While human and mouse TfR2 are highly conserved (82% identity at the amino acid level), cross-species binding experiments are not ideal. They were, however, necessary in this case for a number of reasons. To begin, mouse p97 has been cloned, but is not yet available in the recombinant, soluble form at the quantities necessary for binding experiments. Secondly, while human TfR2 is available, and cloned into TfR- cells, (such as those used earlier in this chapter for the heterodimer experiments) these cells do not function as expected in the binding and uptake experiments. A series of experiments looking at ^{55}Fe-loaded p97 and Tf as well as ^{125}I-p97 and ^{125}I-Tf uptake and cell surface binding were undertaken, and the results were rather surprising. While the TfR1+ cells were able to both bind and internalize Tf, the TfR2+ cells were not. This is in contrast to the published results for TfR2+ cells taking up ^{55}Fe via Tf (Kawabata *et al.*, 1999). In fact, the TfR2+ cells had significantly less iron uptake than the TfR- cells (data

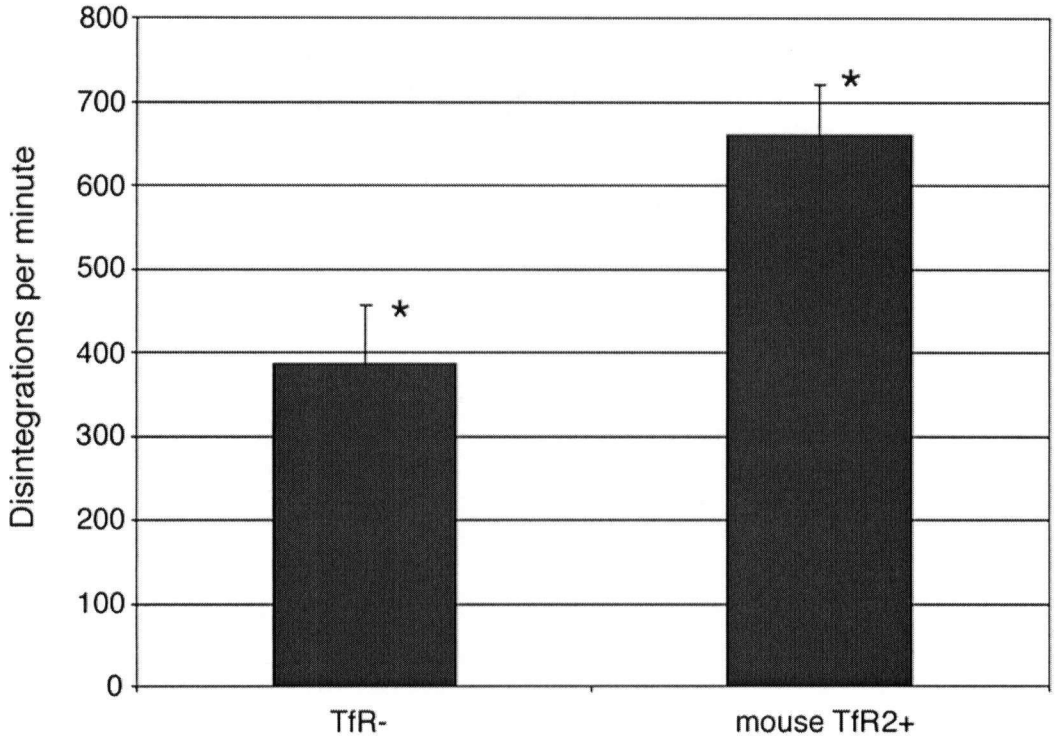

Figure 4.11: Binding of ^{55}Fe-loaded p97 to cells with and without the mouse transferrin receptor 2. TfR- and TfR2+ cells were incubated with ^{55}Fe-p97 on ice, and the bound radioactivity was measured in a scintillation counter. Represents the mean +/- standard deviation for a representative experiment, n=6. *Statistical significance was assessed with Student's t-test ($p<0.005$).

not shown). The TfR2 FLAG-tagged construct was generated by Kawabata and associates to transfect TRVb cells. However, the individual clone of TfR2+ cells used for these experiments is not the same cell clone as that published by the Koeffler group at the Cedars-Sinai Medical Centre, but was instead cloned in Caroline Enns' laboratory at Oregon Health Sciences University. To resolve the discrepancy between the activities of TfR2 in the two cell lines and to be able to draw conclusions about the function of TfR2 with regard to Tf uptake, additional studies on new clones should be undertaken. It is very likely that the unexpected decrease in internalized iron observed in the TfR2+ clones is a result of a problem with the expression of TfR2, or with the integration of the vector into the chromosomes of the cell.

Even though these experiments use mouse TfR2 and human p97, both the uptake of ^{55}Fe via p97 (Figure 4.10) and the cell surface binding of ^{55}Fe-loaded p97 (Figure 4.11) are clear. The differences between the DPM measured in both cases is statistically significant by Student's t-test ($p<0.005$). It seems logical that once the appropriate reagents are generated, the intra-species experiments (mouse p97 binding to mouse TfR2 and human p97 binding to human TfR2) may give even more convincing binding results.

Since p97 is very homologous to Tf, it is likely that the interaction between p97 and TfR2 is similar to that of Tf and TfR2, in terms of the binding pocket. While the binding pocket has not been studied in TfR2, some binding information is known. For example, it has been established that TfR2, like TfR1, binds Tf (although likely with lower affinity) and that TfR2, in contrast to TfR1, does not bind HFE (West *et al.*, 2000). One part of the binding pocket of human TfR1, the RGD motif (arginine, glycine, aspartate at 646-648), is known to be crucial to Tf binding (Dubljevic *et al.*, 1999). A

future experiment that is currently underway involves the mutation of this RGD site (which is fully conserved in both the mouse and human TfR2) by replacing the arginine with a lysine residue. This substitution leads to a reduction of Tf binding to TfR1 by 95% of the wild-type value (Dubljevic *et al.*, 1999). The effect that this mutation has on both p97 and Tf binding will answer some important questions regarding the action of TfR2.

Chapter 5: Conclusions and future directions

The field of iron uptake and transport has generated research interest for many years. Iron is essential to life because it participates in single electron oxidation-reduction reactions involved in a range of important biological processes including the production of ATP (Trinder *et al.*, 2000). Unregulated uptake and transport of iron is detrimental because it has the potential to lead to the formation of reactive oxygen species that cause molecular damage (Sayre *et al.*, 1999). New components of the iron uptake system are being discovered all the time, such as hepcidin, which is a small, soluble protein believed to be involved in communicating the iron storage status of the body to the absorptive cells of the intestine (Fleming and Sly, 2001). On the other hand, the function of some proteins involved in the iron uptake and transport system is still a mystery, despite the fact they were identified long ago. p97 is one of these proteins, with a function that remains controversial. The ability of GPI-p97 to take up iron and deliver the iron to the storage protein ferritin has been demonstrated (Tiong, 2001; Tiong and Jefferies, 2002), and this suggests that some niche does exist for p97 in the iron transport scheme. Some studies, however, have questioned the role of GPI-linked p97 in physiological iron uptake, both because p97 expression is not regulated by iron (Richardson, 2000), and because the Tf/TfR1 iron uptake system seems so efficient as an iron uptake system that additional systems seem redundant. The existence of a soluble form of p97 created through alternative splicing suggests that there maybe a unique function for this form of the protein. Elucidating this function through examining possible receptor interactions has been the major focus of this work.

The interaction of p97 with the most logical receptor choice, TfR1, was characterized with the use of radioligand assays and immunofluorescent labeling Pandex assays. These experiments have shown that p97 does interact with the TfR1 in binding experiments, that the interaction is pH specific (in that it occurs at pH 7.0 but not 6.0), and can be specifically competed with excess unlabeled p97. The binding also seems specific, as excess p97 can compete with the binding of labeled Tf to TfR1, and reduce the binding of Tf by approximately 30%. The failure of p97 to facilitate the internalization of iron via TfR1 indicates that this binding interaction is not likely to function in terms of classical iron uptake into the cell. This does not rule out the possibility that this interaction could function in some other capacity, such as to transport p97 across the BBB from the brain to the blood.

The BIAcore studies were not able to measure any interaction between p97 and TfR1. This indicates that if an interaction does exist between the two proteins, it may require other cellular components in order for the interaction to occur, or that the binding affinity was too low to measure with the sensitivity of the BIAcore. In the future it may be possible to increase the sensitivity of the system by increasing the percentage of the TfR1 that is immobilized on the chip in the proper orientation. In other studies, the TfR1 was coupled to the chip through an anti-His-tag antibody which recognized the His tag on the C-terminus of TfR1, thus a large percentage of the receptor was oriented correctly. In these studies the resonance signal generated for Tf binding was about 3 times that observed in the experiments included here (West *et al.*, 2000).

BIAcore studies were also undertaken to test another theory of p97 function: that due to the presence of an RGD motif in p97 similar to the RGD motifs present in the

ligands of many integrins, p97 may interact with a receptor such as the $\alpha_V\beta_3$ integrin. p97 has been implicated in angiogenesis, since it appears to stimulate vasculogenesis measured in a chick chorioallantoic assay (Sala *et al.*, 2002), thus an association with the integrin $\alpha_V\beta_3$, known to interact with the vascular endothelial growth factor receptor 2, seems possible (Borges *et al.*, 2000; Brooks *et al.*, 1994b). This experiment did not demonstrate binding between p97 and the integrin. The work should be expanded, however, to examine both the possible interaction of p97 with other integrins, and to include the study of binding to integrins in cell based systems, which would allow the interaction with other factors that may be crucial to the interaction.

In the search for other likely candidate receptors for p97, a novel homologue of the TfR1 was discovered through mining of the EST database. This receptor, independently published by Kawabata (Kawabata *et al.*, 1999), shows 45% identity and 66% similarity at the amino acid level, with TfR1. Through various experiments designed to characterize this new receptor, the expression was revealed to be largely restricted to the liver. In embryogenesis, the mouse TfR2 mRNA is present by E15 and continues to increase in expression through E17, in contrast to TfR1 mRNA that is discernable by E7, increases until E15 and decreases by E17. This research has also demonstrated that TfR2 is present on the brain endothelial cells that form the BBB, in contrast with results produced by Kawabata et al. This result is important as soluble p97 has been demonstrated to cross the BBB, and thus candidate receptors for this protein are likely to be expressed in the brain microvasculature (Moroo *et al.*, 2002).

Subcellular localization experiments have indicated that the TfR2 protein is internalized into vesicles that also stain for both EEA1 (a marker of early endosomes) and

clathrin heavy chain. Transferrin receptor 1 is known to localize to these same vesicles during endocytosis, thus it is likely that the two receptors follow the same internalization pathway. One future experiment to confirm this expression involves modification of the internalization signal of the TfR2, to determine if this modification will inhibit internalization of the receptor, as it does with TfR1. Another direction that will be interesting to explore in the future will be whether TfR2 is able to undergo transcytosis in polarized cells in a similar manner to TfR1. Transferrin receptor 1 has a basolateral sorting signal contained within residues 29 to 35 (Dargemont *et al.*, 1993; Odorizzi and Trowbridge, 1997), which do not seem to be highly conserved between the two receptors. Since TfR2 is present in the polarized cells of the BBB, the question of whether it undergoes sorting to the apical or basolateral side of a polarized cell, and if it can undergo transcytosis, are very pertinent.

Interestingly, in transfected cells that over express both TfR1 and TfR2, the receptor is present as a heterodimeric combination of the two receptors. This result must be examined further, as it poses some new and interesting questions. For instance, what unique role, if any, does this heterodimeric receptor play in cells that express both TfR1 and TfR2, such as cells in the erythroid lineage (Kawabata *et al.*, 2001). Since TfR1 is closely regulated by intracellular iron levels, would the heterodimerization of the two proteins confer some level of iron-regulation on whatever function this heterodimeric receptor carries out? The results of these functional experiments could be very interesting and lead to a new level of understanding in cellular iron uptake.

Mouse TfR2, which was isolated from the EST database and sequenced through the technique of "primer walking" to confirm that the full-length cDNA was generated,

displays 40% amino acid identity with mouse TfR1, and 82% amino acid identity with human TfR2. The mouse TfR2, cloned with a myc-tag on the C-terminus for identification, was transfected into both CHO cells and TfR- cells and tested for both p97 binding and iron uptake via p97. Human p97 was able to facilitate the uptake of ^{55}Fe through mouse TfR2, and the p97 was demonstrated to bind to the surface of the cells. These results are intriguing, because while p97 was able to bind to TfR1, the iron uptake or functional aspect of the interaction was not present. With TfR2, the functional aspect seems to occur along with the binding. The next steps in this research are already underway. First, a soluble form of mouse p97 is being generated for use in these studies, so that an inter-species binding system will no longer be necessary. As well, new clones of the human TfR2 in TfR- cells generated in the Enns' laboratory will soon be isolated for further work on the human p97 interaction with TfR2. In collaboration with Pamela Bjorkman's lab at the California Institute of Technology, new soluble recombinant forms of human TfR2 for BIAcore studies are being produced. While the Bjorkman group has produced soluble TfR2 for BIAcore studies in the past (West *et al.*, 2000), a problem with protein stability generated BIAcore results in this study that did not show Tf binding to TfR2 (data not shown), thus were also unsuccessful at demonstrating any interaction with p97. Hopefully this protein stability problem will be rectified in the near future and the binding interactions between p97 and TfR2 can be measured by BIAcore.

Clearly, identification of TfR2 as a receptor of p97 is only the first step toward the ultimate goal of clarifying the function of soluble p97. To reach this final conclusion, functional assays must be developed. The difficulty now will be to design these assays

and try to answer the pressing biological questions such as what p97 does as a soluble, iron binding protein, and why it is increased in Alzheimer disease.

Bibliography

Abbott, N. J., Chugani, D. C., Zaharchuk, G., Rosen, B. R. and Lo, E. H. (1999). Delivery of imaging agents into brain. *Adv Drug Deliv Rev* **37,** 253-277.

Abboud, S. and Haile, D. J. (2000). A novel mammalian iron-regulated protein involved in intracellular iron metabolism. *J Biol Chem* **275,** 19906-12.

Adams, P. C. and Chakrabarti, S. (1998). Genotypic/phenotypic correlations in genetic hemochromatosis: evolution of diagnostic criteria. *Gastroenterology* **114,** 319-23.

Aisen, P. and Leibman, A. (1968). The stability constants of the Fe3+ conalbumin complexes. *Biochem Biophys Res Commun* **30,** 407-13.

Aisen, P. and Leibman, A. (1972). Lactoferrin and transferrin: a comparative study. *Biochim Biophys Acta* **257,** 314-23.

Alemany, R., Vila, M. R., Franci, C., Egea, G., Real, F. X. and Thomson, T. M. (1993). Glycosyl phosphatidylinositol membrane anchoring of melanotransferrin (p97): apical compartmentalization in intestinal epithelial cells. *J Cell Sci* **104,** 1155-62.

Anderson, B. F., Baker, H. M., Norris, G. E., Rumball, S. V. and Baker, E. N. (1990). Apolactoferrin structure demonstrates ligand-induced conformational change in transferrins. *Nature* **344,** 784-7.

Andrews, N. C. (1999). The iron transporter DMT1. *Int J Biochem Cell Biol* **31,** 991-4.

Andrews, N. C. (2000). Iron homeostasis: insights from genetics and animal models. *Nat Rev Genet* **1,** 208-17.

Angel, P. and Karin, M. (1991). The role of Jun, Fos and the AP-1 complex in cell-proliferation and transformation. *Biochim Biophys Acta* **1072,** 129-57.

Attieh, Z. K., Mukhopadhyay, C. K., Seshadri, V., Tripoulas, N. A. and Fox, P. L. (1999). Ceruloplasmin ferroxidase activity stimulates cellular iron uptake by a trivalent cation-specific transport mechanism. *J Biol Chem* **274,** 1116-23.

Aziz, N. and Munro, H. N. (1987). Iron regulates ferritin mRNA translation through a segment of its 5' untranslated region. *Proc Natl Acad Sci U S A* **84,** 8478-82.

Bacon, B. R., Powell, L. W., Adams, P. C., Kresina, T. F. and Hoofnagle, J. H. (1999). Molecular medicine and hemochromatosis: at the crossroads. *Gastroenterology* **116,** 193-207.

Bailey, S., Evans, R. W., Garratt, R. C., Gorinsky, B., Hasnain, S., Horsburgh, C., Jhoti, H., Lindley, P. F., Mydin, A., Sarra, R. and et al. (1988). Molecular structure of serum transferrin at 3.3-A resolution. *Biochemistry* **27,** 5804-12.

Baker, E. N., Baker, H. M., Smith, C. A., Stebbins, M. R., Kahn, M., Hellstrom, K. E. and Hellstrom, I. (1992). Human melanotransferrin (p97) has only one functional iron-binding site. *FEBS Lett* **298,** 215-8.

Bali, P. K. and Aisen, P. (1992). Receptor-induced switch in site-site cooperativity during iron release by transferrin. *Biochemistry* **31,** 3963-7.

Bali, P. K., Zak, O. and Aisen, P. (1991). A new role for the transferrin receptor in the release of iron from transferrin. *Biochemistry* **30,** 324-8.

Baranano, D. E., Wolosker, H., Bae, B. I., Barrow, R. K., Snyder, S. H. and Ferris, C. D. (2000). A mammalian iron ATPase induced by iron. *J Biol Chem* **275,** 15166-73.

Barresi, G. and Tuccari, G. (1994). Immunocytochemical demonstration of melanotransferrin (p97) in thyroid tumors of follicular cell origin. *Pathology* **26,** 127-9.

Bartlett, W. P., Li, X. S. and Connor, J. R. (1991). Expression of transferrin mRNA in the CNS of normal and jimpy mice. *J Neurochem* **57,** 318-22.

Beal, M. F. (1998). Mitochondrial dysfunction in neurodegenerative diseases. *Biochim Biophys Acta* **1366,** 211-23.

Beard, P., Offord, E., Paduwat, N. and Bruggmann, H. (1991). SV40 activates transcription from the transferrin receptor promoter by inducing a factor which binds to the CRE/AP-1 recognition sequence. *Nucleic Acids Res* **19,** 7117-23.

Benito, P., House, W. and Miller, D. (1998). Comparison of oral and intraperitoneal iron supplementation in anaemic rats: a re-evaluation of the mucosal block theory of iron absorption. *Br J Nutr* **79,** 533-40.

Boguski, M. S. (1995). The turning point in genome research. *Trends Biochem Sci* **20,** 295-6.

Boguski, M. S., Lowe, T. M. and Tolstoshev, C. M. (1993). dbEST--database for expressed sequence tags. *Nat Genet* **4,** 332-3.

Borges, E., Jan, Y. and Ruoslahti, E. (2000). Platelet-derived growth factor receptor beta and vascular endothelial growth factor receptor 2 bind to the beta 3 integrin through its extracellular domain. *J Biol Chem* **275,** 39867-73.

Bottomley, S. S., Wolfe, L. C. and Bridges, K. R. (1985). Iron metabolism in K562 erythroleukemic cells. *J Biol Chem* **260,** 6811-5.

Bradbury, M. W. (1997). Transport of iron in the blood-brain-cerebrospinal fluid system. *J Neurochem* **69,** 443-54.

Brightman, M. W. (1992). Ultrastructure of brain endothelium. In *Physiology and Pharmacology of the Blood-brain Barrier* (ed. M. W. B. Bradbury), pp. 549. Berlin; New York: Springer Verlag.

Brooks, P. C., Clark, R. A. and Cheresh, D. A. (1994a). Requirement of vascular integrin alpha v beta 3 for angiogenesis. *Science* **264,** 569-71.

Brooks, P. C., Montgomery, A. M., Rosenfeld, M., Reisfeld, R. A., Hu, T., Klier, G. and Cheresh, D. A. (1994b). Integrin alpha v beta 3 antagonists promote tumor regression by inducing apoptosis of angiogenic blood vessels. *Cell* **79,** 1157-64.

Brown, J. P., Woodbury, R. G., Hart, C. E., Hellstrom, I. and Hellstrom, K. E. (1981). Quantitative analysis of melanoma-associated antigen p97 in normal and neoplastic tissues. *Proc Natl Acad Sci U S A* **78,** 539-43.

Bulaj, Z. J., Griffen, L. M., Jorde, L. B., Edwards, C. Q. and Kushner, J. P. (1996). Clinical and biochemical abnormalities in people heterozygous for hemochromatosis. *N Engl J Med* **335,** 1799-805.

Burke, W., Thomson, E., Khoury, M. J., McDonnell, S. M., Press, N., Adams, P. C., Barton, J. C., Beutler, E., Brittenham, G., Buchanan, A., Clayton, E. W., Cogswell, M. E., Meslin, E. M., Motulsky, A. G., Powell, L. W., Sigal, E., Wilfond, B. S. and Collins, F. S. (1998). Hereditary hemochromatosis: gene discovery and its implications for population-based screening. *Jama* **280,** 172-8.

Bush, A. I., Pettingell, W. H., Multhaup, G., d Paradis, M., Vonsattel, J. P., Gusella, J. F., Beyreuther, K., Masters, C. L. and Tanzi, R. E. (1994). Rapid induction of Alzheimer A beta amyloid formation by zinc. *Science* **265,** 1464-7.

Camaschella, C., Roetto, A., Cali, A., De Gobbi, M., Garozzo, G., Carella, M., Majorano, N., Totaro, A. and Gasparini, P. (2000). The gene TFR2 is mutated in a new type of haemochromatosis mapping to 7q22. *Nat Genet* **25,** 14-5.

Campbell, A. M., Kessler, P. D. and Fambrough, D. M. (1992). The alternative carboxyl termini of avian cardiac and brain sarcoplasmic reticulum/endoplasmic reticulum Ca(2+)-ATPases are on opposite sides of the membrane. *J Biol Chem* **267,** 9321-5.

Casey, J. L., Di Jeso, B., Rao, K. K., Rouault, T. A., Klausner, R. D. and Harford, J. B. (1988). Deletional analysis of the promoter region of the human transferrin receptor gene. *Nucleic Acids Res* **16,** 629-46.

Casey, J. L., Koeller, D. M., Ramin, V. C., Klausner, R. D. and Harford, J. B. (1989). Iron regulation of transferrin receptor mRNA levels requires iron-responsive elements and a rapid turnover determinant in the 3' untranslated region of the mRNA. *Embo J* **8,** 3693-9.

Collawn, J. F., Lai, A., Domingo, D., Fitch, M., Hatton, S. and Trowbridge, I. S. (1993). YTRF is the conserved internalization signal of the transferrin receptor, and a second YTRF signal at position 31-34 enhances endocytosis. *J Biol Chem* **268,** 21686-92.

Collawn, J. F., Stangel, M., Kuhn, L. A., Esekogwu, V., Jing, S. Q., Trowbridge, I. S. and Tainer, J. A. (1990). Transferrin receptor internalization sequence YXRF implicates a tight turn as the structural recognition motif for endocytosis. *Cell* **63,** 1061-72.

Connor, J. R. and Menzies, S. L. (1996). Relationship of iron to oligodendrocytes and myelination. *Glia* **17,** 83-93.

Connor, J. R., Menzies, S. L., Burdo, J. R. and Boyer, P. J. (2001). Iron and iron management proteins in neurobiology. *Pediatr Neurol* **25,** 118-29.

Conrad, M. E., Umbreit, J. N. and Moore, E. G. (1999). Iron absorption and transport. *Am J Med Sci* **318,** 213-29.

Cook, J. D., Skikne, B. S. and Baynes, R. D. (1993). Serum transferrin receptor. *Annu Rev Med* **44,** 63-74.

Crawford, D. H., Jazwinska, E. C., Cullen, L. M. and Powell, L. W. (1998). Expression of HLA-linked hemochromatosis in subjects homozygous or heterozygous for the C282Y mutation. *Gastroenterology* **114,** 1003-8.

Crowe, A. and Morgan, E. H. (1992). Iron and transferrin uptake by brain and cerebrospinal fluid in the rat. *Brain Res* **592,** 8-16.

Cullen, L. M., Summerville, L., Glassick, T. V., Crawford, D. H., Powell, L. W. and Jazwinska, E. C. (1997). Neonatal screening for the hemochromatosis defect [letter]. *Blood* **90,** 4236-7.

Dargemont, C., Le Bivic, A., Rothenberger, S., Iacopetta, B. and Kuhn, L. C. (1993). The internalization signal and the phosphorylation site of transferrin receptor are distinct from the main basolateral sorting information. *Embo J* **12,** 1713-21.

Dautry-Varsat, A., Ciechanover, A. and Lodish, H. F. (1983). pH and the recycling of transferrin during receptor-mediated endocytosis. *Proc Natl Acad Sci U S A* **80,** 2258-62.

de Silva, D., Davis-Kaplan, S., Fergestad, J. and Kaplan, J. (1997). Purification and characterization of Fet3 protein, a yeast homologue of ceruloplasmin. *J Biol Chem* **272,** 14208-13.

Devary, Y., Gottlieb, R. A., Lau, L. F. and Karin, M. (1991). Rapid and preferential activation of the c-jun gene during the mammalian UV response. *Mol Cell Biol* **11,** 2804-11.

Dewan, J. C., Mikami, B., Hirose, M. and Sacchettini, J. C. (1993). Structural evidence for a pH-sensitive dilysine trigger in the hen ovotransferrin N-lobe: implications for transferrin iron release. *Biochemistry* **32,** 11963-8.

Diamond, M. S. and Springer, T. A. (1994). The dynamic regulation of integrin adhesiveness. *Curr Biol* **4,** 506-17.

Dickinson, T. K., Devenyi, A. G. and Connor, J. R. (1996). Distribution of injected iron 59 and manganese 54 in hypotransferrinemic mice. *J Lab Clin Med* **128,** 270-8.

Donovan, A., Brownlie, A., Zhou, Y., Shepard, J., Pratt, S. J., Moynihan, J., Paw, B. H., Drejer, A., Barut, B., Zapata, A., Law, T. C., Brugnara, C., Lux, S. E., Pinkus, G. S., Pinkus, J. L., Kingsley, P. D., Palis, J., Fleming, M. D., Andrews, N. C. and Zon, L. I. (2000). Positional cloning of zebrafish ferroportin1 identifies a conserved vertebrate iron exporter. *Nature* **403,** 776-81.

Dubljevic, V., Sali, A. and Goding, J. W. (1999). A conserved RGD (Arg-Gly-Asp) motif in the transferrin receptor is required for binding to transferrin. *Biochem J* **341,** 11-4.

Duchange, N., Ochoa, A., Plowman, G. D., Roze, A., Amdjadi, M. and Zakin, M. M. (1992). Identification of an enhancer involved in the melanoma-specific expression of the tumor antigen melanotransferrin gene. *Nucleic Acids Res* **20,** 2853-9.

Ekblom, P. and Thesleff, I. (1985). Control of kidney differentiation by soluble factors secreted by the embryonic liver and the yolk sac. *Dev Biol* **110,** 29-38.

Evans, P. and Kemp, J. (1997). Exon/intron structure of the human transferrin receptor gene. *Gene* **199,** 123-31.

Feder, J. N., Gnirke, A., Thomas, W., Tsuchihashi, Z., Ruddy, D. A., Basava, A., Dormishian, F., Domingo, R., Jr., Ellis, M. C., Fullan, A., Hinton, L. M., Jones, N. L., Kimmel, B. E., Kronmal, G. S., Lauer, P., Lee, V. K., Loeb, D. B., Mapa, F. A., McClelland, E., Meyer, N. C., Mintier, G. A., Moeller, N., Moore, T., Morikang, E., Wolff, R. K. and et al. (1996). A novel MHC class I-like gene is mutated in patients with hereditary haemochromatosis. *Nat Genet* **13,** 399-408.

Feder, J. N., Tsuchihashi, Z., Irrinki, A., Lee, V. K., Mapa, F. A., Morikang, E., Prass, C. E., Starnes, S. M., Wolff, R. K., Parkkila, S., Sly, W. S. and Schatzman, R. C. (1997). The hemochromatosis founder mutation in HLA-H disrupts beta2-microglobulin interaction and cell surface expression. *J Biol Chem* **272,** 14025-8.

Feldman, H., Gabathuler, R., Kennard, M., Nurminen, J., Levy, D., Foti, S., Foti, D., Beattie, B. and Jefferies, W. (2001). Serum p97 levels as an aid to identifying Alzheimer's Disease. *Journal of Alzheimer's Disease* **3,** 507-516.

Ferris, C. D., Jaffrey, S. R., Sawa, A., Takahashi, M., Brady, S. D., Barrow, R. K., Tysoe, S. A., Wolosker, H., Baranano, D. E., Dore, S., Poss, K. D. and Snyder, S. H. (1999). Haem oxygenase-1 prevents cell death by regulating cellular iron. *Nat Cell Biol* **1,** 152-7.

Finch, C. (1994). Regulators of iron balance in humans. *Blood* **84,** 1697-702.

Fleming, R. E., Migas, M. C., Holden, C. C., Waheed, A., Britton, R. S., Tomatsu, S., Bacon, B. R. and Sly, W. S. (2000). Transferrin receptor 2: continued expression in mouse liver in the face of iron overload and in hereditary hemochromatosis. *Proc Natl Acad Sci U S A* **97,** 2214-9.

Fleming, R. E., Migas, M. C., Zhou, X., Jiang, J., Britton, R. S., Brunt, E. M., Tomatsu, S., Waheed, A., Bacon, B. R. and Sly, W. S. (1999). Mechanism of increased iron absorption in murine model of hereditary hemochromatosis: increased duodenal expression of the iron transporter DMT1. *Proc Natl Acad Sci U S A* **96,** 3143-8.

Fleming, R. E. and Sly, W. S. (2001). Hepcidin: a putative iron-regulatory hormone relevant to hereditary hemochromatosis and the anemia of chronic disease. *Proc Natl Acad Sci U S A* **98,** 8160-2.

Food, M. R., Rothenberger, S., Gabathuler, R., Haidl, I. D., Reid, G. and Jefferies, W. A. (1994). Transport and expression in human melanomas of a transferrin-like glycosylphosphatidylinositol-anchored protein. *J Biol Chem* **269,** 3034-40.

Forgac, M. (1992). Structure and properties of the coated vesicle proton pump. *Ann N Y Acad Sci* **671,** 273-83.

Fuchs, H., Lucken, U., Tauber, R., Engel, A. and Gessner, R. (1998). Structural model of phospholipid-reconstituted human transferrin receptor derived by electron microscopy. *Structure* **6,** 1235-43.

George, D. K., Ramm, G. A., Powell, L. W., Fletcher, L. M., Walker, N. I., Cowley, L. L. and Crawford, D. H. (1998). Evidence for altered hepatic matrix degradation in genetic haemochromatosis. *Gut* **42,** 715-20.

Gitlin, J. D. (1998). Aceruloplasminemia. *Pediatr Res* **44,** 271-6.

Goldwurm, S. and Powell, L. W. (1997). Haemochromatosis after the discovery of HFE (HLA-H). *Gut* **41,** 855-6.

Grasbeck, R., Majuri, R., Kouvonen, I. and Tenhunen, R. (1982). Spectral and other studies on the intestinal haem receptor of the pig. *Biochim Biophys Acta* **700,** 137-42.

Griffiths, W. J., Kelly, A. L., Smith, S. J. and Cox, T. M. (2000). Localization of iron transport and regulatory proteins in human cells. *Qjm* **93,** 575-87.

Gruenheid, S., Cellier, M., Vidal, S. and Gros, P. (1995). Identification and characterization of a second mouse Nramp gene. *Genomics* **25,** 514-25.

Gunshin, H., Mackenzie, B., Berger, U. V., Gunshin, Y., Romero, M. F., Boron, W. F., Nussberger, S., Gollan, J. L. and Hediger, M. A. (1997). Cloning and characterization of a mammalian proton-coupled metal-ion transporter. *Nature* **388,** 482-8.

Gutierrez, J. A., Yu, J., Rivera, S. and Wessling-Resnick, M. (1997). Functional expression cloning and characterization of SFT, a stimulator of Fe transport [published erratum appears in J Cell Biol 1999 Oct 4;147(1):following 204]. *J Cell Biol* **139,** 895-905.

Hashimoto, S. (2000). Principles of BIACORE. In *Real-Time Analysis of Biomolecular Interactions: Applications of Biacore* (ed. K. Nagata and H. Handa), pp. 256. Toyko: Springer-Verlag.

Hsu, F. (1997). Melanotransferrin. In *Biotechnology*. Vancouver: University of British Columbia.

Hu, D. D., Barbas, C. F. and Smith, J. W. (1996). An allosteric Ca2+ binding site on the beta3-integrins that regulates the dissociation rate for RGD ligands. *J Biol Chem* **271,** 21745-51.

Hynes, R. O. (1987). Integrins: a family of cell surface receptors. *Cell* **48,** 549-54.

Iacopetta, B. J., Rothenberger, S. and Kuhn, L. C. (1988). A role for the cytoplasmic domain in transferrin receptor sorting and coated pit formation during endocytosis. *Cell* **54,** 485-9.

Ikuta, K., Fujimoto, Y., Suzuki, Y., Tanaka, K., Saito, H., Ohhira, M., Sasaki, K. and Kohgo, Y. (2000). Overexpression of hemochromatosis protein, HFE, alters transferrin recycling process in human hepatoma cells. *Biochim Biophys Acta* **1496,** 221-31.

Jazwinska, E. C. and Powell, L. W. (1997). Hemochromatosis and HLA-H: definite! *Hepatology* **25,** 495-6.

Jefferies, W. A., Brandon, M. R., Hunt, S. V., Williams, A. F., Gatter, K. C. and Mason, D. Y. (1984). Transferrin receptor on endothelium of brain capillaries. *Nature* **312,** 162-3.

Jefferies, W. A., Food, M. R., Gabathuler, R., Rothenberger, S., Yamada, T., Yasuhara, O. and McGeer, P. L. (1996). Reactive microglia specifically associated with amyloid plaques in Alzheimer's disease brain tissue express melanotransferrin. *Brain Res* **712,** 122-6.

Jing, S. Q., Spencer, T., Miller, K., Hopkins, C. and Trowbridge, I. S. (1990). Role of the human transferrin receptor cytoplasmic domain in endocytosis: localization of a specific signal sequence for internalization. *J Cell Biol* **110,** 283-94.

Jing, S. Q. and Trowbridge, I. S. (1987). Identification of the intermolecular disulfide bonds of the human transferrin receptor and its lipid-attachment site. *Embo J* **6,** 327-31.

Jolley, M. E., Wang, C. H., Ekenberg, S. J., Zuelke, M. S. and Kelso, D. M. (1984). Particle concentration fluorescence immunoassay (PCFIA): a new, rapid immunoassay technique with high sensitivity. *J Immunol Methods* **67,** 21-35.

Kawabata, H., Germain, R. S., Vuong, P. T., Nakamaki, T., Said, J. W. and Koeffler, H. P. (2000). Transferrin receptor 2-alpha supports cell growth both in iron-chelated cultured cells and in vivo. *J Biol Chem* **275,** 16618-25.

Kawabata, H., Nakamaki, T., Ikonomi, P., Smith, R. D., Germain, R. S. and Koeffler, H. P. (2001). Expression of transferrin receptor 2 in normal and neoplastic hematopoietic cells. *Blood* **98,** 2714-9.

Kawabata, H., Yang, R., Hirama, T., Vuong, P. T., Kawano, S., Gombart, A. F. and Koeffler, H. P. (1999). Molecular cloning of transferrin receptor 2. A new member of the transferrin receptor-like family. *J Biol Chem* **274,** 20826-32.

Kennard, M. L., Feldman, H., Yamada, T. and Jefferies, W. A. (1996). Serum levels of the iron binding protein p97 are elevated in Alzheimer's disease. *Nat Med* **2,** 1230-5.

Kennard, M. L., Richardson, D. R., Gabathuler, R., Ponka, P. and Jefferies, W. A. (1995). A novel iron uptake mechanism mediated by GPI-anchored human p97. *Embo J* **14,** 4178-86.

Kim, D. K., Seo, M.Y., Lim, S.W., Kim, S., Kim, J.W., Carroll, B.J., Kwon, D. Y., Kwon, T., Kang, S.S. (2001). Serum melanotransferrin, p97 as biochemical marker of Alzheimer's disease. *Neuropsychopharmacology* **24,** In press.

Klausner, R. D., Ashwell, G., van Renswoude, J., Harford, J. B. and Bridges, K. R. (1983). Binding of apotransferrin to K562 cells: explanation of the transferrin cycle. *Proc Natl Acad Sci U S A* **80,** 2263-6.

Klomp, L. W. and Gitlin, J. D. (1996). Expression of the ceruloplasmin gene in the human retina and brain: implications for a pathogenic model in aceruloplasminemia. *Hum Mol Genet* **5,** 1989-96.

Knutson, M. D., Levy, J. E., Andrews, N. C. and Wessling-Resnick, M. (2001). Expression of stimulator of Fe transport is not enhanced in Hfe knockout mice. *J Nutr* **131,** 1459-64.

Krause, A., Neitz, S., Magert, H. J., Schulz, A., Forssmann, W. G., Schulz-Knappe, P. and Adermann, K. (2000). LEAP-1, a novel highly disulfide-bonded human peptide, exhibits antimicrobial activity. *FEBS Lett* **480,** 147-50.

Kuhn, L. C., Schulman, H. M. and Ponka, P. (1990). Iron-transferrin requirements and transferrin receptor expression in proliferating cells. In *Iron Transport and Storage* (ed. P. Ponka, R. C. Schulman and R. C. Woodworth), pp. 149-191. Boca Ratan, Fl.: CRC.

Lawrence, C. M., Ray, S., Babyonyshev, M., Galluser, R., Borhani, D. W. and Harrison, S. C. (1999). Crystal structure of the ectodomain of human transferrin receptor. *Science* **286,** 779-82.

Lebron, J. A., Bennett, M. J., Vaughn, D. E., Chirino, A. J., Snow, P. M., Mintier, G. A., Feder, J. N. and Bjorkman, P. J. (1998). Crystal structure of the hemochromatosis protein HFE and characterization of its interaction with transferrin receptor. *Cell* **93,** 111-23.

Levy, J. E., Jin, O., Fujiwara, Y., Kuo, F. and Andrews, N. C. (1999). Transferrin receptor is necessary for development of erythrocytes and the nervous system. *Nat Genet* **21,** 396-9.

Levy, J. E., Montross, L. K. and Andrews, N. C. (2000). Genes that modify the hemochromatosis phenotype in mice. *J Clin Invest* **105,** 1209-16.

Lok, C. N., Chan, K. F. and Loh, T. T. (1996). Transcriptional regulation of transferrin receptor expression during phorbol-ester-induced HL-60 cell differentiation. Evidence for a negative regulatory role of the phorbol-ester-responsive element-like sequence. *Eur J Biochem* **236,** 614-9.

Lok, C. N. and Ponka, P. (1999). Identification of a hypoxia response element in the transferrin receptor gene. *J Biol Chem* **274,** 24147-52.

Lok, C. N. and Ponka, P. (2000). Identification of an erythroid active element in the transferrin receptor gene. *J Biol Chem* .

Lonnerdal, B., Woodhouse, L. R. and Glazier, C. (1987). Compartmentalization and quantitation of protein in human milk. *J Nutr* **117,** 1385-95.

MacGillivray, R. T., Bewley, M. C., Smith, C. A., He, Q. Y., Mason, A. B., Woodworth, R. C. and Baker, E. N. (2000). Mutation of the iron ligand His 249 to Glu in the N-lobe of human transferrin abolishes the dilysine trigger; but does not significantly affect iron release. *Biochemistry* **39,** 1211-6.

MacGillivray, R. T., Moore, S. A., Chen, J., Anderson, B. F., Baker, H., Luo, Y., Bewley, M., Smith, C. A., Murphy, M. E., Wang, Y., Mason, A. B., Woodworth, R. C., Brayer, G. D. and Baker, E. N. (1998). Two high-resolution crystal structures of the recombinant N-lobe of human transferrin reveal a structural change implicated in iron release. *Biochemistry* **37,** 7919-28.

Maines, M. D. (1997). The heme oxygenase system: a regulator of second messenger gases. *Annu Rev Pharmacol Toxicol* **37,** 517-54.

Majuri, R. and Grasbeck, R. (1987). A rosette receptor assay with haem-microbeads. Demonstration of a haem receptor on K562 cells. *Eur J Haematol* **38,** 21-5.

Malecki, E. A., Cook, B. M., Devenyi, A. G., Beard, J. L. and Connor, J. R. (1999a). Transferrin is required for normal distribution of 59Fe and 54Mn in mouse brain. *J Neurol Sci* **170,** 112-8.

Malecki, E. A., Devenyi, A. G., Beard, J. L. and Connor, J. R. (1999b). Existing and emerging mechanisms for transport of iron and manganese to the brain. *J Neurosci Res* **56,** 113-22.

McGraw, T. E., Greenfield, L. and Maxfield, F. R. (1987). Functional expression of the human transferrin receptor cDNA in Chinese hamster ovary cells deficient in endogenous transferrin receptor. *J Cell Biol* **105,** 207-14.

McKie, A. T., Barrow, D., Latunde-Dada, G. O., Rolfs, A., Sager, G., Mudaly, E., Mudaly, M., Richardson, C., Barlow, D., Bomford, A., Peters, T. J., Raja, K. B., Shirali, S., Hediger, M. A., Farzaneh, F. and Simpson, R. J. (2001). An iron-regulated ferric reductase associated with the absorption of dietary iron. *Science* **291,** 1755-9.

McKie, A. T., Marciani, P., Rolfs, A., Brennan, K., Wehr, K., Barrow, D., Miret, S., Bomford, A., Peters, T. J., Farzaneh, F., Hediger, M. A., Hentze, M. W. and Simpson., R. J. (2000). A Novel Duodenal Iron-Regulated Transporter, IREG1, Implicated in the Basolateral Transfer of Iron to the Circulation. *Molecular Cell* **5,** 299-309.

McNagny, K. M. (1990). Identification and Characterization of the Murine BP-3 Antigen. In *Microbiology*, pp. 119. Birmingham: University of Alabama at Birmingham.

McNagny, K. M., Rossi, F., Smith, G. and Graf, T. (1996). The eosinophil-specific cell surface antigen, EOS47, is a chicken homologue of the oncofetal antigen melanotransferrin. *Blood* **87,** 1343-52.

Meehan, R. R., Barlow, D. P., Hill, R. E., Hogan, B. L. and Hastie, N. D. (1984). Pattern of serum protein gene expression in mouse visceral yolk sac and foetal liver. *Embo J* **3,** 1881-5.

Mellman, I. (1996). Endocytosis and molecular sorting. *Annu Rev Cell Dev Biol* **12,** 575-625.

Metz-Boutigue, M. H., Jolles, J., Mazurier, J., Schoentgen, F., Legrand, D., Spik, G., Montreuil, J. and Jolles, P. (1984). Human lactotransferrin: amino acid sequence and structural comparisons with other transferrins. *Eur J Biochem* **145,** 659-76.

Miskimins, W. K., McClelland, A., Roberts, M. P. and Ruddle, F. H. (1986). Cell proliferation and expression of the transferrin receptor gene: promoter sequence homologies and protein interactions. *J Cell Biol* **103,** 1781-8.

Montosi, G., Donovan, A., Totaro, A., Garuti, C., Pignatti, E., Cassanelli, S., Trenor, C. C., Gasparini, P., Andrews, N. C. and Pietrangelo, A. (2001). Autosomal-

dominant hemochromatosis is associated with a mutation in the ferroportin (SLC11A3) gene. *J Clin Invest* **108,** 619-23.

Moos, T. and Morgan, E. H. (1998). Evidence for low molecular weight, non-transferrin-bound iron in rat brain and cerebrospinal fluid. *J Neurosci Res* **54,** 486-94.

Moroo, I., Ujiie, M., Tiong, J. W. C., Walker, B. L. and Jefferies, W. A. (2002). The role of p97 in iron transport across the blood-brain barrier. *Manuscript in preperation.*

Moroo, I., Yamada, T., Gabathuler, R., Kennard, M. L., Nurminen, J. and Jefferies, W. A. (1999). Use of p97 in the diagnosis of Alzheimer's disease. *Alzheimer's Reports* **2,** 353-8.

Motulsky, H. (1995). Intuitive Biostatistics, pp. 386. Oxford: Oxford University Press.

Mukhopadhyay, C. K., Mazumder, B. and Fox, P. L. (2000). Role of hypoxia-inducible factor-1 in transcriptional activation of ceruloplasmin by iron deficiency. *J Biol Chem* **275,** 21048-54.

Mullner, E. W. and Kuhn, L. C. (1988). A stem-loop in the 3' untranslated region mediates iron-dependent regulation of transferrin receptor mRNA stability in the cytoplasm. *Cell* **53,** 815-25.

Nair, M. K., Ebner, K. E. and Cook, J. D. (1990). Isolation and characterization of a transferrin binding protein from rat plasma. *Biochim Biophys Acta* **1035,** 306-12.

Nice, E. C. and Catimel, B. (1999). Instrumental biosensors: new perspectives for the analysis of biomolecular interactions. *Bioessays* **21,** 339-52.

Nicolas, G., Bennoun, M., Devaux, I., Beaumont, C., Grandchamp, B., Kahn, A. and Vaulont, S. (2001). Lack of hepcidin gene expression and severe tissue iron overload in upstream stimulatory factor 2 (USF2) knockout mice. *Proc Natl Acad Sci U S A* **98,** 8780-5.

Nicolas, G., Bennoun, M., Porteu, A., Mativet, S., Beaumont, C., Grandchamp, B., Sirito, M., Sawadogo, M., Kahn, A. and Vaulont, S. (2002). Severe iron deficiency anemia in transgenic mice expressing liver hepcidin. *Proc Natl Acad Sci U S A* **99,** 4596-601.

Niederau, C., Fischer, R., Purschel, A., Stremmel, W., Haussinger, D. and Strohmeyer, G. (1996). Long-term survival in patients with hereditary hemochromatosis. *Gastroenterology* **110,** 1107-19.

Niederau, C., Fischer, R., Sonnenberg, A., Stremmel, W., Trampisch, H. J. and Strohmeyer, G. (1985). Survival and causes of death in cirrhotic and in noncirrhotic patients with primary hemochromatosis. *N Engl J Med* **313,** 1256-62.

Odorizzi, G. and Trowbridge, I. S. (1997). Structural requirements for basolateral sorting of the human transferrin receptor in the biosynthetic and endocytic pathways of Madin-Darby canine kidney cells. *J Cell Biol* **137,** 1255-64.

Osaki, S. and Johnson, D. A. (1969). Mobilization of liver iron by ferroxidase (ceruloplasmin). *J Biol Chem* **244,** 5757-8.

Owen, D. and Kuhn, L. C. (1987). Noncoding 3' sequences of the transferrin receptor gene are required for mRNA regulation by iron. *Embo J* **6,** 1287-93.

Owen, D. J. and Evans, P. R. (1998). A structural explanation for the recognition of tyrosine-based endocytotic signals. *Science* **282,** 1327-32.

Park, C. H., Valore, E. V., Waring, A. J. and Ganz, T. (2001). Hepcidin, a urinary antimicrobial peptide synthesized in the liver. *J Biol Chem* **276,** 7806-10.

Parkkila, S., Parkkila, A. K., Waheed, A., Britton, R. S., Zhou, X. Y., Fleming, R. E., Tomatsu, S., Bacon, B. R. and Sly, W. S. (2000). Cell surface expression of HFE protein in epithelial cells, macrophages, and monocytes. *Haematologica* **85,** 340-5.

Parkkila, S., Waheed, A., Britton, R. S., Bacon, B. R., Zhou, X. Y., Tomatsu, S., Fleming, R. E. and Sly, W. S. (1997a). Association of the transferrin receptor in human placenta with HFE, the protein defective in hereditary hemochromatosis. *Proc Natl Acad Sci U S A* **94,** 13198-202.

Parkkila, S., Waheed, A., Britton, R. S., Feder, J. N., Tsuchihashi, Z., Schatzman, R. C., Bacon, B. R. and Sly, W. S. (1997b). Immunohistochemistry of HLA-H, the protein defective in patients with hereditary hemochromatosis, reveals unique pattern of expression in gastrointestinal tract. *Proc Natl Acad Sci U S A* **94,** 2534-9.

Patel, B. N., Dunn, R. J. and David, S. (2000). Alternative RNA splicing generates a glycosylphosphatidylinositol-anchored form of ceruloplasmin in mammalian brain. *J Biol Chem* **275,** 4305-10.

Plow, E. F., Haas, T. A., Zhang, L., Loftus, J. and Smith, J. W. (2000). Ligand binding to integrins. *J Biol Chem* **275,** 21785-8.

Plowman, G. D. (1986). Characterization and expression of the melanotransferrin (p97) gene. In *Pathology*, pp. 229. Seattle: University of Washington, Seattle.

Poss, K. D. and Tonegawa, S. (1997a). Heme oxygenase 1 is required for mammalian iron reutilization. *Proc Natl Acad Sci U S A* **94,** 10919-24.

Poss, K. D. and Tonegawa, S. (1997b). Reduced stress defense in heme oxygenase 1-deficient cells. *Proc Natl Acad Sci U S A* **94,** 10925-30.

Pytela, R., Pierschbacher, M. D. and Ruoslahti, E. (1985). Identification and isolation of a 140 kd cell surface glycoprotein with properties expected of a fibronectin receptor. *Cell* **40,** 191-8.

Rabin, M., McClelland, A., Kuhn, L. and Ruddle, F. H. (1985). Regional localization of the human transferrin receptor gene to 3q26.2q. *Am J Hum Genet* **37,** 1112-6.

Raffin, S. B., Woo, C. H., Roost, K. T., Price, D. C. and Schmid, R. (1974). Intestinal absorption of hemoglobin iron-heme cleavage by mucosal heme oxygenase. *J Clin Invest* **54,** 1344-52.

Raja, K. B., Simpson, R. J. and Peters, T. J. (1992). Investigation of a role for reduction in ferric iron uptake by mouse duodenum. *Biochim Biophys Acta* **1135,** 141-6.

Ramalingam, T. S., West, A. P., Lebron, J. A., Nangiana, J. S., Hogan, T. H., Enns, C. A. and Bjorkman, P. J. (2000). Binding to the transferrin receptor is required for endocytosis of HFE and regulation of iron homeostasis. *Nat Cell Biol* **2,** 953-7.

Ramm, G. A., Crawford, D. H., Powell, L. W., Walker, N. I., Fletcher, L. M. and Halliday, J. W. (1997). Hepatic stellate cell activation in genetic haemochromatosis. Lobular distribution, effect of increasing hepatic iron and response to phlebotomy. *J Hepatol* **26,** 584-92.

Richardson, D. R. (2000). The role of the membrane-bound tumour antigen, melanotransferrin (p97), in iron uptake by the human malignant melanoma cell. *Eur J Biochem* **267,** 1290-8.

Riedel, H. D., Remus, A. J., Fitscher, B. A. and Stremmel, W. (1995). Characterization and partial purification of a ferrireductase from human duodenal microvillus membranes. *Biochem J* **309,** 745-8.

Roberts, M. R., Han, Y., Fienberg, A., Hunihan, L. and Ruddle, F. H. (1994). A DNA-binding activity, TRAC, specific for the TRA element of the transferrin receptor gene copurifies with the Ku autoantigen. *Proc Natl Acad Sci U S A* **91,** 6354-8.

Robinson, M. S. and Pearse, B. M. (1986). Immunofluorescent localization of 100K coated vesicle proteins. *J Cell Biol* **102,** 48-54.

Roeser, H. P., Lee, G. R., Nacht, S. and Cartwright, G. E. (1970). The role of ceruloplasmin in iron metabolism. *J Clin Invest* **49,** 2408-17.

Rose, T. M., Plowman, G. D., Teplow, D. B., Dreyer, W. J., Hellstrom, K. E. and Brown, J. P. (1986). Primary structure of the human melanoma-associated antigen p97 (melanotransferrin) deduced from the mRNA sequence. *Proc Natl Acad Sci U S A* **83,** 1261-5.

Rosenmund, A., Kuyas, C. and Haeberli, A. (1986). Oxidative radioiodination damage to human lactoferrin. *Biochem J* **240,** 239-45.

Rothenberg, B. E. and Voland, J. R. (1996). beta2 knockout mice develop parenchymal iron overload: A putative role for class I genes of the major histocompatibility complex in iron metabolism. *Proc Natl Acad Sci U S A* **93,** 1529-34.

Rothenberger, S., Food, M. R., Gabathuler, R., Kennard, M. L., Yamada, T., Yasuhara, O., McGeer, P. L. and Jefferies, W. A. (1996). Coincident expression and distribution of melanotransferrin and transferrin receptor in human brain capillary endothelium. *Brain Res* **712,** 117-21.

Rothenberger, S., Iacopetta, B. J. and Kuhn, L. C. (1987a). Endocytosis of the transferrin receptor requires the cytoplasmic domain but not its phosphorylation site. *Cell* **49,** 423-31.

Rothenberger, S., Iacopetta, B. J. and Kuhn, L. C. (1987b). Endocytosis of the transferrin receptor requires the cytoplasmic domain but not its phosphorylation site. *Cell* **49,** 423-31.

Rouault, T. A. (2001). Systemic iron metabolism: a review and implications for brain iron metabolism. *Pediatr Neurol* **25,** 130-7.

Rovati, G. E. (1993). Rational experimental design and data analysis for ligand binding studies: tricks, tips and pitfalls. *Pharmacol Res* **28,** 277-99.

Rovati, G. E. (1998). Ligand-binding studies: old beliefs and new strategies. *Trends Pharmacol Sci* **19,** 365-9.

Roy, C. N., Blemings, K. P., Deck, K. M., Davies, P. S., Anderson, E. L., Eisenstein, R. S. and Enns, C. A. (2002). Increased IRP1 and IRP2 RNA binding activity accompanies a reduction of the labile iron pool in HFE-expressing cells. *J Cell Physiol* **190,** 218-26.

Roy, C. N., Penny, D. M., Feder, J. N. and Enns, C. A. (1999). The hereditary hemochromatosis protein, HFE, specifically regulates transferrin-mediated iron uptake in HeLa cells. *J Biol Chem* **274,** 9022-8.

Roze-Heusse, A., Houbiguian, M. L., Debacker, C., Zakin, M. M. and Duchange, N. (1996). Melanotransferrin gene expression in melanoma cells is correlated with high levels of Jun/Fos family transcripts and with the presence of a specific AP1-dependent ternary complex. *Biochem J* **318,** 883-8.

Rugh, R. (1990). The Mouse: It's reproduction and development: Oxford University Press.

Ruoslahti, E. (1996). RGD and other recognition sequences for integrins. *Annu Rev Cell Dev Biol* **12,** 697-715.

Rutledge, E. A., Green, F. A. and Enns, C. A. (1994). Generation of the soluble transferrin receptor requires cycling through an endosomal compartment. *J Biol Chem* **269,** 31864-8.

Sala, R., Jefferies, W. A., Walker, B., Yang, J., Tiong, J., Law, S. A., Carlevaro, M. F., Vacca, A., Cancedda, R., Cancedda, F. D. and Ribatti, D. (2002). The human melanoma associated protein melanotransferrin promotes endothelial cell migration and angiogenesis in vivo. *Submitted* .

Sassone-Corsi, P. (1994). Goals for signal transduction pathways: linking up with transcriptional regulation. *Embo J* **13,** 4717-28.

Sayre, L. M., Perry, G. and Smith, M. A. (1999). Redox metals and neurodegenerative disease. *Curr Opin Chem Biol* **3,** 220-5.

Schneider, C., Owen, M. J., Banville, D. and Williams, J. G. (1984). Primary structure of human transferrin receptor deduced from the mRNA sequence. *Nature* **311,** 675-8.

Sciot, R., de Vos, R., van Eyken, P., van der Steen, K., Moerman, P. and Desmet, V. J. (1989). In situ localization of melanotransferrin (melanoma-associated antigen P97) in human liver. A light- and electronmicroscopic immunohistochemical study. *Liver* **9,** 110-9.

Sharp, P., Tandy, S., Yamaji, S., Tennant, J., Williams, M. and Singh Srai, S. K. (2002). Rapid regulation of divalent metal transporter (DMT1) protein but not mRNA expression by non-haem iron in human intestinal Caco-2 cells. *FEBS Lett* **510,** 71-6.

Sheth, S. and Brittenham, G. M. (2000). Genetic disorders affecting proteins of iron metabolism: clinical implications. *Annu Rev Med* **51,** 443-64.

Shih, Y. J., Baynes, R. D., Hudson, B. G., Flowers, C. H., Skikne, B. S. and Cook, J. D. (1990). Serum transferrin receptor is a truncated form of tissue receptor. *J Biol Chem* **265,** 19077-81.

Sieweke, M. H., Tekotte, H., Frampton, J. and Graf, T. (1996). MafB is an interaction partner and repressor of Ets-1 that inhibits erythroid differentiation. *Cell* **85,** 49-60.

Sipe, D. M. and Murphy, R. F. (1991). Binding to cellular receptors results in increased iron release from transferrin at mildly acidic pH. *J Biol Chem* **266,** 8002-7.

Stearman, R., Yuan, D. S., Yamaguchi-Iwai, Y., Klausner, R. D. and Dancis, A. (1996). A permease-oxidase complex involved in high-affinity iron uptake in yeast. *Science* **271,** 1552-7.

Stearne, P. A., Pietersz, G. A. and Goding, J. W. (1985). cDNA cloning of the murine transferrin receptor: sequence of trans-membrane and adjacent regions. *J Immunol* **134,** 3474-9.

Stephens, P. E., Ortlepp, S., Perkins, V. C., Robinson, M. K. and Kirby, H. (2000). Expression of a soluble functional form of the integrin alpha4beta1 in mammalian cells. *Cell Adhes Commun* **7,** 377-90.

Sundan, A., Olsnes, S., Sandvig, K. and Pihl, A. (1982). Preparation and properties of chimeric toxins prepared from the constituent polypeptides of diphtheria toxin and ricin. Evidence for entry of ricin A-chain via the diphtheria toxin pathway. *J Biol Chem* **257,** 9733-9.

Thompson, A. M. and Thompson, G. C. (2001). Serotonin projection patterns to the cochlear nucleus. *Brain Res* **907,** 195-207.

Tiong, J. (2001). Metal Binding Properties of p97 and the Trafficking of a Novel Iron Internalizatiion Pathway by GPI-anchored p97. In *Microbiology and Immunology and the Biotechnology Laboratory*, pp. 205. Vancouver: University of British Columbia.

Tiong, J., Tian, M. and Jefferies, W. (2002). A novel iron uptake pathway through caveolae by GPI-anchored p97. *manuscript in preparation* .

Tiong, J. W. C. and Jefferies, W. A. (2002). Metal binding properties of melanotransferrin. , *manuscript in preperation.*

Tong, X., Kawabata, H. and Koeffler, H. P. (2002). Iron deficiency can upregulate expression of transferrin receptor at both the mRNA and protein level. *Br J Haematol* **116,** 458-64.

Townsend, A. and Drakesmith, H. (2002). Role of HFE in iron metabolism, hereditary haemochromatosis, anaemia of chronic disease, and secondary iron overload. *Lancet* **359,** 786-90.

Triguero, D., Buciak, J. and Pardridge, W. M. (1990). Capillary depletion method for quantification of blood-brain barrier transport of circulating peptides and plasma proteins. *J Neurochem* **54,** 1882-8.

Trinder, D., Macey, D. J. and Olynyk, J. K. (2000). The new iron age. *Int J Mol Med* **6,** 607-12.

Turnbull, A., Cleton, F. and Finch, C. A. (1989). The Journal of clinical Investigation, Volume 41, 1962: iron absorption. IV. The absorption of hemoglobin iron. *Nutr Rev* **47,** 51-3.

Umbreit, J. N., Conrad, M. E., Moore, E. G. and Latour, L. F. (1998). Iron absorption and cellular transport: the mobilferrin/paraferritin paradigm. *Semin Hematol* **35,** 13-26.

van der Flier, A. and Sonnenberg, A. (2001). Function and interactions of integrins. *Cell Tissue Res* **305,** 285-98.

Vulpe, C. D., Kuo, Y. M., Murphy, T. L., Cowley, L., Askwith, C., Libina, N., Gitschier, J. and Anderson, G. J. (1999). Hephaestin, a ceruloplasmin homologue implicated in intestinal iron transport, is defective in the sla mouse. *Nat Genet* **21,** 195-9.

Waheed, A., Parkkila, S., Zhou, X. Y., Tomatsu, S., Tsuchihashi, Z., Feder, J. N., Schatzman, R. C., Britton, R. S., Bacon, B. R. and Sly, W. S. (1997). Hereditary hemochromatosis: effects of C282Y and H63D mutations on association with beta2-microglobulin, intracellular processing, and cell surface expression of the HFE protein in COS-7 cells. *Proc Natl Acad Sci U S A* **94,** 12384-9.

Wardrop, S. L. and Richardson, D. R. (1999). The effect of intracellular iron concentration and nitrogen monoxide on Nramp2 expression and non-transferrin-bound iron uptake. *Eur J Biochem* **263,** 41-9.

West, A. P., Jr., Bennett, M. J., Sellers, V. M., Andrews, N. C., Enns, C. A. and Bjorkman, P. J. (2000). Comparison of the interactions of transferrin receptor and

transferrin receptor 2 with transferrin and the hereditary hemochromatosis protein HFE. *J Biol Chem* **275,** 38135-8.

Williams, A. M. and Enns, C. A. (1991). A mutated transferrin receptor lacking asparagine-linked glycosylation sites shows reduced functionality and an association with binding immunoglobulin protein. *J Biol Chem* **266,** 17648-54.

Woodbury, R. G., Brown, J. P., Loop, S. M., Hellstrom, K. E. and Hellstrom, I. (1981). Analysis of normal neoplastic human tissues for the tumor-associated protein p97. *Int J Cancer* **27,** 145-9.

Woodbury, R. G., Brown, J. P., Yeh, M. Y., Hellstrom, I. and Hellstrom, K. E. (1980). Identification of a cell surface protein, p97, in human melanomas and certain other neoplasms. *Proc Natl Acad Sci U S A* **77,** 2183-7.

Xiong, J. P., Stehle, T., Diefenbach, B., Zhang, R., Dunker, R., Scott, D. L., Joachimiak, A., Goodman, S. L. and Arnaout, M. A. (2001). Crystal structure of the extracellular segment of integrin alpha Vbeta3. *Science* **294,** 339-45.

Yamada, T., Tsujioka, Y., Taguchi, J., Takahashi, M., Tsuboi, Y., Moroo, I., Yang, J. and Jefferies, W. A. (1999). Melanotransferrin is produced by senile plaque-associated reactive microglia in Alzheimer's disease. *Brain Res* **845,** 1-5.

Young, S. P., Bomford, A. and Williams, R. (1984). The effect of the iron saturation of transferrin on its binding and uptake by rabbit reticulocytes. *Biochem J* **219,** 505-10.

Yu, J. and Wessling-Resnick, M. (1998). Structural and functional analysis of SFT, a stimulator of Fe Transport. *J Biol Chem* **273,** 21380-5.

Yu, J., Yu, Z. K. and Wessling-Resnick, M. (1998). Expression of SFT (stimulator of Fe transport) is enhanced by iron chelation in HeLa cells and by hemochromatosis in liver. *J Biol Chem* **273,** 34675-8.

Zhou, X. Y., Tomatsu, S., Fleming, R. E., Parkkila, S., Waheed, A., Jiang, J., Fei, Y., Brunt, E. M., Ruddy, D. A., Prass, C. E., Schatzman, R. C., O'Neill, R., Britton, R. S., Bacon, B. R. and Sly, W. S. (1998). HFE gene knockout produces mouse model of hereditary hemochromatosis. *Proc Natl Acad Sci U S A* **95,** 2492-7.

Zoller, H., Koch, R. O., Theurl, I., Obrist, P., Pietrangelo, A., Montosi, G., Haile, D. J., Vogel, W. and Weiss, G. (2001). Expression of the duodenal iron transporters divalent-metal transporter 1 and ferroportin 1 in iron deficiency and iron overload. *Gastroenterology* **120,** 1412-9.